ISSN 2544-4476
e-ISSN 2544-798X

AGRONOMY SCIENCE

wcześniej – formerly

Annales UMCS sectio E Agricultura

VOL. LXXX (4) 2025

UNIWERSYTET PRZYRODNICZY W LUBLINIE

RADA NAUKOWA – SCIENTIFIC BOARD

Imran Aslan (Bingöl, Turcja), Jan Buczek (Polska),
Alessandra Carruba (Palermo, Italy), Dorota Gawęda (Lublin, Polska),
Krzysztof Jankowski (Olsztyn, Polska), Elvyra Jariene (Kowno, Litwa),
Barbara Kołodziej (Lublin, Polska), Ali Hulail Noaema (Al-Muthanna, Irak),
Eleni G. Papazoglou (Ateny, Grecja), Ivan Shuvar (Dublany, Ukraina),
Danuta Sugier (Lublin, Polska), Wiesław Wojciechowski (Wrocław, Polska),
Alena Yakimovich (Mińsk, Białoruś)

REDAKTOR NACZELNY – EDITOR-IN-CHIEF

Aleksandra Głowacka

REDAKTOR WYDAWNICZY – PUBLISHING EDITOR

Renata Zelik

SKŁAD I ŁAMANIE – TYPESETTING TEXT

Małgorzata Grzesiak

© Copyright by Uniwersytet Przyrodniczy w Lublinie – Wydawnictwo, Lublin 2025

ISSN 2544-4476

e-ISSN 2544-798X

Czasopismo jest indeksowane przez – Covered by:

AGRO, Arianta, CAB Abstracts, DOAJ, EBSCO, EuroPub,
Index Copernicus – ICI Journal Master List, Most Wiedzy, Open Policy Finder, PBN, Ulrichsweb
Global Serials Directory

WYDAWNICTWO UNIWERSYTETU PRZYRODNICZEGO W LUBLINIE
ul. Akademicka 15, 20-950 Lublin, tel. 81-445-66-60, https://czasopisma.up.lublin.pl/index.php/as,
e-mail: agronomy.science@up.lublin.pl

AGRONOMY SCIENCE

VOL. LXXX (4) 2025

Table of contents
Spis treści

ROMAN PRAŻAK
Otrzymywanie i charakterystyka mieszańców *Aegilops triuncialis* L. × *Triticum aestivum* L. 5
Obtaining and characterizing of *Aegilops triuncialis* L. × *Triticum aestivum* L. hybrids 22

JACEK GAWROŃSKI, MAGDALENA DYDUCH-SIEMIŃSKA
Molecular identification and genetic diversity assessment of *Mentha* genotypes using SCoT and ISSR DNA markers 23

MICHAŁ KASPROWICZ, KATARZYNA PENTOŚ, WIESŁAW WOJCIECHOWSKI, SEBASTIAN KUJAWA, JASPER TEMBECK MBAH
Advancements in plant protection – the application of machine learning to the detection of maize infestations 39
Zastosowanie uczenia maszynowego w wykrywaniu szkodników kukurydzy

BEATA JACEK
Preliminary assessment of the effectiveness of non-fungicide methods of maize seed treatment 57
Wstępna ocena skuteczności niefungicydowych metod zaprawiania nasion kukurydzy

BARBARA KROCHMAL-MARCZAK, ELŻBIETA PISULEWSKA, BARBARA SAWICKA, PIOTR BARBAŚ, PIOTR PSZCZÓŁKOWSKI
The temperature influence on the energy and germination capacity of seeds and the effect of the substrate on the yield *the withania somnifera* in the conditions of south-eastern Poland 69
Wpływ temperatury na energię i zdolność kiełkowania nasion oraz wpływ podłoża na plonowanie *Withania somnifera* w warunkach Polski południowo-wschodniej

MAGDALENA KAPŁAN, SYLVAIN PLUCHON, KAMILA KLIMEK
Assessment of the impact of growth biostimulants on the effects of stimulating branching in maiden apple tree 89
Ocena wpływu biostymulatorów wzrostu na efekty stymulacji rozgałęzienia u okulantów jabłoni

AGRONOMY SCIENCE

VOL. LXXX (4) 2025

https://doi.org/10.24326/as.2025.5576

Instytut Genetyki, Hodowli i Biotechnologii Roślin, Wydział Agrobioinżynierii,
Uniwersytet Przyrodniczy w Lublinie

e-mail: roman.prazak@up.lublin.pl

ROMAN PRAŻAK https://orcid.org/0000-0002-6920-1017

Otrzymywanie i charakterystyka mieszańców *Aegilops triuncialis* L. × *Triticum aestivum* L.

Obtaining and characterizing of *Aegilops triuncialis* L. × *Triticum aestivum* L. hybrids

Abstrakt. W warunkach polowych wykonano krzyżowania między *Aegilops triuncialis* L. (2n = 4x = 28, genomy *UUCC*) a odmianami pszenicy zwyczajnej *Triticum aestivum* L. (2n = 6x = 42, genomy *AABBDD*) Begra, Monopol, Nawra i Zyta. Celem krzyżowań było poszerzenie zmienności genetycznej pszenicy zwyczajnej. Zdolność do krzyżowania badanych genotypów w warunkach polowych wahała się od 7,14% (*Ae. triuncialis* × Zyta) do 13,33% (*Ae. triuncialis* × Monopol). Ziarniaki mieszańcowe zawiązały się jedynie w przypadku, gdy formą mateczną był *Ae. triuncialis*. Z uzyskanych 22 mieszańcowych ziarniaków F_1 w warunkach *in vitro* wyizolowano 19 zarodków i wyłożono je na pożywkę MS z dodatkiem 10 mg·dm^{-3} IAA (kwas β-indolilo-3-octowy) i 0,04 mg·dm^{-3} kinetyny. Z zarodków F_1 w *in vitro* rozwinęło się 15 siewek. Po 4 tygodniach uzyskane siewki mieszańców przesadzono do doniczek i umieszczono w fitotronie, a następnie w połowie września wysadzono na polu doświadczalnym obok komponentów rodzicielskich. Oceny liczby chromosomów mieszańców dokonano na preparatach rozmazowych komórek merystematycznych wierzchołków korzeni siewek. W czasie sezonu wegetacyjnego z pochew liściowych roślin mieszańcowych pobrano niedojrzałe kłosy do analizy mejozy. Analiza cytologiczna wykazała nieprawidłowości w procesie mikrosporogenezy mieszańców, co wpłynęło na wykształcenie się nieżywotnego pyłku. Część kłosów mieszańców F_1 wykastrowano i zapylono wstecznie pyłkiem pszenicy. Mieszańce F_1 rozmnażano również *in vitro*, wykładając na pożywkę MS z dodatkiem 2 mg·dm^{-3} 2,4-D (kwas 2,4-dichlorofenoksyoctowy) po 100 fragmentów niedojrzałych kwiatostanów w każdej kombinacji krzyżówkowej. Z kalusa wytworzonego przez eksplantaty zregenerowało 5 roślin R_1 w kombinacji *Ae. triuncialis* L. × *T. aestivum* L. Zyta. W fazie dojrzałości pełnej na roślinach mieszańcowych F_1 i R_1 dokonano pomiarów cech biometrycznych, takich jak krzewienie ogólne, długość pędu głównego, średnica drugiego od dołu międzywęźla, długość osadki kłosowej kłosa głównego, zbitość kłosa głównego i płodność kłosa głównego. Mieszańce charakteryzowały się pośrednim w stosunku do form rodzicielskich krzewieniem (15,0–41,0 źdźbeł), średnicą drugiego od dołu

Cytowanie: Prażak R., 2025. Otrzymywanie i charakterystyka mieszańców *Aegilops triuncialis* L. × *Triticum aestivum* L. Agron. Sci. 80(4), 5–22. https://doi.org/10.24326/as.2025.5576

międzywęźla (2,1–2,9 mm), zbitością kłosa głównego (14,6–17,5 kłosków na 1 dm osadki kłosa), krótszymi źdźbłami (43,0–48,3 cm) i osadkami kłosowymi (0,55–0,68 dm) oraz sterylnymi kłosami.

Słowa kluczowe: *Aegilops triuncialis* L., cechy plonotwórcze, pszenica zwyczajna, kultury *in vitro*, mieszańce międzyrodzajowe

WSTĘP

Dla zwiększenia zmienności genetycznej pszenicy zwyczajnej krzyżuje się ją z różnymi gatunkami pokrewnymi z rodzaju *Aegilops* L. [Fakhri i in. 2016, Zhao i in. 2018, Wang i in. 2022, Feldman i Levy 2023]. Gatunki te są opisywane jako źródła pożądanych cech plonotwórczych, odpornościowych (na choroby, szkodniki, zakwaszenie i zasolenie gleby), jakościowych (wysoka zawartość białka i mikroelementów w ziarniakach pszenicy) [Arzani i Ashraf 2016, Prażak i Molas 2017, Prażak i Krzepiłko 2018, Darko i in. 2020, Kiani i in. 2021, Bocianowski i Prażak 2022, Laugerotte i in. 2022, Hadzhiivanova i in. 2025]. *Aegilops triuncialis* L. (genomy *UUCC*) jest przedmiotem zainteresowania hodowców pszenicy jako źródło genów odporności na choroby kłosa [Pilch i in. 1995], rdzę brunatną (*Puccinia recondita*) – *Lr58* [Ijaz i in. 2023], szkodniki [Martín-Sánchez i in. 2003], suszę i zasolenie gleby [Yildiz i in. 2006] oraz charakteryzuje się dużą zawartością białka [Karagoz 2006]. Pochodzi on z Europy Wschodniej i basenu Morza Śródziemnego oraz Azji Zachodniej [Kimber i Feldman 1987]. W naturalnych warunkach *Ae. triuncialis* L. najczęściej rośnie na ugorach, przydrożach, ale dobrze radzi sobie również na użytkach zielonych. W Ameryce Północnej jest to gatunek inwazyjny, występujący głównie na zachodnim wybrzeżu Stanów Zjednoczonych [Zaharieva i Monneveux 2005, Aigner i Woerly 2011]. *Ae. triuncialis* L. jest rzadko wykorzystywany do ulepszania pszenicy zwyczajnej, istnieje niewiele doniesień o udanych krzyżowaniach między tymi dwoma gatunkami. Pilch i in. [1995] zapylali linię mono-5B pszenicy zwyczajnej *T. aestivum* L. Chinese Spring pyłkiem *Ae. triuncialis* L., a następnie powstałego mieszańca krzyżowali wstecznie z *T. aestivum* Chinese Spring. Delibes i in. [1988] w pierwszej kolejności krzyżowali pszenicę tetraploidalną *T. turgidum* L. z *Ae. triuncialis* L., a następnie uzyskane mieszańce F_1 zapylali pyłkiem pszenicy heksaploidalnej. Aghaee-Sarbarzeh i in. [2002] przenieśli odporność na rdzę brunatną z *Ae. triuncialis* L. do pszenicy zwyczajnej przy użyciu indukowanej homeologicznej koniugacji i przy wykorzystaniu genu *Ph1*. Genomowa hybrydyzacja *in situ* (GISH) i analiza markerów DNA (SSR) pozwoliły zidentyfikować u mieszańca pszenicy z *Ae. triuncialis* L. zrekombinowany chromosom 5U z małym końcowym segmentem pochodzącym z ramienia 5AS chromosomu pszenicy [Aghaee-Sarbarzeh i in. 2008]. W krzyżowaniach, w których otrzymuje się niewiele zarodków, wydajność regeneracji żywotnych mieszańców można zwiększyć poprzez indukcję kalusa z fragmentów niedojrzałych kwiatostanów. Zastosowanie pożywki regenerującej o odpowiednim składzie regulatorów wzrostu może zapoczątkować proces organogenezy w tkance kalusowej [Hejnowicz 2002].

Celem badań było otrzymanie mieszańców międzyrodzajowych Ae. triuncialis L. × *T. aestivum* L. oraz ich charakterystyka morfologiczna i cytologiczna.

MATERIAŁ I METODY

Obiektem badań był dziki gatunek *Ae. triuncialis* L. i odmiany pszenicy *T. aestivum* L. Begra, Monopol, Nawra i Zyta. Ziarno *Ae. triuncialis* L. uzyskano z Instytutu Genetyki Roślin Leibnitza i Badań Roślin Uprawnych (IPK) Gatersleben w Niemczech (numer obiektu w banku genów AE 120/78). Pszenice pochodziły z Krajowego Centrum Roślinnych Zasobów Genowych IHAR w Radzikowie. Krzyżowania przeprowadzono na polu doświadczalnym Uniwersytetu Przyrodniczego w Lublinie. W każdej kombinacji zapylono co najmniej dziesięć kłosów. Trzy dni przed kwitnieniem kłosy pszenicy zwyczajnej i *Ae. triuncialis* L. kastrowano i zakładano na nie izolatory z celofanu, aby uniknąć niepożądanego zapylenia. Krzyżowania przeprowadzono przy użyciu świeżego pyłku *Aegilops* lub danej odmiany pszenicy. Po 18 dniach od zapylenia w laboratorium kultur *in vitro* niedojrzałe zarodki mieszańcowe izolowano z ziarniaków i wykładano w warunkach aseptycznych do probówek na pożywkę MS [Murashige i Skoog 1962], z dodatkiem kinetyny – 0,04 $mg \cdot dm^{-3}$ i kwasu indolilo-3-octowego (IAA) – 10,0 $mg \cdot dm^{-3}$ [Chueca i in. 1977]. Ziarniaki były wcześniej odwadniane w 70% alkoholu etylowym i odkażane przez 6 minut w 0,1% roztworze chlorku rtęci ($HgCl_2$), następnie trzykrotnie płukane w sterylnej wodzie. Hodowlę kultur zarodków prowadzono w fitotronie, w temperaturze 23 ±2°C, przy 60–70% wilgotności względnej, 16-godzinnym fotoperiodzie i natężeniu światła 36 $\mu E \cdot m^{-2} \cdot s^{-1}$. Zregenerowane z zarodków rośliny w fazie drugiego liścia przenoszono do doniczek z wyjałowioną ziemią i piaskiem (w stosunku 1 : 1). Po aklimatyzacji od połowy września uprawiano je (podobnie jak genotypy rodzicielskie) na poletkach doświadczalnych o długości 2,0 m i szerokości 1,0 m, w rozstawie rzędów 20 × 10 cm na glebie brunatnej, kompleksu pszennego dobrego, w tych samych warunkach uprawy i nawożenia. Na roślinach mieszańcowych F_1 przeprowadzono krzyżowania wsteczne BC_1 z pszenicami rodzicielskimi, zapylając po 50 wykastrowanych kwiatków w każdej kombinacji.

Analizy cytologiczne. Do obserwacji podziałów mitotycznych pobierano wierzchołki korzeni mieszańców, które po wstępnym traktowaniu mieszaniną wody z lodem przez okres 24 godzin utrwalano w roztworze Carnoya (etanol : kwas octowy = 3 : 1 v/v). Chromosomy liczono pod mikroskopem świetlnym przy powiększeniu 100×. Do obserwacji podziałów mejotycznych z pochew liściowych pobierano młode kłosy z pylnikami zawierającymi komórki macierzyste pyłku i mikrospory na różnym etapie rozwoju i utrwalano je przez trzy godziny w roztworze Carnoya. Utrwalone preparaty przechowywano w 70-procentowym alkoholu etylowym i temperaturze 4°C. W metafazie I obserwowano co najmniej 50 komórek macierzystych pyłku (PMC) wybarwionych acetokarminem. Określano liczbę biwalentów w postaci prętów i pierścieni oraz obecność uniwalentów, triwalentów, kwadriwalentów. W anafazie I obserwowano obecność chromosomów opóźnionych i mostów chromatynowych. Badano również frekwencję mikrojąder, analizując 300 tetrad każdej formy. Pomiary ziaren pyłku wykonano okularem 8× z podziałką, pod obiektywem 40×, a następnie wynik przeliczono na μm. Ziarna pyłku wybarwione acetokarminem na czerwono uznawano za żywotne [Chrząstek 2000]. Wykonano również preparaty rozmazowe komórek kalusa, które barwiono acetokarminem.

Rozmnażanie mieszańców z fragmentów kwiatostanów. Niedojrzałe kłosy mieszańców odwadniano w 70-procentowym alkoholu C_2H_5OH, odkażano w 0,1-procentowym roztworze chlorku rtęci ($HgCl_2$) przez 4 min. Następnie po trzykrotnym przepłukaniu w sterylnej wodzie podzielono je na fragmenty wielkości ok. 0,5 cm i wyłożono do kolb Erlenmeyera o pojemności 150 ml (po 10 szt. na kolbę) na pożywkę MS [Murashige i Skoog 1962], z dodatkiem 2,0 $mg \cdot dm^{-3}$ 2,4-D (kwas 2,4-dichlorofenoksyoctowy) [Prażak 1996]. W każdej kombinacji krzyżówkowej zastosowano po 100 eksplantatów. Hodowlę prowadzono w fitotronie w podobnych warunkach temperatury i oświetlenia jak w przypadku zarodków.

Analiza fenotypowa pojedynków. Rośliny zebrano z pola w fazie dojrzałości pełnej i na 3–5 pojedynkach z każdej formy mieszańcowej oraz na 10 pojedynkach form rodzicielskich analizowano cechy ilościowe, takie jak: krzewienie ogólne (liczba pędów z rośliny), długość pędu głównego, średnicę drugiego od dołu międzywęźla, długość osadki kłosowej, zbitość kłosa głównego (liczbę kłosków przypadających na 1 dm osadki kłosowej), płodność kłosa głównego (liczba ziarniaków przypadających na 1 kłosek).

Analiza statystyczna. Uzyskane wyniki opracowano statystycznie za pomocą analizy wariancji, oceniając istotność różnic testem t-Tukeya przy $\alpha = 0,05$. Do analizy wykorzystano program Statistica v.13.1.

WYNIKI BADAŃ I DYSKUSJA

Najczęściej pierwszym etapem prac mających na celu transfer genów z gatunków *Aegilops* L. do *Triticum* L. jest otrzymanie roślin mieszańcowych pierwszego pokolenia. Dalsze etapy polegają na kolejnych krzyżowaniach wstecznych mieszańców z pszenicą heksaploidalną, prowadzonych jednocześnie z wszechstronną oceną i selekcją.

W prezentowanej pracy przedstawiono wyniki z bezpośredniego krzyżowania dzikiego gatunku *Aegilops* – *A. triuncialis* L. z odmianami pszenicy zwyczajnej *Triticum aestivum* L. (tab. 1).

Rośliny F_1 nie zawiązały ziarniaków. Wynikało to z zaburzeń w mejozie, w efekcie których nie powstały płodne gamety. Zaburzenia te były spowodowane niekompletną koniugacją chromosomów, słabym powinowactwem chromosomów obcych genomów do włókien wrzeciona podziałowego. W metafazie I mejozy mieszańców F_1 *Ae. Triuncialis* × *T. aestivum* L. (*ABDUC*) występowały uniwalenty. Nie było biwalentów zarówno w postaci prętów, jak i pierścieni, a także nie zaobserwowano poliwalentów. Liczba pentad w tych mieszańcach wahała się od 23 do 36. W tetradach widoczne były mikrojądra średnio od 0,28 do 0,33 (tab. 2, ryc. 2D i 2E).

Otrzymywanie roślin drugiego pokolenia w wyniku wstecznego zapylania pyłkiem pszenicy wykastrowanych kłosów mieszańców pierwszego pokolenia napotyka na ogół na jeszcze większe trudności. Bai i in. [1994], krzyżując *Aegilops triaristata* Willd. (genomy *UUMMUnUn*) z *T. aestivum* L. cv. Chinese Spring (genomy *AABBDD*) otrzymali wysokie zawiązywanie mieszańcowych ziarniaków na poziomie od 38,89% do 60,81%. Natomiast w wyniku krzyżowania wstecznego zawiązywanie ziarniaków wahało się jedynie od 0% do 7,14%.

Tabela 1. Rezultaty krzyżowania *Aegilops triuncialis* L. z odmianami *Titicum aestivum* L.
Table 1. Results of crosses between *Aegilops triuncialis* L. and *Triticum aestivum* L. cultivars

Kombinacja krzyżówkowa Cross combination	Liczba zapylonych kwiatków Number of florets pollinated	Zawiązane ziarniaki F_1 F_1 seeds set		Liczba zarodków F_1 w *in vitro* Number of F_1 embryos in *in vitro*				Rośliny F_1 z kultur *in vitro* F_1 plants from *in vitro* cultures	
		liczba number	%	kiełkujących germinating	kalusujących callusing	zamarłych lifeless	razem total	liczba number	%
Ae. triuncialis × *Begra*	82	8	9,76	4	3	1	8	4	50,00
Begra × *Ae. triuncialis*	206	0	0,00	0	0	0	0	0	0,00
Ae. triuncialis × *Monopol*	60	8	13,33	5	0	0	5	5	100,00
Monopol × *Ae. triuncialis*	196	0	0,00	0	0	0	0	0	0,00
Ae. triuncialis × *Nawra*	36	3	8,33	3	0	0	3	3	100,00
Nawra × *Ae. triuncialis*	96	0	0,00	0	0	0	0	0	0,00
Ae. triuncialis × *Zyta*	42	3	7,14	3	0	0	3	3	100,00
Zyta × *Ae. triuncialis*	94	0	0,00	0	0	0	0	0	0,00
Ae. triuncialis × *T. aestivum*	220	22	10,00	15	3	1	19	15	78,95
T. aestivum × *Ae. triuncialis*	592	0	0,00	0	0	0	0	0	0,00

Tabela 2. Analiza cytologiczna mieszańców F_1 *Ae. triuncialis* L. z *T. aestivum* L. i R_1 *Ae. triuncialis* L. × *T. aestivum* L. Zyta
Table 2. Cytological analysis of F_1 *Ae. triuncialis* L. with *T. aestivum* L. hybrids and R_1 *Ae. triuncialis* L. × *T. aestivum* L. Zyta

Analizowane formy Forms analysed	Średnia liczba na komórkę Mean number per cell							Średnia liczba mikrojąder w tetradzie Mean number of micro-nucleiin tetrad	Liczba pentad Number of pentads
	chromosomy chromosomes	uniwalenty univalents	biwalenty bivalents		triwalenty trivalents	kwadriwalenty quadrivalents	chiazmy chiasmata		
			pręty rods	pierścienie rings					
F_1 *Ae. triuncialis* × Begra	35	35,00*	0,00	0,00	0,00	0,00	0,00	0,31*	23
F_1 *Ae. triuncialis* × Nawra	35	35,00*	0,00	0,00	0,00	0,00	0,00	0,28*	28
F_1 *Ae. triuncialis* × Zyta	35	35,00*	0,00	0,00	0,00	0,00	0,00	0,33*	36
R_1 *Ae. Triuncialis* × Zyta	35	33,94*	0,88*	0,16*	0,00	0,00	1,22*	0,24*	19
Zyta	42	0,04	0,36	20,62	0,00	0,00	41,52	0,01	0

* Wynik istotnie różny od pszenicy Zyta przy $\alpha = 0,05$
* Result significantly different in relation to the Zyta wheat at $\alpha = 0.05$

Po zapyleniu wykastrowanych kwiatków obu gatunków uzyskano zawiązywanie ziarniaków na poziomie od 7,14% (*Ae. triuncialis* × Zyta) do 13,33% (*Ae. triuncialis* × Monopol). Ziarniaki mieszańcowe zawiązywały się jedynie w przypadku, gdy formą mateczną był *Aegilops*. Potwierdza to wcześniejsze badania, w których taki kierunek krzyżowania dawał kilkukrotnie większą możliwość uzyskania mieszańców F_1 [Prażak 2001, Mirzaghaderi i in. 2020]. Krzyżowanie *Ae. triuncialis* L. z pszenicą zwyczajną i uzyskanie płodnych mieszańców F_1 jest trudne ze względu na bariery krzyżowalności i brak homologii pomiędzy ich genomami. Jak wynika z badań Chueca i in. [1977], w wyniku krzyżowania pszenicy z gatunkami *Aegilops* tworzą się ziarniaki, ale niektóre z nich są niezdolne do kiełkowania z powodu zamierania zarodków we wczesnej fazie rozwoju. Według tych autorów rośliny mieszańcowe udaje się uzyskać przez wczesną izolację i hodowlę niedojrzałych zarodków w kulturze *in vitro*. W niniejszej pracy z 22-mieszańcowych 18-dniowych ziarniaków F_1 wyizolowano 19 zarodków. Hodowla *in vitro* tych zarodków dała w efekcie 15 roślin F_1 (tab. 1, ryc. 1). Kalusujące zarodki wytwarzały jedynie korzenie. Najwięcej roślin mieszańcowych zregenerowało w kombinacji *A. triuncialis* × Monopol (5). W pozostałych kombinacjach zregenerowały 3–4 rośliny (tab. 1).

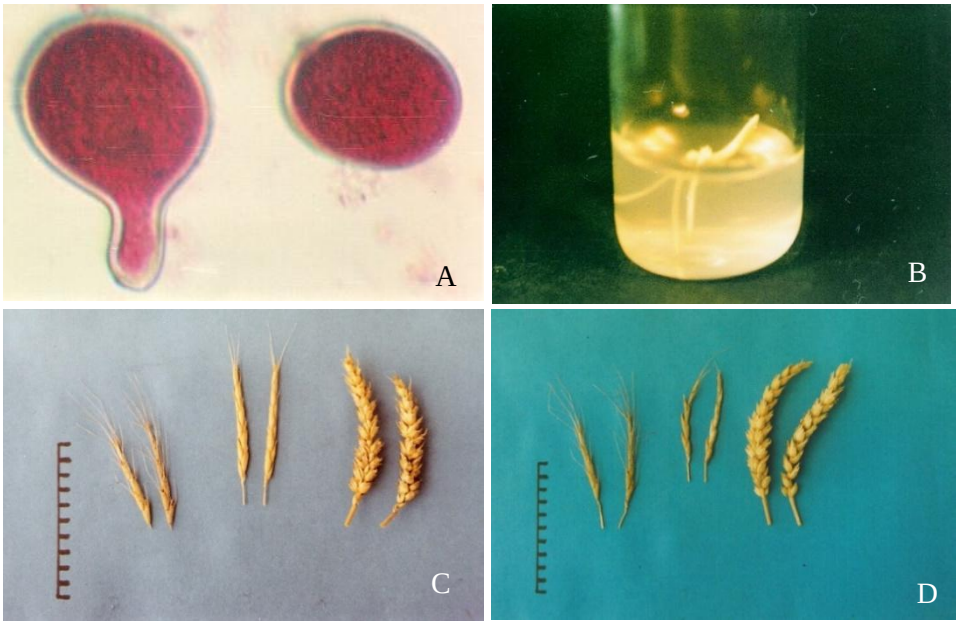

Ryc. 1. Mieszańce F_1 *Ae. triuncialis* L. z *T. aestivum* L.: A) kiełkujące ziarno pyłku pszenicy, B) kiełkujący zarodek mieszańcowy, C) kłosy *Ae. triuncialis* L., mieszańca F_1 pszenicy Monopol, D) kłosy *Ae. triuncialis* L., mieszańca F_1, pszenicy Zyta

Fig. 1. F_1 hybrids of *Ae. triuncialis* L. with *T. aestivum* L.: A) germinating wheat pollen grain, B) germinating hybrid embryo, C) spikes of *Ae. triuncialis* L., F_1 hybrid, wheat Monopol, D) spikes of *Ae. triuncialis* L., F_1 hybrid, wheat Zyta

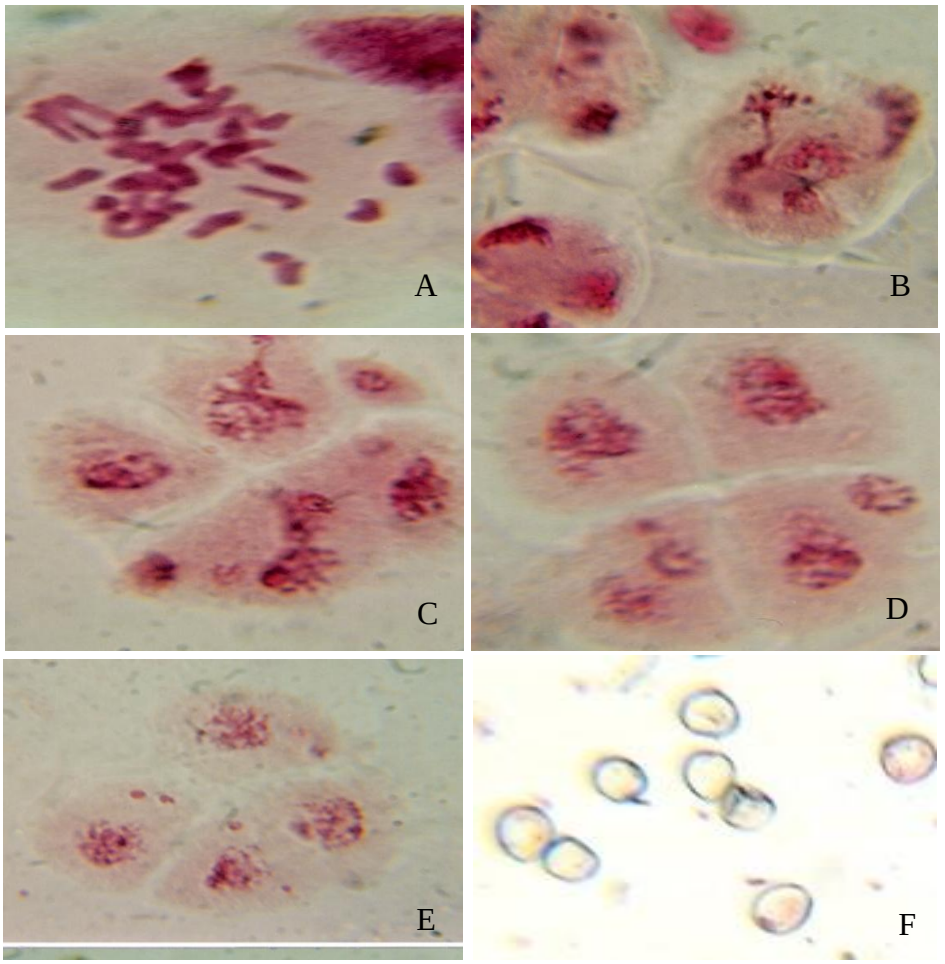

Ryc. 2. Niektóre aspekty mejozy u mieszańca *Ae. triuncialis* L. × *T. aestivum* L. Zyta (2n = 5x = 35): A) metafaza I w PMC, B) późna anafaza II z mostkami i segmentami, nieregularną cytokinezą i chromosomami opóźnionymi, C) poliada z komórkami o różnej wielkości, D) i E) tetrady z mikrojądrami, F) puste ziarna pyłku (odcinek = 45 μm)

Fig. 2. Some aspects of meiosis in *Ae. triuncialis* L. × *T. aestivum* L. Zyta hybrid (2n = 5x = 35): A) metaphase I in PMC, B) late anaphase II with bridges and segments, irregular cytokinesis and lagging chromosomes, C) polyad with cells of different sizes, D) end E) tetrads with micronuclei, F) empty pollen grains (bar = 45 μm)

W przeprowadzonych badaniach w wyniku krzyżowania wstecznego z pszenicą nie uzyskano mieszańców BC_1. Delibes i in. [1988], zapylając pszenicę tetraploidalną *T. turgidum* L. pyłkiem *Ae. triuncialis* L. uzyskali 3 rośliny mieszańcowe F_1. Następnie mieszańce F_1 zapylili pyłkiem pszenicy heksaploidalnej Almatense H-10-15, uzyskując tym

razem 8 roślin, które charakteryzowały się bardzo słabą płodnością, dając 3–5 ziaren na roślinę, bez zauważalnego wzrostu płodności w kolejnych pokoleniach. Mieszańce z *Ae. triuncialis* L. charakteryzowały się mniejszą płodnością niż z *Ae. ventricosa* Tausch. (genomy *DDUnUn*). Według cytowanych autorów genom *D Ae. ventricosa* Tausch. jest bardziej podobny do genomu *D* pszenicy heksaploidalnej niż którykolwiek z dwóch różnych genomów (*CU*) obecnych w *Ae. triuncialis* L., co może prowadzić do bardziej regularnej mejozy w pierwszym przypadku i do prawdopodobnego bardziej rozległego procesu rearanżacji chromosomów w drugim przypadku, z powodu niwelowania efektu działania genu *Ph* przez genom *C* [Delibes i in. 1988].

W badaniach Stefanowskiej i in. [1995] przy krzyżowaniu *Ae. ventricosa* Tausch. z *T. durum* Desf. Grandur zawiązywanie ziarniaków wyniosło 16,67%, a przy krzyżowaniu *Ae. juvenalis* (Tell.) Eig. (genomy *DDMMUU*) z linią pszenicy zwyczajnej CZR 1406 – 41,18%.

Gatunki *Ae. ventricosa* Tausch. (*DDUnUn*) i *Ae. juvenalis* (Tell.) Eig. (genomy *DDMMUU*) zawierają genomy *D*, które są homologiczne do genomu *D* pszenicy, podobnie jak genomy *D Ae. tauchyii* Coss. (*DD*) i *Ae. cylindrica* Host. (*DDCC*). W tych przypadkach transfer genów może odbywać się na zasadzie prostego crossing-over.

Wszystkich 15 pentaploidalnych mieszańców *A. triuncialis* L. z *T. aestivum* L. było całkowicie sterylnych. Pylniki zawierały niezabarwione ziarna pyłku (ryc. 2F). *Ae. triuncialis* L. został zaliczony przez Searsa [1981] do tej samej grupy co gatunki o niskim podobieństwie genomów do *T. aestivum* L., takie jak *Ae. umbellulata* Zhuk. (genomy *UU*) i *Ae. caudata* L., syn. *Ae. markgrafii* (Greuter) Hammer (genomy *CC*). Prawdopodobnie *Ae. triuncialis* powstał w wyniku skrzyżowania tych dwóch gatunków [Mirzaghaderi i in. 2014].

Do rozmnożenia mieszańców F_1 zastosowano również technikę hodowli tkankowej (ryc. 3 i 4). W kulturze *in vitro* może dochodzić do spontanicznego podwojenia liczby chromosomów. Warunki hodowli *in vitro* mogą również przyczynić się do translokacji pomiędzy chromosomami *Aegilops* i *Triticum*. Davies i in. [1986] podają, że rośliny pszenicy zregenerowane wegetatywnie *in vitro* z wykorzystaniem tej metody charakteryzowały się wysoką częstotliwością niehomologicznych translokacji powodujących tworzenie się multiwalentów w czasie mejozy. Feldman [1988] również obserwował obecność multiwalentów w mejozie wywołaną prawdopodobnie translokacjami u mieszańców między *T. aestivum* a amfiploidem *T. turgidum* – *Ae. squarrosa*. Mieszańce były regenerowane z kalusa pochodzącego z hodowli *in vitro* mikrospor.

W przeprowadzonych badaniach do indukcji kalusa wykorzystano niedojrzałe kwiatostany. Z kalusa wytworzonego przez eksplantaty zregenerowało 5 roślin R_1 (5,68% kalusujących eksplanatów) w kombinacji *Ae. triuncialis* L. × *T. aestivum* L. Zyta (tab. 3).

Obserwacje cytologiczne wykazały, że w chaotycznie zbudowanej tkance kalusowej pojawiały się morfogenne obszary, z których tworzyły się zawiązki organów (ryc. 3). Najpierw komórki kalusa przypominały komórki miękiszowe, a potem odróżnicowywały się, przybierając kształt komórek merystematycznych. W wyniku organogenezy na powierzchni kalusa kształtował się wierzchołek przybyszowy, w którym po pewnym czasie różnicował się zawiązek pędu z wierzchołkiem wzrostu i zaczątkami liści i (lub) zawiązek korzenia z wierzchołkiem.

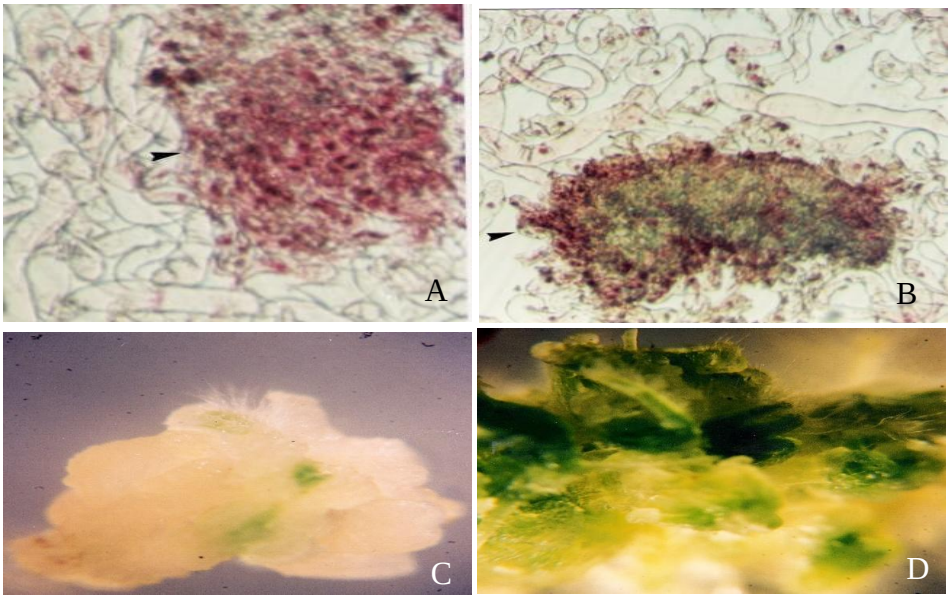

Ryc. 3. Kalus mieszańca F_1 *Ae. triuncialis* L. × *T. aestivum* L. Zyta uzyskany w kulturze *in vitro* z fragmentu kwiatostanu: A) grot wskazuje centrum merystematyczne (odcinek = 50 μm), B) grot wskazuje primordium pędu (odcinek = 100 μm), C) tkanka kalusowa z widocznymi zielonymi centrami różnicowania się zawiązków pędu (odcinek = 3 mm), D) formowanie się pędów (odcinek = 1,0 mm)

Fig. 3. Callus of the F_1 hybrid *Ae. triuncialis* L. × *T. aestivum* L. Zyta obtained in *in vitro* culture from an inflorescence fragment: A) the arrowhead indicates the meristematic center (bar = 50 μm), B) the arrowhead indicates the shoot primordium (bar = 100 μm). C) callus tissue with visible green centers of shoot primordia differentiation (bar = 3 mm), D) shoot formation (bar = 1,0 mm)

Tabela 3. Regeneracja roślin mieszańcowych R_1 w kulturze *in vitro* z fragmentów kwiatostanów F_1 *Ae. triuncialis* × *T. aestivum* L.

Table 3. Regeneration of R_1 *Ae. triuncialis* × *T. aestivum* L. hybrid plants in *in vitro* culture from flower fragments of F_1 *Ae. triuncialis* × *T. aestivum* L.

Mieszańce F_1 F_1 hybrids	Kalusujące eksplantaty na 100 wyłożonych Calloused explants per 100 placed		Zregenerowane w kalusie rośliny R_1 R_1 plants regenerated in callus	
	liczba number	%	liczba number	%
Ae. triuncialis × Begra	72	72	0	0,00
Ae. triuncialis × Monopol	84	84	0	0,00
Ae. triuncialis × Nawra	65	65	0	0,00
Ae. triuncialis × Zyta	88	88	5	5,68

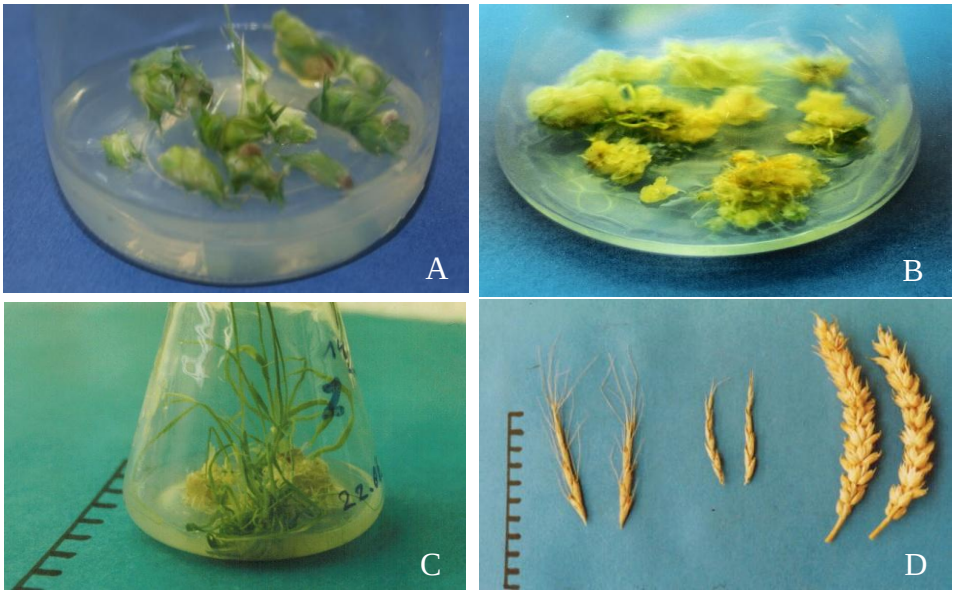

Ryc. 4. Otrzymywanie mieszańców R_1 *Ae. triuncialis* L. × *T. aestivum* L. Zyta w kulturze *in vitro*: A) eksplantaty niedojrzałych kłosów, B) i C) regeneracja pędów i korzeni w kalusie, D) kłosy roślin (od lewej): *Ae. triuncialis* L., mieszaniec R_1, *T. aestivum* L. Zyta
Fig. 4. Obtaining R_1 hybrids *Ae. triuncialis* L. × *T. aestivum* L. Zyta in *in vitro* culture: A) explants of immature spikes, B) i C) regeneration of shoots and roots in callus, D) spikes of plants (from the left): *Ae. triuncialis* L., R_1 hybrid, *T. aestivum* L. Zyta

Tworzenie się wierzchołków przybyszowych wiąże się z naruszeniem regulacji hormonalnej, w wyniku oddzielenia eksplantatu od tkanki macierzystej lub podania regulatorów wzrostu z zewnątrz, głównie auksyn i cytokinin [Hejnowicz 2002].

Kultury *in vitro* fragmentów kwiatostanów przyczyniły się do rozmnożenia mieszańców F_1 i uzyskania dojrzałych roślin R_1 *Ae. triuncialis* × Zyta (ryc. 4). Uzyskano regeneranty R_1 o liczbie chromosomów rośliny dawcy *Ae. triuncialis* L. × *T. aestivum* L. Zyta (2n = 35) – tab. 3. Pentaploidy R_1 *Ae. triuncialis* L. × *T. aestivum* L. (*ABDUC*) zawierały średnio 33,94 uniwalentów, 0,88 biwalentów w formie prętów i 0,16 biwalentów w formie pierścieni. Liczba chiazm w ich przypadku wynosiła średnio 1,22, mikrojąder w tetradach – 0,24, a liczba pentad – 19. W anafazach I i II tworzyły się mostki chromosomowe, chromatydowe i występowały fragmenty chromosomowe oraz nieprawidłowa liczba biegunów, co w konsekwencji prowadziło do powstawania pentad (tab. 2, ryc. 2).

W mieszańcach *Ae. triuncialis* L. × *T. aestivum* L. Zyta analizowano żywotność pyłku i porównywano ją z żywotnością form rodzicielskich. Ziarna pyłku mieszańców F_1 okazały się w 100% puste, a mieszańców R_1 w 94,70%. Natomiast 90,75% ziaren pyłku *Ae. triuncialis* L. i 91,80% pszenicy Zyta było całkowicie wypełnione cytoplazmą (tab. 4). Ziarna pyłku mieszańców F_1 miały wielkość od 44,18 × 40,34 μm (mieszaniec F_1 *Ae. triuncialis* L. z pszenicą Begra) do 45,51 × 41,23 μm (mieszaniec F_1 *Ae. triuncialis* L. z pszenicą Zyta). Mieszaniec R_1 *Ae. triuncialis* L. × Zyta miał ziarna pyłku nieco większe:

46,96 × 41,12 μm. Średnia wielkość ziaren pyłku *Ae. triuncialis* L. wyniosła 51,80 × 47,60 μm. Największe ziarna pyłku miała pszenica Zyta 62,29 × 54,86 μm. W badaniach Chrząstek [2000] wielkość ziaren pyłku pszenicy Grana wyniosła 56,87 × 56,19 μm.

Pylniki mieszańców F_1 miały wielkość od 4,51 × 0,85 mm (mieszaniec F_1 *Ae. triuncialis* L. × Begra) do 4,68 × 0,89 mm (mieszaniec F_1 *Ae. triuncialis* L. × Zyta) – tab. 4.

Mieszaniec R_1 *Ae. triuncialis* L. z pszenicą Zyta miał pylniki nieco większe: 4,73 × 0,86 mm. Średnia wielkość pylników *Ae. triuncialis* L. wyniosła 5,10 × 0,87 mm. Pylniki pszenicy Zyta miały średnią wielkość 4,46 × 0,94 mm (tab. 4). W badaniach Komaki i Tsunewaki [1981] długość pylników 61 odmian pszenicy wahała się od 3,0 do 5,0 mm.

Gatunki traw z rodzaju *Aegilops* należą do form jednorocznych, silnie krzewiących się, wytwarzających bardzo dużo ziarniaków. Przykładowo *Ae. cylindrica* Host wytwarza ponad 100 źdźbeł i ponad 3 tys. ziarniaków. Ziarniaki *Aegilops* pozostają w glebie nawet do 3–5 lat, zachowując zdolność kiełkowania, co pozwala poszczególnym populacjom szybko kolonizować nowe tereny [Zaharieva i Monneveux 2005].

Pszenice krzewią się znacznie słabiej. Analiza pojedynków wykazała, że najwięcej pędów wytworzył dziki gatunek *Ae. triuncialis* – średnio 146,5 na roślinę. Krzewienie mieszańców było pośrednie. Najwięcej pędów wytworzyły mieszańce F_1 i R_1 *Ae. triuncialis* × Zyta, odpowiednio 41,0 i 36,3. Najmniej pędów (średnio 15,0 na roślinę) odnotowano u mieszańców F_1 *Ae. triuncialis* × Monopol. Była to wartość podobna jak u pszenic zwyczajnych. Pszenice wytwarzały średnio od 9,1 (Nawra) do 14,3 (Monopol) pędów na roślinę (tab. 5).

Długość pędu głównego mieszańców była mniejsza od długości pędów obu komponentów rodzicielskich i wynosiła średnio od 43,0 cm (F_1 *Ae. triuncialis* × Nawra) do 48,3 cm (F_1 *Ae. triuncialis* × Begra). Były to wartości istotnie mniejsze od długości pędów dzikiego gatunku (70,4 cm) i od pszenic (79,78–100,80 cm) – tab. 5. Podobnie w środowisku naturalnym gatunki *Aegilops* osiągają wysokość ok. 70 cm [Kimber i Feldman 1987].

Średnica zewnętrzna drugiego od dołu międzywęźla mieszańców mieściła się w granicach od 2,1 do 2,9 mm. Była ona istotnie większa od średnicy dzikiego gatunku (1,46 mm). Wśród mieszańców najgrubsze źdźbła miał F_1 *Ae. triuncialis* × Zyta. U pszenic wartość tej cechy była istotnie większa od mieszańców i wahała się od 4,08 do 5,22 mm (tab. 5).

Większość mieszańców F_1 wytworzyła osadki kłosowe istotnie krótsze od osadek form rodzicielskich. Najdłuższe osadki kłosowe o długości od 0,90 do 0,99 dm odnotowano u pszenic. Nieco krótsze osadki kłosowe miał *Ae. triuncialis*. Osadki kłosowe mieszańców osiągały średnią długość 0,55–0,68 dm (tab. 5, ryc. 1C, 1D, 4D).

Kształt dojrzałych kłosów mieszańców był pośredni w stosunku do form rodzicielskich. Jednak przeważały cechy formy dzikiej (ryc. 1C, 1D, 4D). Największą liczbę kłosków przypadających na 1 dm osadki kłosowej (zbitość kłosa) miały pszenice (od 19,4 do 24,4). Mieszańce charakteryzowały się pośrednią w porównaniu z komponentami rodzicielskimi zbitością kłosów (od 14,6 do 17,5 kłosków na 1 dm osadki kłosa). Zbitość kłosów *Ae. triuncialis* wyniosła 7,5 (tab. 5). We wcześniejszych badaniach [Prażak 1997] kłosy innych mieszańców *Aegilops* sp. z *Triticum* sp. również charakteryzowały się pośrednią zbitością w stosunku do form rodzicielskich.

Tabela 4. Żywotność oraz wymiary ziaren pyłku i pylników mieszańców F_1 i R_1 *Ae. triuncialis* L. z *T. aestivum* L. i *T. aestivum* L. Zyta
Table 4. Viability and dimensions of pollen grains and anthers of F_1 and R_1 hybrids of *Ae. triuncialis* L. with *T. aestivum* L. and *T. aestivum* L. Zyta

Analizowane formy Forms analysed	Ziarna pyłku wypełnione cytoplazmą Pollen grains filled with cytoplasm (%)			Wymiary ziaren pyłku wypełnionych cytoplazmą Dimensions of pollen grains filled with cytoplasm (μm)						Wymiary pylników Anther dimensions (mm)	
				całkowicie entirely		częściowo partly		puste empty			
	całkowicie entirely	częściowo partly	puste empty	długość length	szerokość width	długość length	szerokość width	długość length	szerokość width	długość length	szerokość width
F_1 *Ae. triuncialis* × Begra	0,00	0,00	100,00	0,00	0,00	0,00	0,00	44,18^{fm}	40,34^{fm}	4,51^{f}	0,85
F_1 *Ae. triuncialis* × Monopol	0,00	0,00	100,00	0,00	0,00	0,00	0,00	44,29^{fm}	40,45^{fm}	4,53^{f}	0,86
F_1 *Ae. triuncialis* × Nawra	0,00	0,00	100,00	0,00	0,00	0,00	0,00	45,42^{fm}	41,16^{fm}	4,62^{fm}	0,88
F_1 *Ae. triuncialis* × Zyta	0,00	0,00	100,00	0,00	0,00	0,00	0,00	45,51^{fm}	41,23^{fm}	4,68^{fm}	0,89
R_1 *Ae. triuncialis* × Zyta	0,00	5,30	94,70	0,00^{fm}	0,00	50,85^{m}	44,32^{m}	46,96^{fm}	41,12^{fm}	4,73^{fm}	0,86
Ae. triuncialis	90,75	3,08	6,17	52,00	46,50	44,83	41,00	51,80	47,60	5,10	0,87
Zyta	91,80	1,19	7,01	67,53	64,08	61,57	56,71	62,29	54,86	4,46	0,94

^{f} Wynik istotnie różny od formy matecznej przy $\alpha = 0,05$; ^{m} wynik istotnie różny od formy ojcowskiej przy $\alpha = 0,05$
^{f} Result significantly different from the mother form at $\alpha = 0.05$; ^{m} result significantly different from the paternal form at $\alpha = 0.05$

Tabela 5. Wartości średnie wybranych cech ilościowych u mieszańców F_1 i R_1 *Ae. triuncialis* L. × *T. aestivum* L. oraz ich form rodzicielskich
Table 5. Mean values of some quantitative traits in F_1 and R_1 *Ae. triuncialis* L. × *T. aestivum* L. hybrids and their parental forms

Analizowane formy Forms analysed	Liczba roślin Number of plants	Krzewienie ogólne Total tillering[1]	Długość pędu głównego Length of main shoot (cm)	Średnica drugiego od dołu międzywęźla Diameter of 2nd bottom internode (mm)	Długość osadki kłosowej Length of spike rachis (dm)	Zbitość kłosa głównego Main spike density[2]	Płodność kłosa głównego Main spike fertility[3]
F_1 *Ae. triuncialis* × Begra	4	22,50 [f]	48,30 [fm]	2,35 [fm]	0,68 [m]	15,60 [fm]	0,00 [fm]
F_1 *Ae. triuncialis* × Monopol	5	15,00 [f]	46,00 [fm]	2,50[m]	0,60 [fm]	16,70 [fm]	0,00 [fm]
F_1 *Ae. triuncialis* × Nawra	3	34,00 [f]	43,00 [fm]	2,10[m]	0,55 [fm]	14,60 [fm]	0,00 [fm]
F_1 *Ae. triuncialis* × Zyta	3	41,00 [f]	48,00 [fm]	2,90 [fm]	0,63 [m]	17,50 [fm]	0,00 [fm]
R_1 *Ae. triuncialis* × Zyta	5	36,30 [fm]	46,50 [fm]	2,43 [fm]	0,56 [fm]	14,60 [fm]	0,00 [fm]
Ae. triuncialis	20	146,50	70,40	1,46	0,77	7,50	1,69
Begra	20	12,10	86,50	4,08	0,93	21,10	2,66
Monopol	20	14,30	100,80	4,43	0,90	24,40	2,75
Nawra	20	9,10	79,78	4,62	0,94	20,00	2,16
Zyta	20	12,50	99,88	5,22	0,99	19,40	2,48

[1] liczba pędów z rośliny, [2] liczba kłosków przypadająca na 1 dm osadki kłosa, [3] liczba ziaren przypadająca na 1 kłosek
[f] wynik istotnie różny w stosunku do formy żeńskiej przy $\alpha = 0,05$; [m] wynik istotnie różny w stosunku do formy męskiej przy $\alpha = 0,05$
[1] numer of shoots from plant, [2] number of spikelets per 1 dm of the spike rachis, [3] number of kernels per 1 spikelet
[f] result significantly different in relation to the female form at $\alpha = 0.05$; [m] result significantly different in relation to the male form at $\alpha = 0.05$

Mieszańce nie zawiązały ziarniaków. Natomiast płodność kłosów głównych pszenic wahała się od 2,16 (Nawra) do 2,75 (Monopol). Płodność dzikiego gatunku *Ae. triuncialis* wyniosła 1,69. Słaba płodność mieszańców F_1 pszenicy z gatunkami *Aegilops* wynika z niskiego poziomu koniugacji chromosomów w mejozie lub jej braku [Bai i in. 1994].

Dla zwiększenia płodności form mieszańcowych można zastosować wcześniejsze krzyżowanie *Ae. triuncialis* L. z pszenicami tetraploidalnymi, np. *T. turgidum* L. lub *T. durum* Desf. jako formami pomostowymi [Delibes i in. 1988, Stefanowska i in. 1995]. Inną metodą może być krzyżowanie pszenicy zwyczajnej *T. aestivum* L. mono-*5B* Chinese Spring z *Ae. triuncialis* L., a następnie powstałego mieszańca z *T. aestivum* Chinese Spring [Pilch i in. 1995]. Jeżeli chromosom obcy nie jest homeologiczny do chromosomów pszenicy i nie może z nimi koniugować w mieszańcach pomostowych F_1, można zastosować metody radiacji w celu spowodowania jego fizycznej aktywacji, a następnie w pokoleniu F_2 identyfikować translokacje z obcym chromosomem [Pilch 2005].

WNIOSKI

1. Przy krzyżowaniach odwrotnych *Ae. triuncialis* L. z odmianami pszenicy zwyczajnej Begra, Monopol, Nawra i Zyta ziarniaki mieszańcowe uzyskano jedynie przy zapyleniu *Ae. triuncialis* L. pyłkiem *T. aestivum* L. Średnia zdolność do krzyżowania wyniosła 10,0%, a regeneracja roślin z 18-dniowych zarodków F_1 hodowanych *in vitro* – 78,95%.

2. Wyłożenie fragmentów niedojrzałych kłosów na pożywkę MS z dodatkiem 2,0 $mg \cdot dm^{-3}$ 2,4-D przyczyniło się do uzyskania tkanki kalusowej mieszańców F_1 *Ae. triuncialis* z *Triticum aestivum* L. Najbardziej embriogenny okazał się kalus mieszańców F_1 *Ae. triuncialis* × *T. aestivum* L. Zyta, w którym zregenerowały pędy i korzenie roślin R_1.

3. W porównaniu do form rodzicielskich mieszańce *Ae. triuncialis* z *T. aestivum* L. miały pośrednią liczbę pędów (15,0–41,0), średnicę drugiego od dołu międzywęźla (2,1–2,9 mm) i zbitość kłosa (14,6–17,5 kłosków na 1 dm osadki kłosa) oraz krótsze źdźbła (43,0–48,3 cm) i osadki kłosowe (0,55–0,68 dm). Brak płodności mieszańców F_1 i R_1 oraz brak skuteczności krzyżowań wstecznych BC_1 z pszenicą był spowodowany zaburzeniami w procesie mejozy, które wynikały ze słabej homologii pomiędzy genomami *ABD* pszenicy zwyczajnej i genomami *UC Ae. triuncialis* L.

PIŚMIENNICTWO

Aghaee-Sarbarzeh M., Ferrahi M., Singh S. i in., 2002. PhI-induced transfer of leaf and stripe rust-resistance genes from *Aegilops triuncialis* and *Ae. geniculata* to bread wheat. Euphytica 127, 377–382. https://doi.org/10.1023/A:1020334821122

Aghaee-Sarbarzeh M., Singh H., Dhaliwal H.S., 2008. A microsatellite marker linked to leaf rust resistance transferred from *Aegilops triuncialis* into hexaploid wheat. Plant Breed. 120(3), 259–261. https://doi.org/10.1046/j.1439-0523.2001.00598.x

Aigner P.A., Woerly R.J., 2011. Herbicides and mowing to control barb goatgrass (*Aegilops triuncialis*) and restore native plants in serpentine grasslands. Invas. Plant Sci. Manag. 4(4), 448–457. https://doi.org/10.1614/IPSM-D-11-00027.1

Arzani A., Ashraf M., 2016. Smart engineering of genetic resources for enhanced salinity tolerance in crop plants. Crit. Rev. Plant Sci. 35, 146–189. https://doi.org/10.1080/07352689.2016.1245056

Bai D., Scoles G.J., Knott D.R., 1994. Transfer of leaf rust and stem rust resistance genes from *Triticum triaristatum* to durum and bread wheats and their molecular cytogenetic localization. Genome 37(3), 410–418. https://doi.org/10.1139/g94-058

Bocianowski J., Prażak R., 2022. Genotype by year interaction for selected quantitative traits in hybrid lines of *Triticum aestivum* L. with *Aegilops kotschyi* Boiss. and *Ae. variabilis* Eig. using the additive main effects and multiplicative interaction model. Euphytica 218(11). https://doi.org/10.1007/s10681-022-02967-4

Chrząstek M., 2000. Wpływ dodanych i podstawionych chromosomów żyta (*Secale cereale* L.) cv. Dańkowskie Złote na mejozę oraz niektóre cechy morfologiczne i fizjologiczne pszenicy (*Triticum aestivum* L.) ev. Grana. Rozprawa habilitacyjna. Rozprawy Naukowe Akademii Rolniczej w Lublinie 242. Wyd. AR w Lublinie, Lublin.

Chueca M., Cauderon Y., Tempe J., 1977. Techniques d'obtention d'hybrides Blé tender × *Aegilops* par culture *in vitro* d'embryons immatures. Ann. Amélior. Plantes 27(5), 539–547.

Darko E., Khalil R., Dobi Z. i in., 2020. Addition of *Aegilops biuncialis* chromosomes 2M or 3M improves the salt tolerance of wheat in different way. Sci. Rep. 10(22327). https://doi.org/10.1038/s41598-020-79372-1

Davies P.A., Pallota M.A., Ryan S.A. i in., 1986. Somaclonal variation in wheat: genetic and cytogenetic characterization of alcohol dehydrogenase 1 mutants. Theor. Appl. Genet. 72, 644–653.

Delibes A., López-Braña I., Mena M. i in., 1988. Introgression of *Aegilops triuncialis* into *Triticum aestivum*. A progress report. An. Aula Dei 19(1–2), 189–194.

Fakhri Z., Mirzaghaderi G., Ahmadian S. i in., 2016. Unreduced gamete formation in wheat × *Aegilops* interspecific hybrids is genotype specific and prevented by shared homologous subgenomes. Plant Cell Rep. 35, 1143–1154. https://doi.org/10.1007/s00299-016-1951-9

Feldman M., 1988. Cytogenetic and molecular approaches to alien gene transfer in wheat. Proc. of the Seventh Int. Wheat Genet. Symp. 1, 23–32.

Feldman M., Levy A.A., 2023. *Aegilops* L. W: M. Feldman, A.A. Levy, Wheat evolution and domestication. Springer Nature Link Berlin, Heidelberg, 213–364.

Hadzhiivanova B., Taneva K., Bozhanova V. i in., 2025. Evaluation of yield and quality of advanced durum wheat lines obtained by the distant hybridization method. Bulg. J. Agric. Sci. 62(1), 3–16. https://doi.org/10.61308/CJNU6516

Hejnowicz Z., 2002. Anatomia i histogeneza roślin naczyniowych. Organy wegetatywne. Wyd. Nauk. PWN, Warszawa.

Ijazl M., Afzal A., Shabbir G. i in., 2023. Breeding wheat for leaf rust resistance: past, present and future. Asian J. Agric. Biol. 1, 1–16. https://doi.org/10.35495/ajab.2021.426

Karagoz A., 2006. Hybridization in Turkish *Aegilops* L. Species. Pak. J. Biol. Sci. 9(12), 2243–2248. https://doi.org/10.3923/pjbs.2006.2243.2248

Kiani R., Arzani A., Mirmohammady Maibody S., 2021. Polyphenols, flavonoids, and antioxidant activity involved in salt tolerance in wheat, *Aegilops cylindrica* and their amphidiploids. Front Plant Sci. 12, 493. https://doi.org/10.3389/fpls.2021.646221

Kimber G., Feldman M., 1987. Wild wheat: an introduction. Special Report 35. College of Agriculture, University of Missouri, Columbia, 1–146. https://hdl.handle.net/10355/57430

Komaki M.K., Tsunewaki K., 1981. Genetic studies on the difference of anther length among common wheat cultivar. Euphytica 30, 45–53. https://doi.org/10.1007/BF00033658

Laugerotte J., Baumann U., Sourdille P., 2022. Genetic control of compatibility in crosses between wheat and its wild or cultivated relatives. Plant Biotechnol. J. 20(5), 812–832. https://doi.org/10.1111/pbi.13784

Martín-Sánchez J.A., Gómez-Colmenarejo M., Del Moral J. i in., 2003. A new Hessian fly resistance gene (*H30*) transferred from the wild grass *Aegilops triuncialis* to hexaploid wheat. Theor. Appl. Genet. 106(7), 1248–1255. https://doi.org/10.1007/s00122-002-1182-z

Mirzaghaderi G., Abdolmalaki Z., Ebrahimzadegan R. i in., 2020. Production of synthetic wheat lines to exploit the genetic diversity of emmer wheat and D genome containing *Aegilops* species in wheat breeding. Sci. Rep. 10, 19698. https://doi.org/10.1038/s41598-020-76475-7

Mirzaghaderi G., Houben A., Badaeva E.D., 2014. Molecular-cytogenetic analysis of *Aegilops triuncialis* and identification of its chromosomes in the background of wheat. Mol. Cytogenet. 7(1), 91. https://doi.org/10.1186/s13039-014-0091-6

Murashige T., Skoog F., 1962. A revised medium for rapid growth and bioassay with tobacco tissue cultures. Physiol. Plant. 15, 473–497.

Pilch J., 2005. Możliwości wykorzystania krzyżowania introgresywnego w hodowli pszenicy ozimej *Triticum aestivum* L. Część I. Zastosowanie systemów genetycznych pszenicy *T. aestivum* L. do otrzymania mieszańców pomostowych F_1. Biul. IHAR 235, 31–41. https://doi.org/10.37317/biul-2005-0059

Pilch J., Głowacz E., Kubara-Szpunar Ł. I in., 1995. Mieszance oddalone *Triticum aestivum* L. jako źródła odporności na choroby kłosa. Biul. IHAR 194, 159–167.

Prażak R., 1996. Somatic embryogenesis and plant regeneration of common wheat *Triticum aestivum* L. J. Appl. Genet. 37A, 246–248.

Prażak R., 1997. Charakterystyka morfologiczna mieszańców F_1 *Triticum aestivum* L. i *Triticum durum* Desf. z wybranymi gatunkami *Aegilops* sp. Biul. IHAR 204, 33–42.

Prażak R., 2001. Cross direction for successful production of F_1 hybrids between *Triticum* and *Aegilops* species. Plant Breed. Seed Sci. 45(1), 83–86.

Prażak R., Krzepiłko A., 2018. Evaluation of iron and zinc content in grain of *Aegilops* L. × *Triticum aestivum* L. hybrid lines. J. Elem. 23(2), 545–557. https://doi.org/10.5601/jelem.2017.22.3.1486

Prażak R., Molas J., 2017. Ocena jakości ziarna linii mieszańcowych *Aegilops* L. × *Triticum aestivum* L. Pol. J. Agron. 29, 35–42.

Sears E.R., 1981. Transfer of alien genetic material to wheat. W: L.T. Evans, W.J. Peacock (red.). Wheat science – today and tomorrow. Cambridge University Press, Cambridge, 75–89.

Stefanowska G., Prażak R., Strzembicka A. i in., 1995. Transfer genów z *Aegilops ventricosa* Tausch. i *Aegilops juvenalis* (Thell) Eig. do *Triticum aestivum* L. Biul. IHAR 194, 45–52.

Wang X., Yoo E., Lee S. i in., 2022. Classification of 17 species *Aegilops* using DNA barcoding and SNPs, reveals gene flow among *Aegilops biuncialis*, *Aegilops juvenalis*, and *Aegilops columnaris*. Front. Plant Sci. 13, 984825. https://doi.org/10.3389/fpls.2022.984825

Yildiz M., Terzi H., Arikan E.S., 2006. Seed germination of populations of wild wheat species, *Aegilops biuncialis* and *Ae. triuncialis*: effects of salinity, temperature and photoperiod. Pak. J. Biol. Sci. 9(7), 1299–1305.

Zaharieva M., Monneveux P., 2005. Spontaneous hybridization between bread wheat (*Triticum aestivum* L.) and its wild relatives in Europe. Crop Sci. 46(2), 512–527.

Zhao L., Ning S., Yi, Y. i in., 2018. Fluorescence *in situ* hybridization karyotyping reveals the presence of two distinct genomes in the taxon *Aegilops tauschii*. BMC Genomics 19(3), 1–9. https://doi.org/10.1186/s12864-017-4384-0

Źródło finansowania: Instytut Genetyki, Hodowli i Biotechnologii Roślin, Uniwersytet Przyrodniczy w Lublinie, SUBB.WRH.19.024.

Abstract. Field crosses were performed between *Aegilops triuncialis* L. (2n = 4x = 28, *UUCC* genomes) and the common wheat cultivars *Triticum aestivum* L. (2n = 6x = 42, *AABBDD* genomes) Begra, Monopol, Nawra, and Zyta. The aim of the crosses was to expand the genetic variability of common wheat. The interbreeding ability of tested genotypes under field conditions ranged from 7.14% (*Ae. triuncialis* × Zyta) to 13.33% (*Ae. triuncialis* × Monopol). Hybrid kernels were formed only when the maternal form was *Ae. triuncialis*. From obtained 22 F_1 hybrid kernels, 19 embryos were isolated *in vitro* and plated on MS medium supplemented with 10 mg dm^{-3} IAA (β-indolyl--3-acetic acid) and 0.04 mg dm^{-3} kinetin. F_1 embryos developed into 15 seedlings *in vitro*. After

4 weeks, the hybrid seedlings were transplanted into pots and placed in a growth chamber. Then, in mid-September, they were planted out in the experimental field next to the parental components. Chromosome number of the hybrids were assessed on smear preparations of meristematic cells from the seedling root tips. During the growing season, immature spikes were collected from the leaf sheaths of the hybrid plants for meiosis analysis. Cytological analysis revealed abnormalities in the microsporogenesis process of the hybrids, which resulted in the development of non-viable pollen. Some spikes of the F_1 hybrids were castrated and back-pollinated with wheat pollen. The F_1 hybrids were also propagated *in vitro* by placing 100 fragments of immature inflorescences in each cross combination on MS medium supplemented with 2 mg dm^{-3} 2.4-D (2.4-dichlorophenoxyacetic acid). Five R_1 plants in the *Ae. triuncialis* L. × *T. aestivum* L. Zyta combination were regenerated from callus produced by the explants. At the full maturity stage, biometric traits such as general tillering, main shoot length, diameter of the second internode from the bottom, length of the main spike rachis, main spike density and main spike fertility were measured on F_1 and R_1 hybrid plants. The hybrids were characterized by intermediate tillering (15.0–41.0 stems) compared to their parental forms, a diameter of the second internode from the bottom (2.1–2.9 mm), a dense main spike (14.6–17.5), shorter stems (43.0–48.3 cm) and spike rachis (0.55–0.68 dm), and sterile spikes.

Keywords: *Aegilops triuncialis* L., field traits, common wheat, *in vitro* cultures, intergeneric hybrids

Otrzymano/Received: 28.07.2025
Zaakceptowano/Accepted: 9.10.2025
Opublikowano/Published: 31.12.2025

AGRONOMY SCIENCE

VOL. LXXX (4) 2025

CC BY

https://doi.org/10.24326/as.2025.5594

Department of Genetics and Horticultural Plant Breeding, Institute of Plant Genetics, Breeding and Biotechnology, University of Life Sciences in Lublin, Akademicka 15 Street, 20-950 Lublin, Poland

* e-mail: magdalena.dyduch@up.lublin.pl

JACEK GAWROŃSKI[1] https://orcid.org/0000-0001-9342-5005

MAGDALENA DYDUCH-SIEMIŃSKA[1]* https://orcid.org/0000-0002-6549-7391

Molecular identification and genetic diversity assessment of *Mentha* genotypes using SCoT and ISSR DNA markers

Identyfikacja molekularna i ocena zróżnicowania genetycznego genotypów mięty z wykorzystaniem markerów DNA – SCoT i ISSR

Abstract. The aim of this study was to molecularly identify and assess the genetic diversity of 12 *Mentha* genotypes using, for the first time, two types of DNA markers simultaneously – ISSR (inter simple sequence repeats) and SCoT (start codon targeted). Selected genotypes representing various *Mentha* species and varieties were analyzed to determine the level of genetic similarity and phylogenetic relationships between them. The level of polymorphism obtained for ISSR markers was 71%, while for SCoT it was 88.7%. The obtained data were analyzed, allowing for the assessment of the level of genetic similarity and the construction of dendrograms illustrating the genetic structure of the studied population. Studies indicate that the use of SCoT markers enables the identification of the following genotypes: *Plectranthus amboinicus* (Lour.) Spreng, *Mentha pulegium* L., *Mentha spicata* L. cv. Moroccan, *Mentha suaveolens* Ehrh. var. *variegata* (pineapple mint), *Mentha spicata* L., and *Mentha longifolia* L. ISSR markers, due to the generation of only monomorphic and polymorphic bands, do not allow for the direct identification of any of the studied genotypes. Data from both marker systems indicate significant genetic diversity among the analyzed genotypes, which may be important for breeding programs and the conservation of genetic resources of the *Mentha* genus.

Keywords: DNA polymorphism, genetic diversity ISSR *Mentha*, molecular markers, SCoT, UPGMA methods

Citation: Gawroński J., Dyduch-Siemińska M., 2025. Molecular identification and genetic diversity assessment of *Mentha* genotypes using SCoT and ISSR DNA markers. Agron. Sci. 80(4), 23–37. https://doi.org/10.24326/as.2025.5594

INTRODUCTION

The family *Lamiaceae*, representing the sixth largest group among angiosperms, comprises over 245 genera and approximately 7,886 species with a cosmopolitan distribution. Members of this family are characterized by a high content of essential oils and a wide diversity of secondary metabolites. Owing to these phytochemical properties, numerous *Lamiaceae* species have significant applications in traditional and modern medicine, pharmacology, cosmetics, and aromatherapy, as well as in horticulture for their ornamental and aromatic value [Sofyalıoğlu et al. 2025]. The genus *Mentha*, belongs to the *Lamiaceae* includes more than a dozen wild species and numerous hybrids and cultivated varieties with diverse functional properties [Silva et al. 2006, Mkaddem et al. 2009] and is one of the most important genera with approximately 30 identified species distributed in Europe, Asia, America, Australia, and temperate regions [Dorman et al. 2013]. The systematics of the genus *Mentha* is very complex and still not fully unified. Predisposition of mint to open pollination between wild and cultivated varieties have contributed to the development of numerous cultivars and interspecific hybrids [Jędrzejczyk and Rewers 2018]. The chromosome number in plants of the genus *Mentha* is usually x = 12, but it varies depending on the species and may be: monoploid (basic) number: x = 9, x = 10, x = 12, x = 18, x = 25; while the ploidy level (2n) may be equal to: 2x, 4x, 6x, 8x, 10x [Lawrence 2006]. Within this genus, in addition to variability in the basic chromosome number, polyploidy, and aneuploidy, there is also polymorphism in morphology, the composition of essential oils, and secondary metabolites, depending on the environmental conditions in which the plants are grown. Therefore, morphological, biochemical markers, and even karyological analysis are often unreliable in distinguishing *Mentha* species [Jędrzejczyk and Rewers 2018]. Because, as Devi et al. [2022] report the genus *Mentha* has undergone frequent interspecific hybridization between wild and cultivated populations, which leads to varying basic chromosome count. To distinguish genotypes, DNA markers should be used. In the case of the studied species, the diversity analysis was performed using SRAP [Malik et al. 2019], ISSR [Smolik et al. 2007, Rodrigues et al. 2013, Jędrzejczyk and Rewers 2018, Choupani et al. 2019, Soilhi et al. 2020, Moshrefi-Araghi et al. 2021, Devi et al. 2022, Çelik et al. 2024], RAPD [Khanuja et al. 2000, Ibrahim 2017, Kiełtyka-Dadasiewicz et al. 2017, Ahmad et al. 2018, Panjeshahin et al. 2018], SSR [Vining et al. 2019, Fukui et al. 2022], SCoT [Khan et al. 2017, Salama et al. 2019, Heylen et al. 2021] markers. Molecular marker techniques generate reliable and reproducible results without being influenced by environmental factors. In the analysis of genetic similarity, it is recommended to use two types of primers to scan a large area of the genome. SCoT exploits the gene regions flanking the ATG initiation codon [Collard and Mackill 2009], while ISSR markers can amplify the flanking regions of the target microsatellite [Sabboura et al. 2016]. Therefore, in this study, for the first time, the ISSR and SCoT marker systems were used simultaneously for the studied set of genotypes. Information on the genetic diversity and relationships among different species in *Mentha* genus may produce new insights and give a better understanding of the distribution of genetic diversity and is necessary for germplasm collection, conservation and breeding program. The aim of this study was to conduct molecular identification of various mint genotypes. Molecular analyses were conducted to develop rapid and precise species identification, determine interspecific and intraspecific variability within the genus, and describe relationships between genotypes.

MATERIALS AND METHODS

DNA extraction

Samples of healthy leaves from 10 randomly selected plants grown at the Experimental Farm of the Department of Vegetable and Medicinal Plants of the University of Life Sciences in Lublin (51°14'53"N, 2°34'13"E) were collected. DNA was isolated in two replications, for every listed in table 1 genotypes. DNA was extracted following the CTAB method described by Doyle and Doyle [1987]. The DNA concentration was determined using Thermo Scientific Nanodrop spectrophotometer. Test samples were diluted to a final concentration 25 ng μl^{-1}.

Table 1. The list of genotypes

Species	Code
Mentha suaveolens Ehrh. var. *variegata* (pineapple mint)	G1
Mentha suaveolens Ehrh.	G2
Mentha pulegium L.	G3
Mentha longifolia L.	G4
Plectranthus amboinicus (Lour.) Spreng. (Mexican mint)	G5
Mentha piperita L. var. *officinalis* Sole f. *rubescens* Camus	G6
Mentha spicata L.	G7
Mentha spicata var. *crispa* cv. Persian	G8
Mentha spicata L. cv. Moroccan	G9
Mentha rotundifolia L. Huds.	G10
Mentha piperita L. var. *citrata* Ehrh.	G11
Mentha spicata L. var. *crispa*	G12

ISSR analysis

A total of 30 ISSR primers (Sigma-Aldrich) were initially screened, of which 13 produced clear, reproducible banding patterns. These primers were selected for subsequent analyses. PCR amplification was performed in a final reaction volume of 15 µL, containing 130 µM dNTPs, 1.5 mM $MgCl_2$, 1 U of Taq DNA polymerase, 1× reaction buffer, 470 pM primer, and 60 ng of genomic DNA. Amplification reactions were carried out in a gradient thermal cycler (Biometra GmbH) using the following program: an initial denaturation step at 94°C for 7 min; followed by 35 cycles of denaturation at 94°C for 30 s, primer annealing at the primer-specific annealing temperature (Tm) for 30 s, and extension at 72°C for 2 min; with a final extension step at 72°C for 7 min.

SCoT analysis

Fifteen 18-base primers selected from 25 arbitrary primers were used for PCR amplification. DNA amplification of SCoT markers was carried out in a final volume of 10 µl containing 0.5 U of Taq DNA Polymerase (Fermentas), 0.8 µl of oligonucleotide primer (0.8 µM), 1 µM dNTPs, 1 × PCR buffer with $MgCl_2$, and 25 ng of genomic DNA as a template. Amplification was performed in a gradient thermal cycler (Biometra GmbH) with the following reaction conditions: initial predenaturation at 94°C for 3 min, followed by 35 denaturation cycles at 94°C for 1 min, annealing at 50°C for 1 min, and extension at 72°C for 2 min. The final extension was carried out for 5 min at 72°C with the holding temperature of 4°C.

DNA data analysis

PCR products were separated on 1.5% agarose gels stained with ethidium bromide and electrophoresed at a constant voltage of 3 V cm^{-1} until the bromophenol blue tracking dye reached the end of the gel. The gel was visualized in a UV transilluminator and photographed using GeneSnap ver. 7.09 (SynGene) gel documentation system. NZYDNA Ladder III (NZYtech; ISSR) and MassRuler DNA Ladder Mix (Thermo Scientific; SCoT) were used to establish molecular weight of the products. ISSR and SCoT amplification products that were clearly distinguishable and reproducible were scored. Bands were recorded in a binary format: presence (1) or absence (0). A band was considered monomorphic if it was present in all analyzed individuals. Polymorphic bands were those observed only in specific genotypes, while specific bands referred to those uniquely present in a single individual. The unique combination of bands produced by each primer was defined as its banding pattern.

Statistical analysis

The similarity coefficient between the studied genotypes in the ISSR and SCoT analysis was assessed according to the Dice formula [Nei 1979]. Cluster analysis was conducted using the UPGMA (unweighted pair-group method with arithmetic mean) distance method implemented in the PAST software [Hammer 2001]. PAST software was also used for the principal component analysis (PCA).

RESULTS AND DISCUSSION

ISSR-PCR amplification

In this study, a total of 136 allelic bands were detected that could be assessed using 13 different ISSR markers in 12 *Mentha* genotypes. Of these, 97 were found to be polymorphic, representing 71 percent polymorphism. Thirty-nine monomorphic bands were also detected, representing an average of three bands per primer. Primer ISSR12 generated the maximum number of bands (14), while primers ISSR3 and ISSR8 generated the minimum number (8). Band sizes ranged from 350 to 3800 bp (tab. 2). No specific bands were identified in the sample. Therefore, the marker sequences used in the study did not allow identification of any of the studied genotypes. However, according to Jędrzejczyk and

Rewers [2018], ISSR markers are useful in identifying *Mentha* species. The ISSR markers used by Çelik et al. [2024] to analyze various mint genotypes generated 100% polymorphic bands, which, similarly to our study, make identification impossible. In the study by Sabbour et al. [2016], no specific bands were identified. The primers used generated only polymorphic bands. The studies by the cited authors show significant differences in the average number of bands generated by primer, which in the case of the first author was 17.5 and the second 3.42. Our results are situated between these values (10.5). This may be due to the sequence of markers used and the genetic diversity of the plant material analyzed. The average polymorphism of 71% obtained in our study should be considered moderate, especially in the context of the study by Çelik et al. [2024], where it reached 100%. However, it was higher compared to the value of 65% reported by Choupani et al. [2019]. A high value of this parameter is observed when, among all amplicons, those that can be considered polymorphic predominate, and this most often happens in the analysis of a genetically diverse group of genotypes.

Table 2. Starter sequence and assessment of the number and type of products generated with the ISSR primers used in the study

Number of starter	Starter sequence	Number of PCR products				Polymorphism (%)	Range (bp)
		total	polymorphic	monomorphic	specific		
ISSR 1	VBV$(AC)_7$*	11	10	1	0	90.9	400–3800
ISSR 2	BDB$(CA)_7$	10	10	0	0	100.0	500–3200
ISSR 3	HBH$(CT)_7$	8	4	4	0	50.0	500–1500
ISSR 4	GCV$(TC)_7$	11	8	3	0	72.7	400–2300
ISSR 5	BDV$(AG)_7$	11	5	6	0	45.5	400–1500
ISSR 6	HVHTG$(TTG)_4$T	9	7	2	0	77.8	400–1400
ISSR 7	BDBCA$(CCA)_4$C	10	7	3	0	70.0	500–1400
ISSR 8	BDM$(CAG)_5$	8	4	4	0	50.0	400–2300
ISSR 9	$(GAA)_6$	11	11	0	0	100.0	400–2800
ISSR 10	$(ATG)_6$	11	7	4	0	63.6	400–3200
ISSR 11	$(TGG)_6$	11	7	4	0	63.6	350–1500
ISSR 12	$(GATA)_5$	14	8	6	0	57.1	400–2000
ISSR 13	$(GACA)_5$	11	9	2	0	81.8	350–1500
Total		136	97	39	0	–	350–3800
Mean		10.46	7.46	3.0	–	71.0	–

*V – not T; B – not A; H – not G; D – not C

The genetic similarity coefficient between the studied genotypes calculated using the Dice method ranged from 0.56 to 0.88 (tab. 3). As a result of clustering the genotypes, a dendrogram was generated which can be divided into three main clusters (fig. 1a). The first two have only one genotype each: *M. spicata* var. *crispa* and *Mentha piperita* var. *citrata*, respectively. In cluster III, comprising a total of 10 genotypes, two subclusters should be distinguished: A and B. Subcluster III A consisted of *M. suaveolens* and *M. suaveolens* var. *variegata* (for which the similarity coefficient was 0.79), joined by *Plectranthus amboinicus*. Subcluster III B contained the largest group of objects (7). The first clusters within it were formed by *M. spicata* var. *crispa* Persian and *M. piperita* var. *officinalis*, and then *M. spicata*, *M. longifolia, M. spicata* cv. Maroccan, *M. pulegium*, and finally *M. rotundifolia* were added. According to Vining et al. [2022], *M. spicata* is a hybrid whose parental forms are *M. suaveolens* and *M. longifolia*. Dendrogram analysis indicates that these forms are located in different subclusters of cluster III – III A and III B, respectively. At the same time, *M. spicata* and *M. spicata* cv. Maroccan are located in subcluster III B, indicating their greater similarity to the paternal form. Gobert et al. [2002], Choupani et al. [2019] point out the high similarity between *M. longifolia* and *M. spicata* based on their studies. The study by Naseem et al. [2024] indicates the joint clustering of the *M. spicata* hybrid and the parent forms *M. suaveolens* and *M. longifolia*. Taxonomy defines *M. piperita* as a hybrid between *M. spicata* and *M. aquatica*, and according to Momeni et al. [2006] shows greater similarity to *M. spicata* than to *M. aquatica*. This is confirmed by the results of our study, as both these genotypes were grouped together, and the genetic similarity coefficient was 0.88. A similar relationship between the studied objects is indicated by Soilhi et al. [2020]. According to Choupani et al. [2019], *M. piperita* and *M. longifolia* are highly similar, and our findings support this view with a genetic similarity value of 0.85. However, it should be noted that *M. piperita* is grouped into separate clusters, which was also observed by Çelik et al. [2024]. The authors suggest that this may be due to backcrossing. Relationships between *Mentha* accessions were assessed using PCA (fig. 2). For ISSR markers, principal component analysis (fig. 2a) revealed that the variance of the first two components accounted for 50.39% of the total variance. The first axis, accounting for 35.05% of the variance, separated genotypes G12, G11, and G5, G2, and G1, of which the first two formed single clusters in the dendrogram, while the remaining three formed cluster IIIa from the remaining genotypes. The second axis, accounting for 15.34% of the variance, essentially separated genotypes G4 and G7 from the remaining five (G3, G6, G8, G9, and G10), which constituted cluster IIIB in the dendrogram. The results of the PCA analysis are consistent with the results of the cluster analysis. PCA also confirms the results obtained by UPGMA clustering for SCoT markers (fig. 2b). The first axis, explaining 40.60% of the variance, separated genotypes G3, G5, and G11 from the others except G1, while the second axis, accounting for 16.89% of the variance, partially divides the objects of cluster IV dendrogram and genotype G3.

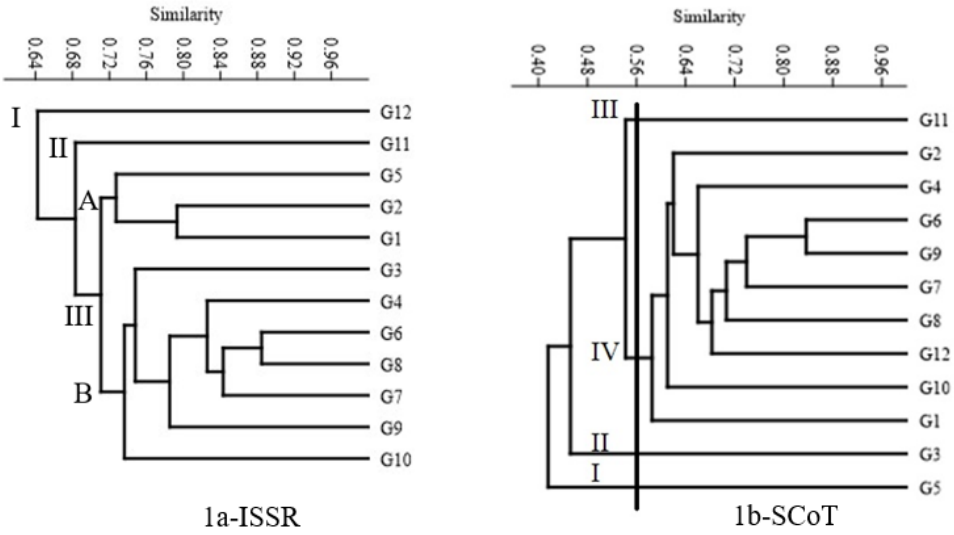

Fig. 1. UPGMA dendrogram of genetic similarity generated by ISSR (1a) and SCoT (1b) markers for 12 *Mentha* genotypes

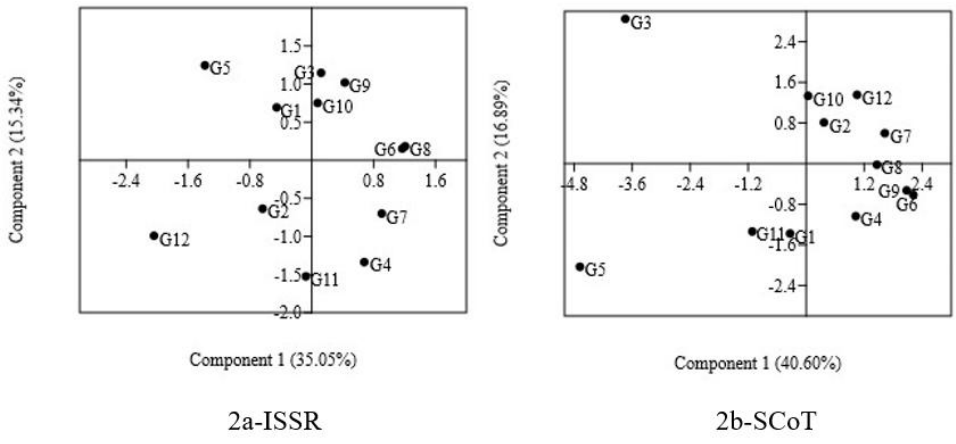

Fig. 2. Principal component analysis of 12 *Mentha* accessions with ISSR (2a) and SCoT (2b) markers

Table 3. Matrix of genetic similarity between the studied genotypes obtained on the basis of ISSR below the diagonal and SCoT above diagonal markers

	G1	G2	G3	G4	G5	G6	G7	G8	G9	G10	G11	G12
G1	1.00	0.55	0.40	0.61	0.47	0.63	0.55	0.59	0.60	0.58	0.55	0.56
G2	0.79	1.00	0.46	0.62	0.36	0.64	0.63	0.65	0.57	0.57	0.47	0.62
G3	0.73	0.67	1.00	0.39	0.37	0.41	0.48	0.42	0.43	0.54	0.41	0.58
G4	0.69	0.80	0.70	1.00	0.48	0.71	0.62	0.67	0.67	0.60	0.54	0.63
G5	0.76	0.69	0.70	0.65	1.00	0.45	0.36	0.43	0.42	0.40	0.43	0.40
G6	0.76	0.73	0.80	0.85	0.69	1.00	0.73	0.71	0.84	0.63	0.59	0.70
G7	0.74	0.70	0.71	0.82	0.67	0.86	1.00	0.70	0.75	0.57	0.57	0.72
G8	0.76	0.73	0.77	0.81	0.65	0.88	0.82	1.00	0.71	0.66	0.49	0.61
G9	0.72	0.69	0.76	0.76	0.73	0.80	0.78	0.80	1.00	0.62	0.65	0.70
G10	0.70	0.74	0.74	0.70	0.67	0.74	0.72	0.78	0.74	1.00	0.45	0.62
G11	0.70	0.63	0.71	0.73	0.60	0.70	0.75	0.73	0.63	0.65	1.00	0.56
G12	0.68	0.71	0.66	0.68	0.68	0.64	0.65	0.57	0.64	0.59	0.56	1.00

G1 – Mentha suaveolens Ehrh. var. variegata (pineapple mint); G2 – Mentha suaveolens Ehrh.; G3 – Mentha pulegium L.; G4 – Mentha longifolia L.; G5 – Plectranthus amboinicus (Lour.) Spreng. (Mexican mint); G6 – Mentha piperita L. var. officinalis Sole f. rubescens Camus; G7 – Mentha spicata L.; G8 – Mentha spicata var. crispa cv. Persian; G9 – Mentha spicata L. cv. Moroccan; G10 – Mentha rotundifolia L. Huds.; G11 – Mentha piperita L. var. citrata Ehrh.; G12 – Mentha spicata L. var. crispa

SCoT-PCR amplification

Molecular markers are used to assess genetic diversity, study population structure, and investigate relatedness between individuals. A relatively new marker technique used in DNA research is the start codon targeted (SCoT) polymorphism method, developed by Collard and Mackill [2009]. It utilizes dominant and repetitive markers based on the region surrounding the ATG translation initiation codon. This method is based on the polymerase chain reaction (PCR) using single primers, 18 nucleotides in length. In this study, fifteen SCoT primers were analyzed, and their sequences, along with the generated products, are listed in table 4. All primers produced a total of 157 bands, averaging more than 10 bands per primer. The percentage of polymorphism obtained ranged from 75% to 100%, averaging 88.7% for the fifteen primers mentioned above. A slightly lower value of this parameter at 56.8% was observed in 4 mint species by Salama et al. [2019]. Specific products generated by ten primers (SCoT 2, SCoT 3, SCoT 4, SCoT 5, SCoT 7, SCoT 9, SCoT 10, SCoT 12, SCoT 14, and SCoT 15) were also detected. A total of 14 products were obtained, with an average of 1.4 bands for primers amplifying these products. Primers SCoT 8, SCoT 9, and SCoT 15 generated monomorphic products. All the above-mentioned primers produced only one band of this type. The size of the obtained products ranged between 350 and 4200 bp. The usefulness of SCoT markers in the characterization of mint species is indicated by Salama et al. [2019] and Heylen et al. [2021]. Salama et al. [2019] identified specific amplicons generated by some primers allowing the identification of the species *M. sativa*, *M. spicata*, *M. piperita* and the subspecies *M. longifolia* subsp. *typhoides* and *schimperi*. The possibility of identifying *M.* × *piperita* cultivars with this marker system was indicated by Khan et al. [2017], and with the RAPD marker system by Kiełtyka-Dadasiewicz et al. [2017]. This is confirmed by the results of this study, which enable the identification of six of the twelve genotypes tested, which include: *Plectranthus amboinicus* – using primers SCoT 2, 3, 4, 10 and 14 generating a total of 6 specific fragments, *Mentha pulegium* L. using primer SCoT 7, *Mentha spicata* L. cv. Moroccan using primers SCoT 5 and 9, *Mentha suaveolens* Ehrh. var. *variegata* (pineapple mint) using starter SCoT 2 and 4, *Mentha spicata* L. using starter SCoT 12, and *Mentha longifolia* L. using starter SCoT 15 (tab. 5).

The genetic similarity coefficient assessed according to the Dice formula between 12 studied genotypes is presented in table 3. The similarity ranged from 0.36 to 0.84. The highest similarity occurred between *Mentha piperita* L. var. *officinalis* Sole f. *rubescens* Camus and *Mentha spicata* L. cv. Moroccan while the lowest between *Mentha suaveolens* and *Plectranthus amboinicus* and *Plectranthus amboinicus* and *Mentha spicata* L.

Table 4. Starter sequence and assessment of the number and type of products generated with the SCoT primers used in the study

Number of starter	Starter sequence	Number of PCR products				Polymorphism (%)	Range (bp)
		total	polymorphic	monomorphic	specific		
SCoT 1	CAACAATGGCTACCACCA	11	11	0	0	100	650–3500
SCoT 2	CAACAATGGCTACCACCC	12	10	0	2	83.3	450–4200
SCoT 3	CAACAATGGCTACCACCT	9	8	0	1	88.8	850–2700
SCoT 4	CAACAATGGCTACCACGT	13	11	0	2	84.6	550–3200
SCoT 5	CAACAATGGCTACCAGCC	8	7	0	1	87.5	650–4200
SCoT 6	ACGACATGGCGACCGCGA	17	17	0	0	100.0	250–3500
SCoT 7	ACCATGGCTACCACCGAC	9	7	0	2	77.7	550–3200
SCoT 8	ACCATGGCTACCACCGAG	10	9	1	0	90.0	550–3200
SCoT 9	ACCATGGCTACCACCGCC	8	6	1	1	75.0	350–4200
SCoT 10	ACCATGGCTACCACCGGC	10	8	0	2	80.0	350–2400
SCoT 11	CCATGGCTACCACCGCCG	9	9	0	0	100.0	450–3500
SCoT 12	CCATGGCTACCACCGGAG	10	9	0	1	90.0	350–2300
SCoT 13	ACGACATGGCGACCAGCG	10	10	0	0	100.0	550–2500
SCoT 14	ACGACATGGCGACCACGT	9	8	0	1	88.8	450–2500
SCoT 15	CCATGGCTACCACCGGCA	12	10	1	1	83.3	450–2700
Total		157	140	3	14	–	350-4200
Mean		10.5	9.3	0.2	0.9	88.7	–

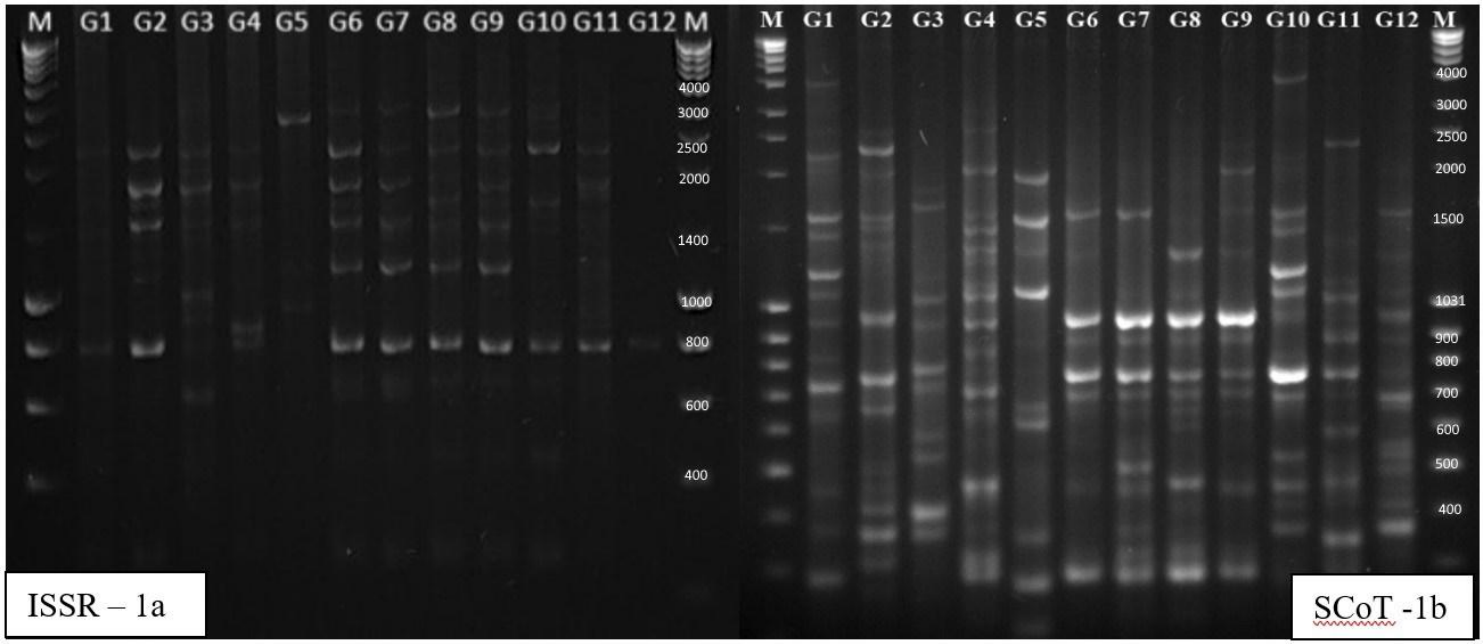

M – standard of DNA fragment size; G1 – *Mentha suaveolens* Ehrh. var. *variegata* (pineapple mint); G2 – *Mentha suaveolens* Ehrh.; G3 – *Mentha pulegium* L.; G4 – *Mentha longifolia* L.; G5 – *Plectranthus amboinicus* (Lour.) Spreng. (Mexican mint); G6 – *Mentha piperita* L. var. *officinalis* Sole f. *rubescens* Camus; G7 – *Mentha spicata* L.; G8 – *Mentha spicata* var. *crispa* cv. Persian; G9 – *Mentha spicata* L. cv. Moroccan; G10 – *Mentha rotundifolia* L. Huds.; G11 – *Mentha piperita* L. var. *citrata* Ehrh.; G12 – *Mentha spicata* L. var. *crispa*

Fig. 3. Fingerprints of twelve *Mentha* genotypes using ISSR 2 (1a) and SCoT 6 (1b) primer

Table 5. SCoT markers specific to *Mentha*

Species names	SCoT primer	Specific band size (bp)
M. suaveolens Ehrh. var. *variegata* G1	SCoT2	4200
	SCoT4	1500
Mentha pulegium L. G3	SCoT7	1700
	SCoT7	800
Mentha longifolia L. G4	SCoT15	1200
Plectranthus amboinicus (Lour.) Spreng G5	SCoT2	1400
	SCoT3	2700
	SCoT4	650
	SCoT10	1200
	SCoT10	450
	SCoT14	1400
Mentha spicata L. G7	SCoT12	1700
Mentha spicata L. cv. Moroccan G9	SCoT5	650
	SCoT9	2500

The analysis of genetic similarity generated using SCoT markers was presented in the form of a dendrogram (fig. 1b). The dendrogram intersection at 0.56, which is the average value for all analyzed genotypes, allows for the identification of four distinct clusters. Three of these clusters include single genotypes: *Mentha piperita* var. *citrata*, *Mentha pulegium*, and *Plectrantus amboinicus* – Mexican mint, the latter of which was the most distant from all the others. In cluster IV, composed of nine genotypes, the first cluster was formed by *M. piperita* var. *officinalis* and *M. spicata* cv. Moroccan. Subsequently, the remaining genotypes were added to this cluster, and finally *M. suaveolens* var. *variegata*. However Khan et al. [2017] in their study of genetic diversity using SCoT markers did not group *Mentha piperita* and *Mentha spicata* genotypes into separate clusters, but rather combined them with *M. cardiaca* and *M. viridis* into one large cluster. The genotypes present in cluster IV were characterized by a high level of similarity ranging from 0.55 to 0.84. Among them, *M. spicata* and *M. longifolia* were used by Salama et al. [2019] in the analysis using SCoT markers and by Ibrahim [2017] using RAPD markers. The authors report similarity between *M. spicata* and *M. longifolia* at 0.45 and 0.44, respectively, for the marker systems used. This is reflected in the results of this study, as these species formed one cluster, and the similarity value was even higher than the reported results and amounted to 0.62. In turn, the study by Vining et al. [2019] using SSR markers indicate a joint grouping of *M. suaveolens* and *M. longifolia* genotypes. This relationship is confirmed by the cluster IV observed in our study, which includes both aforementioned species. Phylogenetic tree analyses conducted by Thakur et al. [2016] indicate grouping of *M. piperita* and *M. citrata* in one cluster and *M. spicata* in a separate one. Genetic similarity determined by SCoT markers within the *M. spicata* species, represented by three genotypes, should be considered high, as it ranged from 0.70 to 0.75. This was reflected

in the formation of the second cluster on the dendrogram between *M. spicata* and *M. spicata* cv. Maroccan. Furthermore, the same cluster included *M. suaveolens* and *M. longifolia*, which, according to Vining et al. [2022], are parental forms of this species, and their direct similarity was estimated at 0.62. Therefore, using SCoT markers allows for the assessment of genetic diversity within the studied genus, allowing for effective differentiation of even forms with close phylogenetic relationships.

CONCLUSION

Genetic improvement of *Mentha* should integrate both morphological and molecular data, as accessions with similar morphology often differ at the molecular level. Molecular diversity databases are thus valuable tools for breeding and analysing novel intra and interspecific hybrids. SCoT markers, due to their primer design based on conserved start codon regions, are predominantly distributed within gene rich regions on both DNA strands, enhancing their relevance for functional genomic studies. Unlike ISSR markers, which target repetitive non-coding regions, SCoT markers are more likely to amplify coding sequences, including regions associated with pseudogenes and transposable elements, providing greater insight into gene-associated polymorphisms. Additionally, the efficiency of SCoT markers is influenced by the precise distance between primer binding sites, contributing to their reproducibility and specificity. These advantages make SCoT a more informative and functionally relevant tool compared to ISSR for assessing genetic diversity and structure *Mentha* genus. Selected primers generating unique bands can be used to precisely identify specific genotypes.

REFERENCES

Ahmad İ., Khan S.U., Khan A. et al., 2018. Reassessment of *Mentha* species from Kunhar River catchment using morphological and molecular markers. Anadolu J. Aegean Agric. Res. Inst. 28(1), 6–12.

Choupani A., Shojaeiyan A., Maleki M., 2019. Genetic relationships of Iranian endemic mint species, *Mentha mozaffariani* Jamzad and some other mint species revealed by ISSR markers. BioTechnologia 100, 19–28. https://doi.org/10.5114/bta.2019.83208

Çelik C., Seraj N.A., Yasak S. et al., 2024. Molecular characterization and genetic relationships in different mint (*Mentha* L.) species with ISSR marker technique. Biol. Bull. 51(4), 959–968. https://doi.org/10.1134/S106235902360616X

Collard B.C., Mackill D.J., 2009. Start codon targeted (SCoT) polymorphism: a simple novel DNA marker technique for generating gene-targeted markers in plants. Plant Mol. Biol. Rep. 27, 86–93. https://doi.org/10.1007/s11105-008-0060-5

Devi A., Iqbal T., Ahmad Wani I. et al., 2022. Assessment of variability among morphological and molecular characters in wild populations of mint [*Mentha longifolia* (L.) L.] germplasm. Saudi J. Biol. Sci. 29, 3528–3538. https://doi.org/10.1016/j.sjbs.2022.02.013

Dorman H.D., Koşar M., Kahlos K. et al., 2013. Antioxidant properties and composition of aqueous extracts from *Mentha* species, hybrids, varieties, and cultivars. J. Agric. Food Chem. 51, 4563–4569. https://doi.org/10.1021/jf034108k

Doyle J.J., Doyle J.L., 1987. A rapid DNA isolation procedure for small quantities of fresh leaf tissue. Phytochem. Bull. 19, 11–15.

Fukui Y., Saito M., Nakamura N. et al., 2022. Classification of Southeast Asian mints (*Mentha* spp.) based on simple sequence repeat markers. Breed. Sci. 72, 181–187. https://doi.org/10.1270/jsbbs.21058

Gobert V., Moja S., Colson M. et al., 2002. Hybridization in the section *Mentha* (Lamiaceae) inferred from AFLP markers. Am. J. Bot. 89, 2017–2023. https://doi.org/10.3732/ajb.89.12.2017

Hammer Ø., Harper D.A.T., Ryan P.D., 2001. Past: Paleontological statistics software package for education and data analysis. Palaeontol. Electron. 4, 9.

Heylen O.C.G., Debortoli N., Marescaux J. et al., 2021. A revised phylogeny of the *Mentha spicata* clade reveals cryptic species. Plants 10, 819. https://doi.org/10.3390/plants10040819

Ibrahim H.M., 2017. Assessment of genetic diversity and relationships of five *Mentha* species using RAPD marker. Curr. Sci. Int. 6, 271–277.

Jędrzejczyk I., Rewers M., 2018. Genome size and ISSR markers for *Mentha* L. (Lamiaceae) genetic diversity assessment and species identification. Ind. Crops Prod. 120, 171–179. https://doi.org/10.1016/j.indcrop.2018.04.062

Khan N., Singh S., Singh Dhawan S., 2017. Development of species-specific SCoT markers and analysis of genetic diversity among *Mentha* genotypes. Int. J. Innov. Sci. Engineer. Technol. 4, 2348–7968.

Khanuja S.P.S., Shasany A.K., Srivastava A. et al., 2000. Assessment of genetic relationships in *Mentha* species. Euphytica 111, 121–125. https://doi.org/10.1023/A:1003829512956

Kiełtyka-Dadasiewicz A., Okoń S., Ociepa T. et al., 2017. Morphological and genetic diversity among peppermint (*Mentha* × *piperita* L.) cultivars. Acta Sci. Pol. Hortorum Cultus 16, 151–161. https://doi.org/10.24326/asphc.2017.3.15

Lawrence B.M., 2006. Mint. The Genus Mentha. CRC Press, Boca Raton. https://doi.org/10.1201/9780849307980

Malik R.H., Shah S.M., Khan A.R. et al., 2019. Evaluation of sequence related amplified polymorphic markers for genetic characterization of *Mentha* species. Phillipine J. Crop Sci. 44, 71–76.

Mkaddem M., Bouajila J., Ennajar M. et al., 2009. Chemical composition and antimicrobial and antioxidant activities of *Mentha* (*longifolia* L. and *viridis*) essential oils. J. Food Sci. 74, M358–M363. https://doi.org/10.1111/j.1750-3841.2009.01272.x

Momeni S., Shiran B., Razmjoo K., 2006. Genetic variation in Iranian mints on the bases of RAPD analysis. Pak. J. Biol. Sci. 9, 1898–1904. https://doi.org/10.3923/pjbs.2006.1898.1904

Moshrefi-Araghi A., Nemati H., Azizi M. et al., 2021. Association of genetic structure and diversity in Iranian wild germplasms of *Mentha longifolia* L. based on phenotypical, biochemical, and molecular markers. Chem. Biodivers. 18, e2001044. https://doi.org/10.1002/cbdv.202001044

Naseem I., Khan M.A., Habib U. et al., 2025. Morphological profiling and DNA barcoding revealed genetic diversity and phylogeny of Mentha species cultivated in Pakistan. Genet. Resourc. Crop Evol. 72(3), 2977–2995. https://doi.org/10.1007/s10722-024-02140-x

Nei M., Li W., 1979. Mathematical model for studying genetic variation in terms of restriction endonucleases. Proc. Natl. Acad. Sci. USA 76, 5269–5273.

Panjeshahin Z., Sharifi-Sirchi G., Samsampour D., 2018. Genetic and morphological diversity of wild mint *Mentha longifolia* (L.) Hudson subsp. *noeana* (Briq.) Briq. in south- and southeastern Iran. *J. Med. Plants By-products* 7(1), 105–115. https://doi.org/10.22092/jmpb.2018.116741

Rodrigues L., van den Berg C., Póvoa O. et al., 2013. Low genetic diversity and significant structuring in the endangered *Mentha cervina* populations and its implications for conservation. Biochem. Syst. Ecol. 50, 51–61. https://doi.org/10.1016/j.bse.2013.03.007

Sabboura D., Yacoub R., Lawand S., 2016. Assessment of genetic relationships among *Mentha* species. Int. J. ChemTech Res. 9, 462–468. https://doi.org/10.1023/A:1003829512956

Salama A.M., Osman E.A., El-Tantawy A.A., 2019. Taxonomical studies on four *Mentha* species grown in Egypt through morpho-anatomical characters and SCoT genetic markers. Plant Arch. 19, 2273–2286.

Silva D., Vieira R., Alves R. et al., 2006. Mint (*Mentha* spp.) germplasm conservation in Brazil. Rev. Bras. Pl. Med. 8, 27–31.

Sofyalıoğlu E., Sevindik E., Gübeş İ. et al., 2025. Phylogenetic analysis of endemic *Sideritis* L. spp. (*Lamiaceae*) in Türkiye based on chloroplast *trn*L-F, *mat*K, and *rbc*L DNA sequences. Genet. Resourc. Crop Evol**.** 72(4), 4381–4391. https://doi.org/10.1007/s10722-024-02225-7

Smolik M., Rzepka-Plevnes D., Jadczak D. et al., 2007. Morphological and genetic variability of chosen *Mentha* species. Herba Pol. 53, 90–97.

Soilhi Z., Trindade H., Vicente S. et al., 2020. Assessment of the genetic diversity and relationships of a collection of *Mentha* spp. in Tunisia using morphological traits and ISSR markers. J. Hortic. Sci. Biotechnol. 95, 483–495. https://doi.org/10.1080/14620316.2019.1702482

Thakur V.V., Tiwari S., Tripathi N. et al., 2016. DNA barcoding and phylogenetic analyses of Mentha species using *rbc*L sequences. Ann. Phytomed. 5(1), 59–62

Vining K.J., Pandelova I., Hummer K. et al., 2019. Genetic diversity survey of *Mentha aquatica* L. and *Mentha suaveolens* Ehrh., mint crop ancestors. Genet. Resour. Crop Evol. 66, 825–845. https://doi.org/10.1007/s10722-019-00750-4

Vining K.J., Pandelova I., Lange I. et al., 2022. Chromosome-level genome assembly of *Mentha longifolia* L. reveals gene organization underlying disease resistance and essential oil traits. G3 Genes Genomes Genet. 12(8), jkac112. https://doi.org/10.1093/g3journal/jkac112

Source of funding: This research was funded by the statutory activity of the University of Life Sciences in Lublin (Grant No. SUBB.WRH.19.023.RiO).

Received: 1.09.2025
Accepted: 17.10.2025
Published: 31.12.2025

AGRONOMY SCIENCE

VOL. LXXX (4) 2025

https://doi.org/10.24326/as.2025.5569

[1] Institute of Agricultural Engineering, Wroclaw University of Environmental and Life Sciences, Chełmońskiego 37b, 51-630 Wrocław, Poland
[2] Institute of Agroecology and Plant Production, Wroclaw University of Environmental and Life Sciences, Grunwaldzki 24A, 50-363 Wrocław, Poland
[3] Department of Biosystems Engineering, Poznań University of Life Sciences, Wojska Polskiego 50, 60-627 Poznań, Poland

* e-mail: katarzyna.pentos@upwr.edu.pl

MICHAŁ KASPROWICZ https://orcid.org/0009-0006-1224-061X

KATARZYNA PENTOŚ*[1] https://orcid.org/0000-0002-0666-1948

WIESŁAW WOJCIECHOWSKI[2] https://orcid.org/0000-0002-2011-2427

SEBASTIAN KUJAWA[3] https://orcid.org/0000-0002-5461-9170

JASPER TEMBECK MBAH[1] https://orcid.org/0000-0002-8888-6672

Advancements in plant protection – the application of machine learning to the detection of maize infestations

Zastosowanie uczenia maszynowego w wykrywaniu szkodników kukurydzy

Abstract. Plant infestations cause significant economic losses in agriculture, necessitating rapid and accurate detection for optimized agrotechnical operations and reduced environmental pollution. This study addresses this challenge by proposing a customized convolutional neural network (CNN) architecture for detecting corn leaf worm infestations in maize. The research focuses on developing unique CNN models through extensive experimentation, systematically adjusting hyperparameters like optimizers, filter numbers, and kernel sizes. The study's main contributions include the design of an accurate CNN classifier, and its implementation in a user-friendly smartphone application. The research highlights the importance of hyperparameter tuning in CNN performance, demonstrating that optimal configurations lead to high accuracy (up to 95% for accuracy, precision, recall, specificity, and F1-score). While the current model focuses on a single pest, the findings underscore the potential of custom CNN classifiers in vision systems for automated crop inspection, offering a promising solution for minimizing crop losses and the environmental impact of chemical plant protection products.

Keywords: corn leaf worm, convolutional neural network, plant protection, image recognition

Citation: Kasprowicz M., Pentoś K., Wojciechowski W., Kujawa S., Mbah J.T., 2025. Advancements in plant protection – the application of machine learning to the detection of maize infestations. Agron. Sci., 80(4), 39–55. https://doi.org/10.24326/as.2025.5569

INTRODUCTION

The aetiology of plant diseases is multifactorial, with biotic stressors (pathogens, fungi, bacteria, and insects) and abiotic stressors (weather, soil conditions, and chemicals) both playing a role [Oliveira 2019]. Plant diseases have the potential to cause significant damage to agricultural crops, resulting in reduced yields. In the event of a large-scale attack, this can even lead to the complete failure of a crop, with serious economic consequences [Li et al. 2020, Khanramaki et al. 2021]. In order to reduce the negative impact of diseases on crop quality and yield, it is necessary to detect them quickly. This is a challenging task due to the labour-intensive and time-consuming nature of traditional methods of pest and diseases detection and identification. Furthermore, farmers often lack the necessary knowledge to identify diseases or insects, which can result in the inappropriate application of agrochemicals with negative environmental consequences.

Maize is one of the three most important crops in the world, along with rice and wheat. However, since the end of the second decade of the twenty-first century, it has ranked second in terms of area sown. A number of factors have contributed to this state of affairs, the most significant of which are its versatility of use (as fodder, food, and for industrial and energy purposes), high yields, and the advancement of breeding progress (including the development of hybrid cultivars and the breeding of early-maturing cultivars). The earlier maturation of the cultivars permits their cultivation in cooler climates with a shorter growing season. Poland provides an illustrative example, where the area planted with this species increased nearly threefold (2.84 times) over a 10-year period (2010–2020) [FAOSTAT 2024]. It is regrettable that the expansion of maize cultivation is leading to an intensification of pest pressure, particularly from those species that have been identified as the most problematic. Until recently, the European corn borer (*Ostrinia nubilalis* H.) and the frit fly (*Oscinella frit* L.) were considered the most significant pests in Europe. However, more recently, the western corn rootworm (*Diabrotica virgifera* KeConte) has emerged as a growing concern, and with the anticipated effects of climate change, the corn leaf worm (*Spodoptera frugiperda*) may become a prominent issue in the near future.

The corn leaf worm is a polyphagous pest that most often attacks plants of the panicle, nightshade, cabbage family, as well as many vegetables. Of the cereals, it is most dangerous in maize crops. Its grey-brown front and white back wings are distinguished by distinct brown veins. The voracious larvae are the most damaging, and their distinctive feature is the inverted Y on their head. They cause leaf skeletonization, which significantly reduces photosynthetic capacity of crops. They also often damage flower buds, plant growth tips and even cobs and grain, resulting in reduced maize yield and quality. As reported by van der Berg et al. [2021], yield losses of up to 30% to 70% have been documented in the Americas, while losses of 11% to 100% have been observed in Africa. The corn leaf worm is mainly known for causing significant damage to crops in South America, however, there have been observations of its migration to colder regions of the world. Despite being considered a thermophilic species, the pest has also been observed in cooler regions, including Europe [Jeger et al. 2018, Babendreier et al. 2022].

The efficacy of the utilisation of agrochemicals is contingent upon the prompt identification of crop diseases. The expeditious advancement of image recognition algorithms employing machine learning in recent years has rendered the real-time identification of selected crop pests and diseases. One limitation of this method of detecting threats to crops

is the necessity to represent the effects of infection in the image. Additionally, the acquisition of images at different crop growth stages and under different lighting conditions is important because these factors affect the quality of the classification. Based on image data, machine learning-based vision systems for automatic detection of pests and crop infections are being developed. Image processing with SVM classifier was utilised by Ebrahimi et al. [2017] to detect of thrips on the strawberry canopies in greenhouses. Mohan et al. [2016] developed system for detection and recognition of brown spot disease, leaf blast disease and bacterial blight disease in paddy plants. The methods used were AdaBoost classifier for detection and k-Nearest Neighbour (k-NN) and Support Vector Machine (SVM) algorithms for recognition.

In recent years, deep learning methods based on convolutional neural networks (CNNs) have become a widely used tool in agriculture for the purpose of solving classification problems. Examples of such applications include the detection of weeds [Gao et al. 2020, Hasan et al. 2021], plant water stress identification [Kamarudin et al. 2021], yield prediction [Srivastava et al. 2022], crop type classification [Kussul et al. 2017], as well as vegetable and fruit quality assessment [Gill et al. 2022]. There are also numerous applications related to the detection of pests and crop diseases [Jiao et al. 2020, Wang et al. 2020, Xu et al. 2022, Yang et al. 2022]. The availability of open databases containing images that can be used as training data represents a significant advantage in the construction of systems for plant diseases and insects recognition. Ferentinos [2018] employed an open database comprising 87,848 images of plants belonging to 25 different species. The database was utilized to train five convolutional neural network architectures, namely AlexNet, AlexNet-OWTBn, GoogLeNet, Overfeat, and VGG. The VGG model yielded the most optimal results, with a success rate of 99.53%. The RGB insect images from the three publicly available insect datasets were employed by Thenmozhi and Reddy [2019] to train a CNN architecture. The authors compared their model with pre-trained models such as AlexNet, ResNet, and VGG. The original images were converted to grayscale. The CNN model developed in this work demonstrated superior performance to the pre-trained models with transfer learning, achieving classification accuracy approximately 2% higher for the tested datasets. The PlantVillage dataset [Hughes and Salathe 2015] which contains images of common diseases across a range of crops, has been used by some researchers [Mohanty et al. 2016, Barbedo 2018, Ferentinos 2018]. Computer vision systems that employ convolutional neural networks are integral components of comprehensive solutions, including harvesting robots [Jia et al. 2020], automated sprayers [Khan et al. 2021, Storey et al. 2022], and smartphone applications, which facilitate the prediction of yields [Coviello et al. 2020] and the identification of weeds, pests, and crop diseases [Loyani and Machuve 2021, Lanjewar and Panchbhai 2023].

This study evaluates the performance of custom-designed convolutional neural network architectures on images of maize plants, with a focus on how varying hyperparameters affect model accuracy and efficiency. Unlike traditional studies that rely on pre-existing architectures, the authors developed unique CNN architectures through extensive experimentation, with numerous iterations and refinements ultimately yielding the presented model. To optimize performance, the architecture was tested under varying hyperparameters, including different optimizers, the number of filters, and kernel sizes. This exploration led to the investigation of 25 distinct models, each differing in parameters such as batch size, dropout rate, and optimizer type. By systematically adjusting these parameters,

we gained insights into how specific choices impact the model's accuracy and computational efficiency, providing valuable guidance for CNN design in agricultural image classification tasks. Furthermore, a CNN classifier was implemented in a smartphone application to create a rapid detection tool for maize infestation by corn leaf worms, designed for use in field conditions.

MATERIALS AND METHODS

Custom CNN model

Convolutional neural networks represent an advanced deep learning architecture that has significantly transformed computer vision and image analysis tasks. CNNs are built to automatically and progressively learn spatial feature hierarchies directly from input data, adapting to patterns at multiple levels of abstraction. This architecture makes the neural network particularly well-suited for tasks involving image and video recognition, classification, and segmentation. The fundamental building blocks of a CNN include convolutional layers, pooling layers, and fully connected layers. Convolutional layers apply a set of learnable filters to the input, each detecting specific features at various locations. Pooling layers reduce the spatial dimensions of the feature maps, providing a form of translational invariance. Fully connected layers, typically used at the end of the network, combine these features for final classification or regression tasks.

The proposed custom CNN model's design (fig. 1) incorporates convolutional layers with multiple kernel sizes spread across them, dropout layers, max-pooling, normalization, and an early stopping feature. The selection of this structure was informed by the findings of preliminary research. In the course of this research, 10 CNNs were examined. The results of the accuracy dependence on the number of adjustable parameters are presented in table 1.

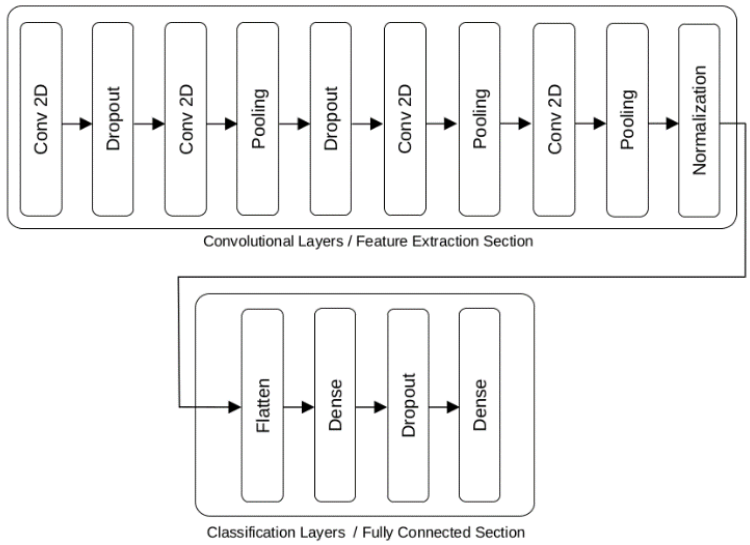

Fig. 1. Building blocks of the model

Table 1. The accuracy of the custom CNN models of various structures

No.	Number of parameters	Accuracy
1	23,907,650	0.71
2	23,907,842	0.94
3	22,245,186	0.76
4	93,506	0.72
5	2,424,802	0.62
6	11,169,218	0.79
7	23,077,282	0.68
8	10,104,418	0.66
9	31,874	0.87
10	66,599,572	0.95

Despite its strengths, the complexity of the proposed CNN model may introduce potential challenges, as larger kernel sizes (7×7 and 9×9) significantly increase the number of parameters, potentially resulting in longer training times and higher memory requirements. This can be problematic, especially when computational resources are limited and/or when training a significantly larger amount of data. Additionally, the risk of overfitting remains, particularly with a high number of parameters (tab. 2), or in case the training data is insufficient. To mitigate these issues, we employed the Early Stopping callback from the Keras library, which halts training when the validation loss ceases to improve, preventing overfitting. Early Stopping was configured with a patience of five epochs to accommodate minor fluctuations without prematurely stopping the training. This approach ensures that the model achieves optimal performance while efficiently utilizing computational resources.

Table 2. The summary of the custom CNN model

Layer (type)	Output shape	Number of parameters
Conv2D	(400, 400, 32)	896
Dropout	(400, 400, 32)	–
Conv2D	(400, 400, 64)	51,264
MaxPooling	(133, 133, 64)	–
Dropout	(133, 133, 64)	–
Conv2D	(133, 133, 128)	401,536
Pooling	(44, 44, 128)	–
Conv2D	(44, 44, 256)	2,654,464
MaxPooling	(22, 22, 256)	–
Normalization	(22, 22, 256)	1,024
Flatten	123,904	–
Dense	512	63,439,360
Dropout	512	–
Dense	2	51,026

Such CNN architecture offers significant advantages – using varying kernel sizes enables the network to capture both fine details and larger structures in the images. For example, a 3 × 3 kernel is effective at detecting small features, while larger kernels (5 × 5, 7 × 7, and 9 × 9) are better suited for recognizing bigger patterns and even entire objects. Dropout layers serve a critical role in regularization by randomly deactivating a certain fraction of neurons during training, thereby reducing the risk of overfitting and enhancing the model's generalization capabilities. Max-pooling layers further reduce the feature map dimensions and the number of parameters, mainly to lower the computational load. Normalization layers stabilize the training process by making activation distributions more predictable, leading to a faster and more stable outcome.

This CNN model has several structural and functional advantages for image-based tasks. The number of filters, starting with 32 filters and progressively increasing up to 256 allows the model to learn hierarchical representations. Initial layers capture basic features (like edges and textures) with fewer filters, while deeper layers capture more complex patterns and object parts with more filters. With four convolutional layers, the model can gradually increase abstraction levels. This depth helps the network capture both low-level and high-level spatial hierarchies in the data. By varying kernel sizes (3, 5, 7, and 9), the model learns to detect features at multiple scales within each layer. Smaller kernels focus on fine-grained details, while larger kernels cover broader spatial regions. This can help capture both small and large patterns within images, improving robustness and accuracy, especially if objects vary in scale within the dataset. Dropout layers with rates of 0.25 and 0.5 help reduce overfitting by randomly „dropping out" a fraction of neurons during each training step, ensuring the model doesn't become overly reliant on specific paths within the network. This is especially important in deeper networks. Batch normalization applied before the fully connected layers stabilizes the training process by normalizing layer outputs, accelerating convergence, and further reducing overfitting. Each MaxPooling layer progressively reduces the spatial dimensions of feature maps, which lowers computational load, enabling efficient training on large images (e.g., 400 × 400 input size) as well as helping the network focus on the most prominent features, as MaxPooling selects the strongest activations, aiding in translation invariance. After flattening, a dense layer with 512 neurons serves as a feature synthesizer, integrating information from all previous layers before the final classification. The ReLU activation in this dense layer supports effective learning and gradient flow. A final softmax layer with two outputs is suitable for binary classification, producing probabilities for each class, which is intuitive for tasks with two possible labels.

A key feature of the model training process is the use of an Early Stopping function, which prevents the network from utilizing the full number of epochs (set to 100 in this case) if it reaches a plateau in performance. This approach allows the model to halt training as soon as validation performance stabilizes, saving computational resources and preventing overfitting by avoiding unnecessary training cycles. Setting a high number of epochs (100) provides enough time for the network to learn complex patterns within the maize dataset. However, Early Stopping, along with dropout and batch normalization layers, acts as a balance to prevent overfitting, ensuring that the model does not continue learning beyond the point of optimal generalization. The dropout layer, in particular, with variations tested from 0.0 to 0.49, introduces controlled regularization by randomly deactivat-

ing certain neurons during training. This reduces dependency on specific neurons, enhancing generalization capability. Interestingly, dropout 0.5 causes the model to crash and run out of memory.

Dataset overview

The images employed in this study to train the neural network were sourced from Kaggle's „corn leaf infection dataset" [Acharya 2020]. This dataset encompasses images of corn leaves, illustrating both healthy specimens and those affected by pathogens such as the larvae of *Spodoptera frugiperda* (fall armyworm moth). The training set consists of 3770 images, with 1794 images representing healthy leaves and 1976 images representing infected leaves. During training, this data set was divided into training and validation sets in a ratio of 3 : 1. The test set contains 454 images with 204 healthy and 250 infected leaves. Illustrative images utilised for the training of the models are depicted in figure 2.

Given the high-definition nature of the original images, data preprocessing was imperative. This preprocessing included resizing the images to a uniform resolution, normalizing pixel values to standardize the dataset. These preprocessing steps were essential to ensure the dataset was adequately prepared for effective neural network training, thereby improving the models' accuracies in identifying healthy and infected corn leaves under various conditions.

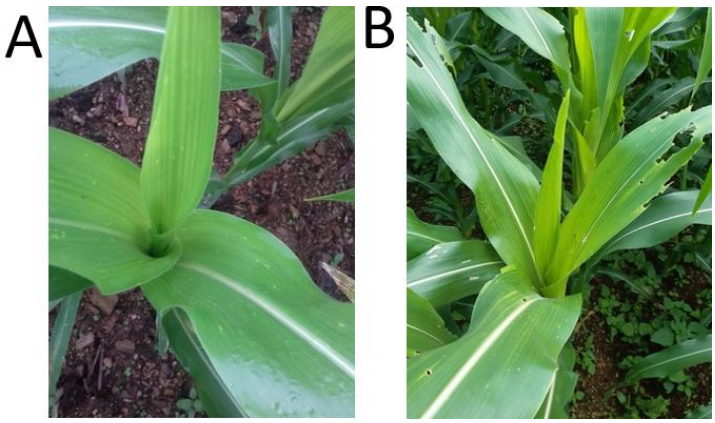

Fig. 2. Images of healthy (A) and infected (B) plant

Data pre-processing and model parameters

The original high-definition images in the dataset were resized to a resolution of 400 × 400 pixels to accommodate memory limitations. Consequently, the training set was converted into a four-dimensional tensor with dimensions 3770 × 400 × 400 × 3, representing the number of training images, the size of each image (400 × 400 pixels), and the three RGB colour channels. Similarly, the test set was converted into a four-dimensional tensor with dimensions 451 × 400 × 400 × 3. This tensor format facilitates the input of image data into the neural network for training and subsequent evaluation of the model's performance on unseen data. The dataset was pre-labeled, and a manual verification process was

conducted to ensure label accuracy. The custom CNN model was employed using the TensorFlow framework. The study involved over 25 experiments, each training a new neural network on the same dataset and comparing the aggregate results. These variations were driven by adjustments in hyperparameters to identify the optimal configuration for accurate disease detection.

The hyperparameters considered during the experiments included the number of epochs (set to 100), a validation split of 25%, and batch sizes of either 32 or 64. Dropout rates varied from 0% to 49% (0%, 10%, 30%, and 49%) to assess their impact on model regularization and performance. Additionally, various optimizers, such as SGD, Adam, Ada, and Adadelta, were utilized to determine the most effective optimization strategy for this specific task. These systematic variations and evaluations were critical in refining the model to achieve high accuracy in distinguishing between healthy and diseased corn leaves, demonstrating the robustness and versatility of the CNN approach in agricultural diagnostics.

The CNN models were developed using python programming language, utilizing libraries such as NumPy, which is a fundamental tool for array manipulation and computation. It is widely recognized and utilized in the development and implementation of artificial neural networks. Complementing NumPy, the pandas library extends its functionality, serving as a versatile and comprehensive tool for data manipulation and analysis, a kind of „Swiss army knife" in the realm of data science. Creation, training and deployment of neural networks were performed based on libraries associated with neural networks – specifically Keras and TensorFlow. After training, the model was deployed for use in the production phase. The neural network was trained based on the TPU (Tensor Processing Unit) architecture, enabling the efficient execution of artificial neural networks on the Google Colab platform, which leverages cloud computing resources.

Evaluation metrics

The following metrics were used to evaluate the quality of the CNN models:

$$\text{Accuracy} = \frac{\text{TN} + \text{TP}}{\text{TN} + \text{TP} + \text{FN} + \text{FP}}$$

$$\text{Precision} = \frac{\text{TP}}{\text{TP} + \text{FP}}$$

$$\text{Recall} = \frac{\text{TP}}{\text{TP} + \text{FN}}$$

$$\text{Specificity} = \frac{\text{TN}}{\text{TN} + \text{FP}}$$

$$\text{F1} - \text{score} = \frac{2 \cdot \text{Precission} \cdot \text{Recall}}{\text{Precission} + \text{Recall}}$$

where TP (true positive) and FP (false positive) are the number of correctly and incorrectly classified images of infected plants. TN (true negative) and FN (false negative) are the number of correctly and incorrectly classified images of non-infected plants.

RESULTS

In order to obtain an optimal model for the classification of images of maize leaves infected and non-infected by corn leaf worms, a range of values for batch size, dropout and different types of optimisers were tested. The results show notable trends and some striking contrasts in CNN performance based on hyperparameter variations, as summarised in table 3.

Table 3. The time of training and error metrics for models tested (the best model is marked in bold)

No.	Optimiser	Batch size	Dropout	Time	Accuracy	Precision	Recall	Specificity	F1-score
1	SGD	64	0	5:17:18	0.95	0.98	0.90	0.99	0.94
2	SGD	64	0.1	1:20:59	0.93	0.94	0.94	0.93	0.94
3	SGD	64	0.3	5:28:35	0.76	0.58	0.98	0.66	0.73
4	SGD	64	0.49	2:45:03	0.55	1.00	0.55	–	0.71
5	**SGD**	**32**	**0**	**3:48:12**	**0.95**	**0.96**	**0.95**	**0.95**	**0.95**
6	SGD	32	0.1	5:37:00	0.87	0.78	0.97	0.78	0.86
7	SGD	32	0.3	2:40:45	0.90	0.90	0.91	0.88	0.91
8	SGD	32	0.49	1:58:05	0.55	1.00	0.55	–	0.71
9	Adam	64	0	2:01:56	0.59	1.00	0.57	1.00	0.73
10	Adam	64	0.1	2:10:37	0.57	1.00	0.56	1.00	0.72
11	Adam	64	0.3	2:04:28	0.64	1.00	0.60	0.98	0.75
12	Adam	64	0.49	2:04:00	0.58	0.69	0.61	0.54	0.64
13	Adam	32	0	3:37:54	0.84	0.99	0.78	0.99	0.87
14	Adam	32	0.1	4:02:02	0.60	1.00	0.58	1.00	0.73
15	Adam	32	0.3	2:30:59	0.62	1.00	0.59	1.00	0.75
16	Adam	32	0.49	2:08:37	0.55	1.00	0.55	–	0.71
17	Adadelta	64	0	4:48:49	0.91	0.98	0.82	0.98	0.89
18	Adadelta	64	0.1	2:06:07	0.71	1.00	0.65	0.99	0.79
19	Adadelta	64	0.3	2:05:50	0.55	1.00	0.55	–	0.71
20	Adadelta	64	0.49	1:12:27	0.55	1.00	0.55	–	0.71
21	Adadelta	32	0	7:54:10	0.92	0.97	0.90	0.96	0.93

Utilising the Adadelta optimiser with a batch size of 32 and a dropout greater than 0, the training process encountered an issue pertaining to inadequate memory resources, thus resulting in its failure.

The findings reveal considerable variability in accuracy of models and computational time across different configurations, underscoring the critical role of tuning the hyperparameters in optimizing CNN performance for this specific task. The choice of optimizer significantly affects accuracy. In general, the best results were obtained with optimiser SGD and the weakest with optimiser Adam. With the SGD optimiser, the F1-score ranged from 0.71 to 0.95, while with Adam optimizer the F1-score ranged from 0.64 to 0.87. The F1-score is defined as the harmonic mean of the precision and recall, and is widely regarded as a metric that correctly indicates the reliability of a model [Vujovic 2021]. The most common metric utilised for the assessment of classification models is accuracy,

which indicates the percentage of correctly classified cases. Nevertheless, it must be noted that this particular metric is not sufficiently comprehensive in order to provide a full and detailed assessment of the quality of the classifier, particularly in instances where the classes are imbalanced [Chicco and Jurman 2020]. In this work, the test set was reasonably well balanced, and when employing the SGD optimiser, accuracy was in the range of 0.55 to 0.95, with a value of 0.55 occurring in two models where all cases were classified as infected. In the context of plant disease diagnosis, the classifier can be utilised as a component of a decision-making system, in conjunction with a vision system, to determine the application of a plant protection product. The utilisation of chemical plant protection products in situations where they are not required has deleterious consequences for the environment and the economic aspect of crop management. Conversely, the non-application of plant protection products in the event of a disease outbreak can lead to yield losses. Consequently, the classifier developed in this study places significant emphasis on metrics such as recall and specificity. Recall signifies the probability of accurately predicting positive cases, whereas specificity ensures the precision of negative classifications [Baldi et al. 2000]. It was observed that models which achieved high F1-scores and accuracy values also exhibited high recall and specificity values when employing the SGD optimiser. The findings revealed no substantial impact of batch size on the quality of the models obtained. However, it was observed that smaller batch sizes (32) frequently exhibited marginal superiority over larger ones (64). In contrast, the selection of dropout probability proved to be of significant importance. The incorporation of dropout into CNNs is intended to reduce the number of parameters that require adjustment during model training, thereby counteracting the issue of overfitting and reducing the necessary training time. The experimental findings demonstrated that the introduction of dropout typically resulted in a reduction in training time. However, models that employed a low dropout probability value exhibited higher classification quality. For all optimisers employed, the highest classification quality was attained for a batch size of 32 and dropout of 0. Models with longer training times did not necessarily result in higher accuracy, indicating that resource allocation might be optimized by reducing training time without significantly impacting performance.

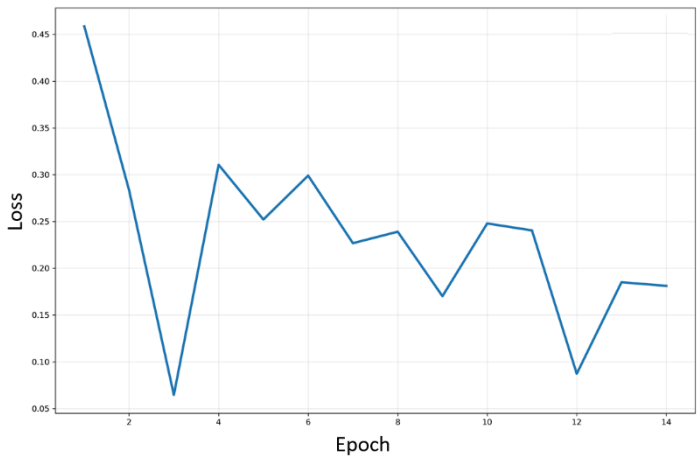

Fig. 3. Loss graph of the best model

The study identified the following models as the most effective classifiers: models 1, 2, 5, 7 and 21. The majority of the metrics analysed for these models exceeded 0.9. Model 5, for which all metrics reached a value of at least 0.95, can be considered the most effective. The loss graph of this model is presented in figure 3 and the confusion matrix showing the classification results is shown in figure 4. The results of the study suggest that a combination of SGD optimiser, low dropout and smaller batch size tends to give optimal results for this CNN on the maize dataset, providing the best possible balance between regularisation and model complexity, thus enhancing the model's ability to generalise well across the dataset.

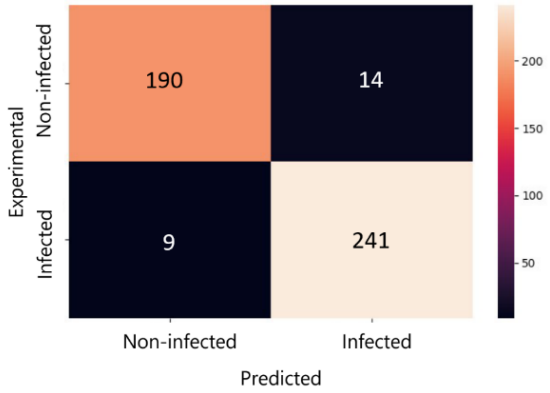

Fig. 4. Confusion matrix obtained from test dataset for the best model

In a departure from standard practice, the authors employ the Softmax function in the final layer for binary classification, even though it is typically used in multi-class scenarios [Duan et al. 2003]. Consequently, the proposed method proves more efficient than the conventional sigmoid function.

The mobile application for the detection of maize infestation by corn leaf worms

The application leverages Discord as a platform to facilitate seamless user interaction while offloading the computational tasks of image recognition and classification to a hosted cloud environment. This approach offers significant advantages. First, since Discord is a widely accessible platform, any user with a phone and a Discord account can use the application without requiring additional installations, making it universally accessible and user-friendly. Additionally, Discord provides a safe and robust environment where user management and communication security are inherently managed, reducing the need for developers to address these aspects independently. By focusing computational resources solely on the cloud-based image classification, the system achieves optimized performance, as it does not expend resources on user interface maintenance or peripheral features.

Furthermore, the hosted environment collects all images uploaded by users, enabling ongoing, seamless improvement of the neural network model through continuous training with real-world data. This process allows for smooth, quick, and painless updates to the

network's capabilities, as the CNN can be re-trained with new data, improving accuracy and adaptability over time. Importantly, users benefit from these updates without needing to adjust or update anything on their devices, as all upgrades are handled directly in the cloud. This architecture thus ensures that users experience consistently enhanced functionality without the complexity or inconvenience of manual updates, making the application both highly accessible and continuously refined. Additionally, as only the initial image transfer is necessary for classification, the application remains effective even with weak internet connectivity, maximizing usability in diverse network environments.

The presented classification system integrates a convolutional neural network with a user-friendly messaging interface. The application employs a pretrained deep learning model built using TensorFlow/Keras framework to perform binary classification of plant images into „infected" or „healthy" categories. The system architecture comprises four primary components: a Discord bot interface utilizing the Discord.py library for user interaction, a CNN model for image classification, an image preprocessing module leveraging PIL (Pillow) for image manipulation, and a comprehensive logging system for tracking user interactions and analysis results. The preprocessing pipeline standardizes input images through RGB conversion, resizing to 400 × 400 pixels, and normalization before feeding them to the neural network, ensuring consistent model performance across various input format files up to 8 MB in size.

The system workflow operates through command-based interactions where users submit plant images via Discord attachments and execute classification using the "!check" command. Upon receiving an image, the application performs multi-stage validation including file format verification, size constraints checking, and image integrity assessment before processing. The CNN model processes the normalized image tensor through batch expansion and generates predictions with binary output corresponding to disease presence or absence. The implementation incorporates robust error handling mechanisms at multiple levels – model loading, image processing, Discord API communication, and file operations – while maintaining comprehensive audit trails through structured logging. This integration of machine learning capabilities with a widely-adopted communication platform provides an accessible and efficient solution for rapid plant health assessment, demonstrating the practical application of deep learning in agricultural disease detection systems. The application is deployed and accessible through the Discord platform on a dedicated server named Traynia, providing users with direct access to the classification service.

Figure 5 demonstrates the application's functionality. As demonstrated in figure 5A, the primary user interface enables the uploading of a photograph of a plant. As demonstrated in figure 5B, the image that has been uploaded for the purposes of evaluation is displayed. As demonstrated in figure 5C, the application yielded the anticipated outcome.

The presented model has the potential for implementation not only on mobile devices, but also as a component of a vision system installed on a drone, for example. The implementation of such a system has the potential to facilitate the monitoring of crops, with a particular focus on large-scale crops. The early and accurate detection of plant infestations facilitates rapid action to control the pest. This approach has the potential to assist in the mitigation of crop losses and the reduction of the adverse economic and environmental consequences associated with the utilisation of chemical plant protection products.

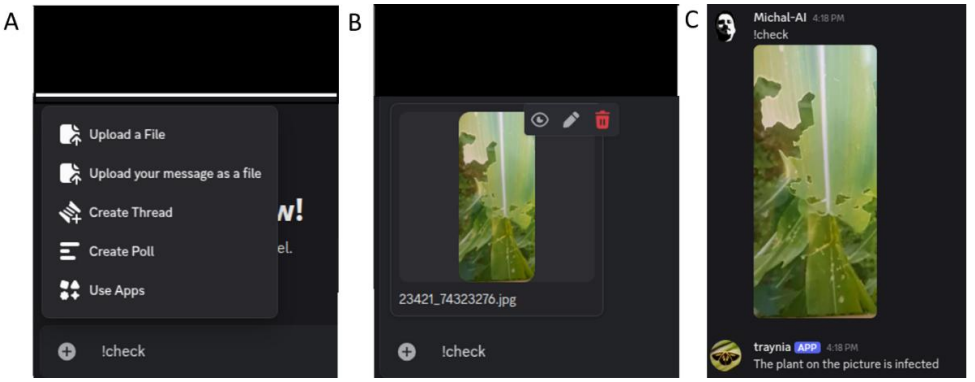

Fig. 5. The example of the functionality of the application. A – the primary user interface, B – the image that has been submitted for analysis, C – the result of the classification

DISCUSSION

Vision systems supported by artificial intelligence tools are becoming increasingly popular in agricultural applications. Convolutional networks are often used in such solutions because of their ability to extract accurate features automatically. They enable accurate classification of various objects, such as pests. Qureshi et al. [2024] proposed a system based on CNN to classify the severity levels of maize stalk rot. The system recognised six classes of stalk rot with an accuracy of 83.58%.

Models based on convolutional networks can work accurately even on devices that do not have large memory resources, such as smartphones. This makes it easy for farmers to use applications that use CNNs. Such applications include the detection and identification of pests and plant diseases. Mallick et al. [2023] presented a CNN model based on MobileNetV2 architecture for detection of six different types of mung bean diseases and four types of pests. They optimised the model and reduced its size from 20.6 MB to 6.02 MB, achieving 93.65% accuracy for the test dataset. This enabled the model to be implemented as a native application on the Android platform. Berka et al. [2023] developed a CNN-based application called CactiViT. The application used a visual image transformer to diagnose cactus cochineal with an average accuracy of 88.34%. The CactiViT mobile application allows the assessment of the health status of cacti based on images captured by the user. Lanjewar and Parab [2024] tested a customised CNN and four pre-trained deep CNNs to recognise citrus leaf diseases (black spot, melanose, canker and greening). The high-accurate (accuracy of 98%, and F1-score of 99%) optimised CNN with 15 layers and a size of 1.68 MB was deployed to the platform as a service cloud and released to the users as a link. Similar research was carried out by Peyal et al. [2023] for diseases of tomato and cotton crops. Their custom CNN model outperformed VGG-16, VGG-19, Inception-V3, MobileNet and MobileNetV2, achieving an accuracy of 97.36% and an F1-score of 97%. The model was implemented as an Android application that can detect 12 different diseases in an average time of 4.84 ms.

It is evident that both transfer learning-based CNNs (e.g., MobileNet, ResNet) and custom CNNs (e.g., the one under discussion) are effective. As demonstrated in this research, the technology is employed in the field of precision agriculture for the purpose of detecting plant diseases and pests. Nevertheless, the decision to develop and optimise a custom CNN classifier constitutes a significant methodological contribution of this study. Whilst transfer learning offers rapid deployment, the architecture presented here focuses on systematic hyperparameter tuning (including optimisers, filter numbers and kernel sizes) to achieve optimal performance for the specific task of detecting corn leaf worm infestations. Additionally, the architecture presented in this study was selected based on preliminary research, which involved training various CNN architectures. Each of the architectures examined was associated with a distinct number of adjustable parameters. Despite the network with a considerably reduced number of parameters (No. 2 in table 1) attaining only marginally lower levels of accuracy, the remaining metrics also exhibited diminished values (precision = 0.93, recall = 0.94, and F1-score = 0.94). In circumstances where the implementation of the model is constrained by limited resources, it is recommended to select that model without a substantial compromise in the quality of classification.

The rigorous approach presented in this study demonstrates that it is possible to achieve state-of-the-art detection accuracy (up to 95% across all key metrics: accuracy, precision, recall, specificity, and F1-score) using a lighter, less complex model dedicated solely to this single-pest problem. This is a critical factor for practical application. Typically, custom models are smaller in size and computationally more efficient, enabling their seamless implementation in user-friendly mobile applications for direct use in the field. Consequently, the high accuracy, when combined with the low computational overhead of the custom architecture, yields a significant practical advantage, namely the ability to execute real-time, highly localized detection. This capacity enables agricultural practitioners to transition from conventional, prophylactic spraying to precision chemical application in affected areas, thereby optimising the utilisation of plant protection products from both economic (cost reduction) and environmental (reduced chemical runoff) perspectives.

CONCLUSIONS

In the field of agriculture, infestations of plant life have been demonstrated to result in considerable economic losses. The rapid and accurate detection of diseases and pest attacks is instrumental in optimising agrotechnical operations, thereby minimising production costs and environmental pollution. The issue is especially pronounced in the context of large-scale crop cultivation, where effective monitoring and management of plant health become particularly challenging. In such cases, the combination of modern vision systems with machine learning algorithms has been proven to be a highly effective solution. Such systems can be installed, for example, on drones and thus automate the crop inspection process. The findings of our research suggest that custom CNN classifiers can be utilised in such systems. The identification of the optimal set of hyperparameters for the model is a prerequisite for the creation of an accurate classifier. In the case of the proposed model, the levels of accuracy, precision, recall, specificity, and F1-score were

determined to be at the 95% level. Moreover, the findings of this study demonstrated that the optimisation of the hyperparameters of model and the training process exerted a substantial influence on the model's accuracy. Depending on these hyperparameters, we obtained models ranging from highly inaccurate to those that may have practical applications. The limitation of this work is that the model has been trained on data concerning only one type of pest. Consequently, the model is capable of accurately identifying leaf damage caused exclusively by corn leaf worm infestations. It is important to note that images showing similar damage caused by other factors, such as hail or other pests, may be classified by the model as corn leaf worm damage. The results presented herein refer to preliminary research that focused on the possibility of using custom CNN structures to recognise plant infestations. Future research will entail the development of models capable of recognising various diseases and pest attacks. In addition to employing convolutional networks for this purpose, it is also planned to utilise quantum tensors, which will facilitate more accurate image analysis, including fine details and interpretation.

REFERENCES

Acharya R., 2020. Corn Leaf Infection Dataset, https://www.kaggle.com/datasets/qramkrishna/corn-leaf-infection-dataset [access: 04.15.2023].

Babendreier D., Toepfer S., Bateman M. et al., 2022. Potential management options for the invasive moth spodoptera frugiperda in Europe. J. Econ. Entomol. 115(6), 1772–1782. https://doi.org/10.1093/JEE/TOAC089

Baldi P., Brunak S., Chauvin Y. et al., 2000. Assessing the accuracy of prediction algorithms for classification: an overview. Bioinformatics 16(5), 412–424. https://doi.org/10.1093/BIOINFORMATICS/16.5.412

Barbedo J.G.A., 2018. Impact of dataset size and variety on the effectiveness of deep learning and transfer learning for plant disease classification. Comput. Electron. Agric. 153, 46–53. https://doi.org/10.1016/J.COMPAG.2018.08.013

Berka A., Hafiane A., Es-Saady Y. et al., 2023. CactiViT: Image-based smartphone application and transformer network for diagnosis of cactus cochineal. Artif. Intell. Agric. 9, 12–21. https://doi.org/10.1016/J.AIIA.2023.07.002

Chicco D., Jurman G., 2020. The advantages of the Matthews correlation coefficient (MCC) over F1 score and accuracy in binary classification evaluation. BMC Genomics 21(1), 1–13. https://doi.org/10.1186/s12864-019-6413-7

Coviello L., Cristoforetti M., Jurman G. et al., 2020. GBCNet: In-field grape berries counting for yield estimation by dilated CNNs. Appl. Sci. 10(14), 4870. https://doi.org/10.3390/APP10144870

Duan K., Keerthi S.S., Chu W. et al., 2003. Multi-category classification by soft-max combination of binary classifiers. In: T. Windeatt, F. Roli (eds), Multiple classifier systems. MCS 2003. Springer–Berlin–Heidelberg. https://doi.org/10.1007/3-540-44938-8_13

Ebrahimi M.A., Khoshtaghaza M.H., Minaei S. et al., 2017. Vision-based pest detection based on SVM classification method. Comput. Electron. Agric. 137, 52–58. https://doi.org/10.1016/J.COMPAG.2017.03.016

FAOSTAT, 2024. https://www.fao.org/faostat/en/#data/QV [access: 23.10.2024].

Ferentinos K.P., 2018. Deep learning models for plant disease detection and diagnosis. Comput. Electron. Agric. 145, 311–318. https://doi.org/10.1016/J.COMPAG.2018.01.009

Gao J., French A.P., Pound M.P. et al., 2020. Deep convolutional neural networks for image-based *Convolvulus sepium* detection in sugar beet fields. Plant Methods 16(1), 1–12. https://doi.org/10.1186/s13007-020-00570-z

Gill H.S., Khalaf O.I., Alotaibi Y. et al., 2022. Multi-model CNN-RNN-LSTM based fruit recognition and classification. Intell. Autom. Soft Comput. 33(1), 637–650. https://doi.org/10.32604/IASC.2022.022589

Hasan A.S.M.M., Sohel F., Diepeveen D. et al., 2021. A survey of deep learning techniques for weed detection from images. Comput. Electron. Agric. 184, 106067. https://doi.org/10.1016/J.COMPAG.2021.106067

Hughes D.P., Salathe M., 2015. An open access repository of images on plant health to enable the development of mobile disease diagnostics. arXiv, 1511.08060. https://doi.org/10.48550/arXiv.1511.08060

Jeger M., Bragard C., Caffier D. et al., 2018. Pest risk assessment of *Spodoptera frugiperda* for the European Union. EFSA J. 16(8). https://doi.org/10.2903/J.EFSA.2018.5351

Jia W., Tian Y., Luo R. et al., 2020. Detection and segmentation of overlapped fruits based on optimized mask R-CNN application in apple harvesting robot. Comput. Electron. Agric. 172, 105380. https://doi.org/10.1016/J.COMPAG.2020.105380

Jiao L., Dong S., Zhang S. et al., 2020. AF-RCNN: An anchor-free convolutional neural network for multi-categories agricultural pest detection. Comput. Electron. Agric. 174, 105522. https://doi.org/10.1016/J.COMPAG.2020.105522

Kamarudin M.H., Ismail Z.H., Saidi N.B., 2021. Deep learning sensor fusion in plant water stress assessment: a comprehensive review. Appl. Sci. 11(4), 1403. https://doi.org/10.3390/APP11041403

Khan S., Tufail M., Khan M.T. et al., 2021. Deep-learning-based spraying area recognition system for unmanned-aerial-vehicle-based sprayers. Turk. J. Elec. Eng. Comp. Sci. 29(1), 241–256. https://doi.org/10.3906/elk-2004-4

Khanramaki M., Askari Asli-Ardeh E., Kozegar E., 2021. Citrus pests classification using an ensemble of deep learning models. Comput. Electron. Agric. 186, 106192. https://doi.org/10.1016/J.COMPAG.2021.106192

Kussul N., Lavreniuk M., Skakun S. et al., 2017. Deep learning classification of land cover and crop types using remote sensing data. IEEE Geosci. Remote Sens. Lett. 14(5), 778–782. https://doi.org/10.1109/LGRS.2017.2681128

Lanjewar M.G., Panchbhai K.G., 2023. Convolutional neural network based tea leaf disease prediction system on smart phone using paas cloud. Neural Comput. App. 35(3), 2755–2771. https://doi.org/10.1007/S00521-022-07743-y

Lanjewar M.G., Parab J.S., 2024. CNN and transfer learning methods with augmentation for citrus leaf diseases detection using PaaS cloud on mobile. Multimed. Tools App. 83(11), 31733–31758. https://doi.org/10.1007/S11042-023-16886-6

Li Y., Wang H., Dang L.M. et al., 2020. Crop pest recognition in natural scenes using convolutional neural networks. Comput. Electron. Agric. 169, 105174. https://doi.org/10.1016/J.COMPAG.2019.105174

Loyani L., Machuve D., 2021. A deep learning-based mobile application for segmenting tuta absoluta's damage on tomato plants. Eng. Technol. Appl. Sci. Res. 11(5), 7730–7737. https://doi.org/10.48084/ETASR.4355

Mallick M.T., Biswas S., Das A.K. et al., 2023. Deep learning based automated disease detection and pest classification in Indian mung bean. Multimed. Tools App. 82(8), 12017–12041. https://doi.org/10.1007/S11042-022-13673-7

Mohan K.J., Balasubramanian M., Palanivel S., 2016. Detection and recognition of diseases from paddy plant leaf images. Int. J. Comput. App. 144(12), 975–8887.

Mohanty S.P., Hughes D.P., Salathé M., 2016. Using deep learning for image-based plant disease detection. Front. Plant Sci. 7, 215232. https://doi.org/10.3389/FPLS.2016.01419

Bosco de Oliveira A. (ed.), 2019. Abiotic and biotic stress in plants. IntechOpen. https://doi.org/10.5772/intechopen.77845

Peyal H.I., Nahiduzzaman M., Pramanik M.A.H. et al., 2023. Plant disease classifier: detection of dual-crop diseases using lightweight 2D CNN architecture. IEEE Access 11, 110627–110643. https://doi.org/10.1109/ACCESS.2023.3320686

Qureshi S.H., Khan D.M., Razzaq A. et al., 2024. Comparison of conventional and computer-based detection of severity scales of stalk rot disease in maize. Sabrao J. Breed. Genet. 56(1), 292–301. https://doi.org/10.54910/SABRAO2024.56.1.26

Srivastava A.K., Safaei N., Khaki S. et al., 2022. Winter wheat yield prediction using convolutional neural networks from environmental and phenological data. Sci. Rep. 12(1), 1–14. https://doi.org/10.1038/s41598-022-06249-w

Storey G., Meng Q., Li B., 2022. Leaf disease segmentation and detection in apple orchards for precise smart spraying in sustainable agriculture. Sustainability 14(3), 1458. https://doi.org/10.3390/SU14031458

Thenmozhi K., Srinivasulu Reddy U., 2019. Crop pest classification based on deep convolutional neural network and transfer learning. Comput. Electron. Agric. 164, 104906. https://doi.org/10.1016/J.COMPAG.2019.104906

van den Berg J., Britz C., du Plessis H., 2021. Maize Yield response to chemical control of *Spodoptera frugiperda* at different plant growth stages in South Africa. Agriculture 11(9), 826. https://doi.org/10.3390/AGRICULTURE11090826

Vujovic Z., 2021. Classification model evaluation metrics. Int. J. Adv. Comput. Sci. Appl. 12(6). https://doi.org/10.14569/IJACSA.2021.0120670

Wang J., Li Y., Feng H. et al., 2020. Common pests image recognition based on deep convolutional neural network. Comput. Electron. Agric. 179, 105834. https://doi.org/10.1016/J.COMPAG.2020.105834

Xu W., Sun L., Zhen C. et al., 2022. Deep learning-based image recognition of agricultural pests. Appl. Sci. 12(24), 12896. https://doi.org/10.3390/APP122412896

Yang C., Teng Z., Dong C. et al., 2022. In-field citrus disease classification via convolutional neural network from smartphone images. Agriculture 12(9), 1487. https://doi.org/10.3390/AGRICULTURE12091487

Data availability statement: The software used in the study are openly available in repository: https://bazawiedzy.upwr.edu.pl/info/researchdata/UPWR0067067009ef4735aefdad4793e1b6df/.

The source of funding: Wrocław University of Environmental and Life Sciences.

Received: 9.07.2025
Accepted: 19.11.2025
Published: 31.12.2025

AGRONOMY SCIENCE

VOL. LXXX (4) 2025

https://doi.org/10.24326/as.2025.5548

Department of Plant Physiology and Biotechnology, Faculty of Technology and Life Sciences, University of Rzeszów, Ćwiklinskiej 2, 35-601 Rzeszów, Poland

e-mail: bjacek@ur.edu.pl

BEATA JACEK https://orcid.org/0000-0001-8517-2095

Preliminary assessment of the effectiveness of non-fungicide methods of maize seed treatment

Wstępna ocena skuteczności niefungicydowych metod zaprawiania nasion kukurydzy

Abstract. Many plant diseases are transmitted through seeds. Thus, seed dressing is the first and most important protective measure. It promotes germination, increases seed vigour, improves rooting, and effectively controls pathogens. Due to the reduction of chemical plant protection products on the market, new products are being sought. Therefore, the aim of the present study was to preliminarily assess non-fungicidal methods that significantly reduce seed contamination before sprouting and do not affect germination rates and initial maize growth. The following non-fungicidal seed surface-sterilisation methods were tested: hypochlorous acid, sodium and calcium hypochlorite, peracetic acid and non-ionic nanosilver for 5, 10, 20 or 30 minutes of soaking. Dish and pot experiments were carried out. Among the tested treatments, hypochlorous acid and calcium hypochlorite were the most effective, resulting in the least seed contamination and the highest maize germination. These treatments also significantly enhanced plant height, root elongation and its fresh weight. However, the remaining treatment methods using sodium hypochlorite, peracetic acid and nanosilver were ineffective. Additionally, a pot experiment was carried out to evaluate the effect of non-fungicide seed treatments. The positive effect of hypochlorous acid and calcium hypochlorite on germination capacity, plant growth and weight, as well as its physiological condition, was also confirmed.

Keywords: calcium hypochlorite, hypochlorous acid, seed dressing, germination, natural plant protection products

INTRODUCTION

In contemporary agriculture, farmers face increasing challenges due to climate change, biodiversity loss, and environmental degradation [Gai and Wang 2024]. At the same time, there has been a noticeable rise in plant diseases caused by bacterial, fungal,

Citation: Jacek B., 2025. Preliminary assessment of the effectiveness of non-fungicide methods of maize seed treatment Agron. Sci. 80(4), 57–67. https://doi.org/10.24326/as.2025.5548

and viral pathogens. According to Nazarov et al. [2020], in favourable conditions, diseases can affect up to 70–80% of the total plant population, and crop yields can decline by as much as 80–98%. Thus, the threat from crop diseases continues to grow, posing a risk to food security and agricultural productivity. Chemical control has long been the mainstay of plant disease management. However, one significant problem in recent years has been the progressive reduction of chemical plant protection products on the market, largely due to regulatory and environmental concerns. Therefore, there is a need to develop more environmentally friendly, safe, and sustainable integrated control strategies and technologies for plant diseases.

Pathogens affect plants at various stages of agricultural production, ranging from seed germination to growth, harvest, and storage. The basic condition for achieving high yields with good quality parameters is the use of high-quality seed material as well as its proper dressing. Seed dressing is a common agricultural practice that improves germination rates, protects against pathogens, and enhances crop productivity. These treatments are of great importance in the development of vigorous and healthy plants from the initial stages of growth [Madruga et al. 2023].

Many plant diseases are transmitted through seeds that are colonised by various bacteria and fungi, and some may be detrimental to the germination and subsequent growth of seedlings [Hong et al. 2023, Surovy et al. 2023]. The result of this damage is a reduction and deterioration in the quality of the obtained crops. Thus, seed treatment is essential and beneficial for all crops, aiming to eliminate and control pathogens that attack seeds, seedlings and plants [Madruga et al. 2023]. It is particularly crucial for maize seeds, which can be susceptible to a range of fungal pathogens, including those belonging to the *Fusarium* genus. Thus, maize seed treatment is the first and most important protective measure during the early stages of its growth. This treatment can significantly increase germination velocity, resulting in improved seedling establishment, particularly under varying environmental conditions [Rossini et al. 2024]. Furthermore, seed dressing inhibits post-emergent diseases, contributing to better plant health [Yang et al. 2022, Kardava et al. 2023].

Due to the withdrawal of chemical dressings from the market, it is necessary to explore alternative methods of dressing seed material before sowing. Maize is an important agricultural crop, ranking third globally in both harvested area and total production [Tobiasz-Salach et al. 2023]. It can be used for fodder, food, and industrial and energy purposes, as well as in the phytoremediation process. Non-fungicide maize seed treatment methods offer viable alternatives to chemical products, particularly in light of growing concerns about pesticide use and its impact on health and the environment. These methods must focus on promoting germination, increasing seed vigour and effectively controlling pathogens. Therefore, the aim of the present study was to preliminarily assess non-fungicidal methods that can significantly reduce seed contamination before sprouting and do not adversely affect germination rates and the appropriate growth of maize.

MATERIAL AND METHODS

The maize seeds came from the 2024 harvest. The following seed dressing methods were used: soaking in 0.05% hypochlorous acid (produced by Bio ActiW), 10% sodium hypochlorite or 10% calcium hypochlorite (Chempur), 1% peracetic acid (Pol-Aura) and

0.01% non-ionic colloidal nanosilver (Uni-Farma). All seeds were soaked in these solutions for 5, 10, 20 or 30 minutes and then washed in sterile distilled water to remove the solution.

After the surface sterilisation, the maize seeds were placed in a 90 mm Petri dish with Potato Dextrose Agar (PDA) medium. The experiment included five replicates for each treatment and time point, with each replicate containing five seeds. The control consisted of undressed seeds. All plates were incubated at 28°C for 4 days. Then, the Petri dishes with seeds were placed in the phytotron at 20°C/15°C under a 14-hour/10-hour (day/night) photoperiod. Germination energy was assessed after 4 days, and germination capacity after 10 days. The percentage of seed infection was calculated at 4 and 14 days after the start of the experiment. Additionally, shoot and root length, as well as fresh root mass, were measured after one month of growth.

At the same time, the experiment was conducted in a greenhouse from June to July 2025. The maize seeds were sown in plastic pots filled with a mixture of Jiffy and QTS substrates (1 : 1, volume basis). Five surface-sterilised seeds were planted in each pot. Three replications for each treatment and sterilisation time point were performed. The plants were grown in a greenhouse at 25°C (±5) and 80–90% relative humidity for 4 weeks. The watering was performed based on water demand. Then, the shoot length and diameter, average root length and above-ground and below-ground mass of plants were determined. The index of leaf greenness (relative chlorophyll content) expressed in SPAD units was recorded using a portable Chlorophyll Meter SPAD-502 Plus.

Statistical analysis was performed using Statistica v.13.1. An ANOVA and the LSD mean separation test were used at a significance level of 0.05.

RESULTS AND DISCUSSION

Seed dressing is the first and most important protective measure during the early stages of plant growth [Kowalska and Łukaszyk 2022]. It can significantly increase crop yield by improving germination, stimulating root development, enhancing nutrient uptake and protecting plants against diseases [Madruga et al. 2023]. However, the number of registered chemical seed dressings in Poland has been decreasing annually [Kowalska and Łukaszyk 2022]. Additionally, chemical dressings are not allowed in organic farming. Therefore, new, environmentally friendly and non-invasive methods of eliminating pathogens from seed coats are being sought.

Different degree of effectiveness of the treatments used in reducing the level of surface contamination of the maize seed was found. After 14 days, seed infection ranged from 3 to 100%. The most effective was peracetic acid, but it significantly reduced seed germination, even after 5 minutes of soaking (tab. 1). Furthermore, after treatment with peracetic acid for more than 20 min, the maize seeds lost their ability to germinate (fig. 1). Similarly, Wilson [1976] found that the germination of wheat and soybean seeds was reduced after treatment with peracetic acid. Effective disinfectants must significantly reduce seed contamination without significantly reducing the germination percentage. Thus, peracetic acid cannot be recommended for corn dressing. Nevertheless, peracetic acid is gaining increasing attention as a powerful disinfectant, particularly within the agricultural and food processing sectors [Hopkins et al. 2003, Lee et al. 2016, Şehirli et al. 2020]. Its broad-spectrum antimicrobial activity allows it to inactivate various microorganisms, particularly bacteria and fungi, effectively.

Table 1. The effect of different seed treatments on germination and growth of maize plants using the agar method

Time of treatment (min)	Seed infection (%)		Germination energy (%)	Germination capacity (%)	Shoot length (cm)	Root length (cm)	Root mass (g)
	after 4 days	after 14 days					
control							
0	80 ^{C}	100 ^{C}	52 ^{BC}	60 ^{B}	0.9 ^{A}	1.9 ^{AB}	0.020 ^{AB}
hypochlorous acid							
5	4 ^{a}	12 ^{a}	76 ^{a}	96 ^{a}	5.7 ^{a}	18.1 ^{ab}	0.352 ^{a}
10	0 ^{a}	8 ^{a}	72 ^{a}	92 ^{a}	10.3 ^{b}	21.6 ^{b}	0.536 ^{a}
20	0 ^{a}	0 ^{a}	64 ^{a}	76 ^{a}	6.9 ^{ab}	16.3 ^{ab}	0.450 ^{a}
30	0 ^{a}	0 ^{a}	64 ^{a}	84 ^{a}	8.2 ^{ab}	14.8 ^{a}	0.391 ^{a}
$\bar{x}$	1 ^{A}	5 ^{A}	69 ^{C}	87 ^{C}	7.8 ^{B}	17.7 ^{D}	0.432 ^{D}
sodium hypochlorite							
5	0 ^{a}	8 ^{a}	40 ^{a}	64 ^{a}	0.8 ^{a}	4.3 ^{a}	0.105 ^{a}
10	4 ^{a}	4 ^{a}	40 ^{a}	60 ^{a}	1.0 ^{a}	4.6 ^{a}	0.122 ^{a}
20	0 ^{a}	8 ^{a}	44 ^{a}	68 ^{a}	1.1 ^{a}	5.4 ^{a}	0.168 ^{a}
30	0 ^{a}	4 ^{a}	36 ^{a}	48 ^{a}	0.9 ^{a}	2.6 ^{a}	0.056 ^{a}
$\bar{x}$	1 ^{A}	6 ^{A}	40 ^{B}	60 ^{B}	1.0 ^{A}	4.2 ^{B}	0.116 ^{B}
calcium hypochlorite							
5	16 ^{a}	24 ^{a}	72 ^{ab}	92 ^{b}	7.2 ^{a}	4.8 ^{a}	0.107^{a}
10	12 ^{a}	16 ^{a}	56 ^{a}	84^{ab}	8.9 ^{ab}	9.2 ^{ab}	0.261 ^{ab}
20	12 ^{a}	12 ^{a}	56 ^{a}	80^{a}	10.0 ^{ab}	13.2 ^{bc}	0.360 ^{b}
30	0 ^{a}	4 ^{a}	80 ^{b}	84^{ab}	12.1 ^{b}	14.6 ^{c}	0.307 ^{b}
$\bar{x}$	10 ^{B}	14 ^{B}	66 ^{C}	85^{C}	9.6 ^{C}	10.5 ^{C}	0.259 ^{C}
peracetic acid							
5	0 ^{a}	0 ^{a}	0 ^{a}	16^{a}	1.2 ^{b}	7.4 ^{c}	0.154 ^{b}
10	4 ^{a}	8 ^{a}	0 ^{a}	48^{a}	0.9 ^{b}	3.2 ^{b}	0.083 ^{ab}
20	0 ^{a}	4 ^{a}	0 ^{a}	0^{a}	0.2 ^{a}	0.0 ^{a}	0.000 ^{a}
30	0 ^{a}	0 ^{a}	0 ^{a}	0^{a}	0.0 ^{a}	0.0 ^{a}	0.000 ^{a}
$\bar{x}$	1 ^{A}	3 ^{A}	0 ^{A}	16^{A}	0.6 ^{A}	2.8 ^{AB}	0.062 ^{AB}
non-ionic nanosilver							
5	88 ^{a}	100 ^{a}	40 ^{a}	40^{a}	0.7 ^{a}	1.2 ^{a}	0.010 ^{a}
10	96 ^{a}	100 ^{a}	44 ^{a}	44^{a}	0.8 ^{a}	1.5 ^{a}	0.014 ^{a}
20	100 ^{a}	100 ^{a}	56 ^{a}	56^{a}	1.0 ^{a}	1.0 ^{a}	0.008 ^{a}
30	100 ^{a}	100 ^{a}	60 ^{a}	64^{a}	1.0 ^{a}	2.1 ^{a}	0.017 ^{a}
$\bar{x}$	96 ^{D}	100 ^{C}	50 ^{B}	51^{B}	0.9 ^{A}	1.4 ^{A}	0.012 ^{A}

Different letters within the columns indicate significant differences ($p < 0.05$) according to the LSD test, ower-case letters indicate significant differences among treatment time periods ($p < 0.05$) according to the LSD test

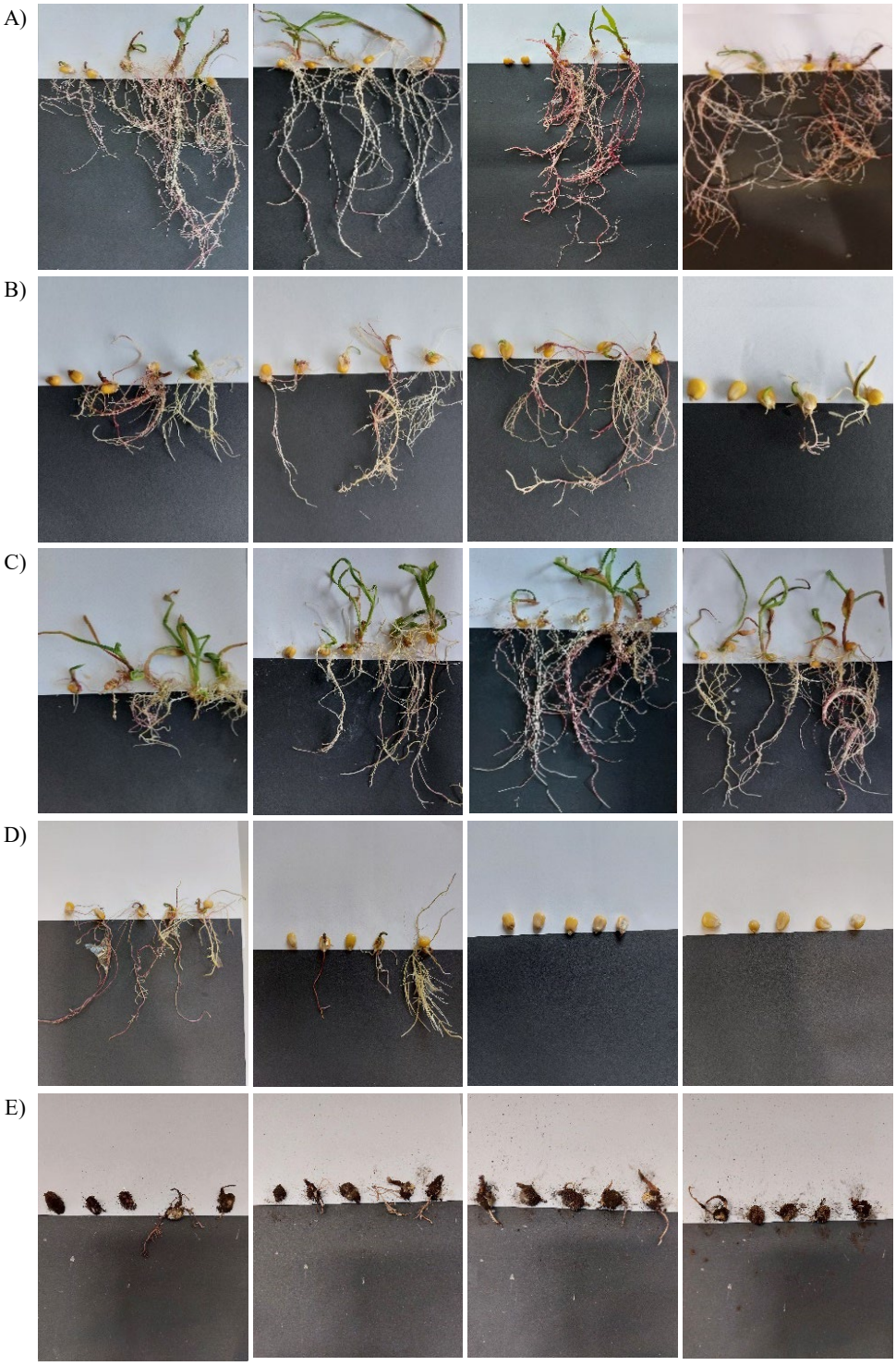

Fig. 1. Comparison of maize growth and development depending on the seed treatment: A) hypochlorous acid, B) sodium hypochlorite, C) calcium hypochlorite, D) peracetic acid, E) non-ionic nanosilver

One promising method of seed treatment is the use of hypochlorous acid. Several studies have demonstrated that this treatment reduces microbiological contamination on seed surfaces [Goo and Koo 2020, Gilbert et al. 2023, Saikumar et al. 2023]. In this study, this effect was confirmed, as on average, 95% of the maize seeds were not infected. Furthermore, seed infection was completely eliminated by 20- and 30-minute treatments with hypochlorous acid. This capacity for microbial reduction is crucial, as surface contamination can adversely affect seed germination and subsequent plant health. At the same time, seed treatment with hypochlorous acid showed a 27% improvement in germination capacity compared to the control. It suggests that this treatment can be a beneficial method for enhancing seed germination. However, hypochlorous acid must be prepared fresh, as it is unstable and loses its antimicrobial effectiveness within a few days [Gilbert et al. 2023].

The calcium hypochlorite prevented the growth of microbial contaminants present on the maize seed surface to a lesser extent. After 2 weeks, 14% of the maize seeds were infected using the agar method. However, the effectiveness of this treatment increased with the length of soaking time, from 24% to 4% (tab. 1). It can be assumed that the longer the treatment time, the better the effect of seed sterilisation and the greater the reduction in pathogens. Additionally, the use of calcium hypochlorite significantly increased maize germination capacity compared to the control (tab. 1). After 10 days, 85% of the seeds had germinated, a substantially higher rate than the untreated seeds. Similarly, Dempsey and Walker [1973] found that calcium hypochlorite was an effective surface disinfectant of pepper seed and did not reduce germination. Calcium hypochlorite has also been previously tested for the disinfection of alfalfa seeds and sprouts against *Escherichia coli* and *Salmonella enterica* [Gandhi and Matthews 2003, Ding et al. 2013, Kim et al. 2025].

Sodium hypochlorite is a substance commonly used for explant surface decontamination in *in vitro* plant cultures [Yildiz and Ekiz 2014, Hesami et al. 2017, Bošnjak Mihovilović et al. 2024]. In the present study, the sodium hypochlorite significantly eliminated maize seed infection, but the germination rate was similar to that of untreated seeds. This result is consistent with Dempsey and Walker [1973]. They reported that sodium hypochlorite was more effective in sterilising pepper seeds than calcium hypochlorite, but its germination was reduced. On the other hand, Gilbert et al. [2023] obtained different results. They reported that sodium hypochlorite was an effective treatment for reducing fungal growth on seeds, without harming germination rates. However, they used a lower solution concentration – 0.6% instead of 10%. Similarly, the use of nanosilver showed a comparable germination to the control. Additionally, it was found that there is a relationship between the duration of silver treatment and the germination capacity of seeds. Longer exposure to silver was associated with a higher rate of maize seed germination, from 40% to 64%. However, under the silver treatment, all seeds were contaminated by fungal pathogens within 14 days. Nevertheless, the positive impacts of silver nanoparticles have been noted in agriculture [Khan et al. 2023, Rahman et al. 2023, de Almeida Junior et al. 2024, Al Salama et al. 2025].

The impact of non-fungicide seed dressing solutions on the initial growth and development of maize plants was also determined. Among the tested treatments, hypochlorous

acid and calcium hypochlorite were the most effective, with the lowest rate of contamination and the highest germination rates. Additionally, surface sterilisation treatment does not appear to impact the growth of shoots and roots. Maize plants treated with hypochlorous acid and calcium hypochlorite exhibited significantly higher growth compared to the control (tab. 1, fig. 1). These treatments significantly increased plant height, root elongation and its fresh weight. Furthermore, longer exposure to calcium hypochlorite was observed to stimulate shoot growth and root elongation. All other treatments proved to be inhibitors of plant growth. The treatment of maize seeds with nanosilver, peracetic acid and sodium hypochlorite resulted in statistically similar growth of seedlings compared to the untreated control. It can be assumed that microbiological infections at the seed germination stage can inhibit rooting and further plant growth. Moreover, longer exposure to peracetic acid significantly reduced shoot length and root development.

At the same time, a pot experiment was established. After 10 days, the untreated maize seeds germinated at a level of 60%. Similarly, the application of sodium hypochlorite resulted in the same germination rate as the control. In contrast, peracetic acid completely inhibited maize germination, even after 5 min of soaking. Particularly, the use of hypochlorous acid and calcium hypochlorite increased the maize germination capacity (tab. 2). The results of the pot experiment were consistent with those obtained using the agar plate method.

Maize plants treated with calcium hypochlorite exhibited improved growth compared to untreated plants. The plants were on average over 80 cm in height and almost 1 cm in diameter, with roots extending over 20 cm. This seed treatment method was found to be the most effective treatment, resulting in improved shoot and root elongation, particularly during the 20- and 30-minute treatments (tab. 2). Hypochlorous acid treatment was also effective for initial maize growth and development. These plants reached a length of almost 80 cm and a shoot base diameter of nearly 0.8 cm. Faster seed germination is crucial for successful corn growth, as it allows for earlier emergence and reduces the time plants are vulnerable to diseases, pests, and environmental stress. Thus, this leads to better overall growth and potentially higher yields.

In turn, sodium hypochlorite, commonly used for sterilisation, limited the development of maize plants during the studied exposure periods. Similarly, silver nanoparticles, while used for their antimicrobial properties, also inhibited the early stages of maize development. A slower seed germination rate was also observed in silver treatments. However, the use of silver treatment has been shown to have a significant impact on the physiological state of plants. The highest SPAD leaf greenness index was found for silver-treated maize plants. Peracetic acid completely inhibited seed germination, regardless of the treatment duration. Similarly, Vines et al. [2003] found that peracetic acid has phytotoxic effects.

Plant mass production is also a crucial factor in determining plant yield [do Moraes Gatti et al. 2023]. In this study, the fresh shoot mass ranged from 13 to 20 g, while the fresh root mass ranged from 4 to 10 g per plant after a month. The use of calcium hypochlorite proved to be the most effective strategy for increasing the underground and aboveground mass of maize (tab. 2). Longer exposure to calcium hypochlorite was observed to stimulate shoot growth and root elongation. Similarly, the use of hypochlorous acid contributed to increased shoot and root mass.

Table 2. Effect of different seed treatments on maize seed germination and growth in pot experiment

Time of treatment (min)	Germination capacity (%)	Shoot length (cm)	Shoot diameter (mm)	Average root length (cm)	Fresh shoot mass (g)	Fresh root mass (g)	SPAD index
control							
0	60 ^{BC}	74.2 ^{BC}	7.3^{BC}	18.0^{BC}	13.9^{BC}	4.3 ^{B}	34.4 ^{BC}
hypochlorous acid							
5	93 ^{a}	79.8 ^{a}	8.3^{a}	20.0^{a}	17.2 ^{a}	6.7 ^{a}	34.0 ^{a}
10	87 ^{a}	80.0 ^{a}	5.8^{a}	19.8^{a}	19.2 ^{a}	9.2 ^{a}	34.7 ^{a}
20	80 ^{a}	77.6 ^{a}	9.4^{a}	21.9^{a}	13.6 ^{a}	7.8 ^{a}	33.6 ^{a}
30	80 ^{a}	75.3 ^{a}	8.0^{a}	19.0^{a}	17.7 ^{a}	7.5 ^{a}	33.1 ^{a}
$\bar{x}$	85 ^{D}	78.2 ^{C}	7.7^{B}	20.0^{CD}	17.2 ^{BC}	7.8 ^{C}	33.9 ^{B}
sodium hypochlorite							
5	53 ^{a}	76.8 ^{b}	7.7 ^{a}	17.3 ^{a}	14.2 ^{a}	3.7 ^{a}	33.7 ^{b}
10	53 ^{a}	70.3 ^{ab}	7.6 ^{a}	18.2 ^{a}	17.6 ^{a}	5.6 ^{a}	31.7 ^{ab}
20	73 ^{a}	57.9 ^{a}	5.7 ^{a}	14.9 ^{a}	9.7 ^{a}	3.5 ^{a}	29.3 ^{a}
30	60 ^{a}	63.5 ^{ab}	5.9 ^{a}	16.7 ^{a}	10.1 ^{a}	2.7 ^{a}	33.6 ^{b}
$\bar{x}$	60 ^{BC}	67.4 ^{B}	6.8 ^{B}	16.8^{B}	13.1 ^{B}	4.0 ^{B}	32.0 ^{B}
calcium hypochlorite							
5	100 ^{b}	77.2 ^{a}	9.1 ^{a}	18.2 ^{a}	16.6 ^{a}	7.6 ^{a}	35.9 ^{a}
10	73 ^{a}	80.8 ^{a}	9.4 ^{a}	21.0 ^{a}	19.1 ^{a}	9.2 ^{a}	35.0 ^{a}
20	50 ^{a}	84.5 ^{a}	10.7 ^{a}	24.6 ^{a}	20.5 ^{a}	13.8 ^{b}	37.9 ^{a}
30	67 ^{a}	88.2 ^{a}	10.2 ^{a}	22.7 ^{a}	22.0 ^{a}	10.9 ^{ab}	37.2 ^{a}
$\bar{x}$	72 ^{CD}	83.0 ^{C}	9.8 ^{C}	21.7 ^{D}	19.8 ^{C}	10.3 ^{D}	36.4 ^{C}
peracetic acid							
5	0 ^{a}	0.0 ^{a}	0.0 ^{a}	0.0 ^{a}	0.0 ^{a}	0.0 ^{a}	0.0 ^{a}
10	0 ^{a}	0.0 ^{a}	0.0 ^{a}	0.0 ^{a}	0.0 ^{a}	0.0 ^{a}	0.0 ^{a}
20	0 ^{a}	0.0 ^{a}	0.0 ^{a}	0.0 ^{a}	0.0 ^{a}	0.0 ^{a}	0.0 ^{a}
30	0 ^{a}	0.0 ^{a}	0.0 ^{a}	0.0 ^{a}	0.0 ^{a}	0.0 ^{a}	0.0 ^{a}
$\bar{x}$	0 ^{A}	0.0 ^{A}	0.0 ^{A}	0.0 ^{A}	0.0 ^{A}	0.0 ^{A}	0.0 ^{A}
non-ionic nanosilver							
5	40 ^{a}	81.8 ^{b}	8.9 ^{a}	18.4 ^{a}	15.9 ^{ab}	8.6 ^{b}	41.3 ^{a}
10	40 ^{a}	86.0 ^{b}	7.3 ^{a}	18.1 ^{a}	21.3 ^{b}	6.4 ^{ab}	39.1 ^{a}
20	60 ^{ab}	73.9 ^{ab}	7.4 ^{a}	17.0 ^{a}	10.3 ^{ab}	3.8 ^{a}	37.3 ^{a}
30	80 ^{b}	59.3 ^{a}	5.0 ^{a}	15.0 ^{a}	8.6 ^{a}	3.2 ^{a}	33.4 ^{a}
$\bar{x}$	53 ^{B}	76.1 ^{BC}	7.5 ^{B}	17.3^{B}	13.7 ^{B}	5.8 ^{BC}	38.3 ^{C}

Different letters within the columns indicate significant differences ($p < 0.05$) according to the LSD test, lowercase letters indicate significant differences among treatment time periods ($p < 0.05$) according to the LSD test

CONCLUSIONS

Seed dressing is the most effective method for protecting plants from diseases during the early growth stages. However, one significant problem in recent years has been the progressive reduction of chemical plant protection products on the market. Preliminary studies on non-fungicide seed treatments are promising in maize protection. The use of calcium hypochlorite and hypochlorous acid significantly reduced the seed-borne pathogens, which is beneficial during the period of seed germination. These treatments also enhanced the germination capacity and improved maize plant growth and root development. It was observed that longer exposure to calcium hypochlorite stimulated shoot growth and root elongation. Thus, the use of calcium hypochlorite and hypochlorous acid is a promising method for seed treatment. These treatments can be used as a supplement to chemical plant protection products. However, the research was conducted under *in vitro* and greenhouse conditions and further studies are needed. It is also necessary to extend the research to include field experiments. It should be noted, however, that products used for sterilisation may disturb the microbiological balance under natural conditions.

In contrast, peracetic acid, which significantly reduces microbial growth and significantly reduces seed germination, will not be an effective method for maize seed surface sterilisation. Exposure to peracetic acid significantly reduced the shoot length and root development of maize plants. The remaining seed treatment methods using sodium hypochlorite and nanosilver were also ineffective. Moreover, the silver nanoparticles cannot eliminate all pathogens from the seed coat. Silver nanoparticle treatments were included solely as an experimental option, tested under controlled *in vitro* and greenhouse conditions, and not as a recommended method for field-ready use. Nanoparticle-based treatments are currently not considered standard, environmentally friendly practices in agriculture.

REFERENCES

Al Salama Y., Alghoraibi I., Zein R. et al., 2025. Silver nanoparticles seed priming for sustainable enhancement of durum wheat growth, yield, and nutrient enrichment. Instit. Engineer. Technol. Nanobiotechnol. 1, 6152486. https://doi.org/10.1049/nbt2/6152486

Bošnjak Mihovilović A., Kereša S., Lazarević B. et al., 2024. The use of sodium hypochlorite and plant preservative mixture significantly reduces seed-borne pathogen contamination when establishing *in vitro* cultures of wheat (*Triticum aestivum* L.) seeds. Agriculture 14, 556. https://doi.org/10.3390/agriculture14040556

de Almeida Junior J.H.V., Brignoli F.M., Neto M.E. et al., 2024. Synthesis of silver and cobalt nanoparticles and assessment of their effects on Environ. Saf. 287, 117257. https://doi.org/10.1016/j.ecoenv.2024.117257

Dempsey A.H., Walker J.T., 1973. Efficacy of calcium and sodium hypochlorite for seed treatment of pepper. Hortscience 8(4), 328–329.

Ding H., Fu T.J., Smith M.A., 2013. Microbial contamination in sprouts: how effective is seed disinfection treatment?. J. Food Sci. 78(4), R495–R501. https://doi.org/10.1111/1750-3841.12064

do Moraes Gatti V.C., da Silva Barata H., Silva V.F.A. et al., 2023. Influence of calcium on the development of corn plants grown in hydroponics. AgriEngineering 5, 623–630. https://doi.org/10.3390/agriengineering5010039

Gai Y., Wang H., 2024. Plant disease: a growing threat to global food security. Agronomy 14, 1615. https://doi.org/10.3390/agronomy14081615

Gandhi M., Matthews K.R., 2003. Efficacy of chlorine and calcinated calcium treatment of alfalfa seeds and sprouts to eliminate *Salmonella*. Int. J. Food Microbiol. 87, 301–306. https://doi.org/10.1016/S0168-1605(03)00108-9

Gilbert G.S., Diaz A., Bregoff H.A., 2023. Seed disinfestation practices to control seed-borne fungi and bacteria in home production of sprouts. Foods 12, 747. https://doi.org/10.3390/foods12040747

Goo S.G., Koo J., 2020. Establishment of rice bakanae disease management using slightly acidic hypochlorous acid water. J. Life Sci. 30(2), 178–185. https://doi.org/10.5352/JLS.2020.30.2.178

Hesami M., Daneshvar M.H., Lotfi-Jalalabadi A., 2017. The effect of sodium hypochlorite on control of *in vitro* contamination and seed germination of *Ficus religiosa*. Iran. J. Plant Physiol. 7(4), 2157–2162. https://doi.org/10.22034/ijpp.2017.537980

Hong J.K., Baek J., Park S.R., Lee G.S. et al., 2023. A new protocol to mitigate damage to germination caused by black layers in maize (*Zea mays* L.) seeds. Agriculture 13, 2147. https://doi.org/10.3390/agriculture13112147

Hopkins D.L., Thompson C.M., Hilgren J. et al., 2003. Wet seed treatment with peroxyacetic acid for the control of bacterial fruit blotch and other seedborne diseases of watermelon. Plant Dis. 87(12), 1495–1499. https://doi.org/10.1094/PDIS.2003.87.12.1495

Kardava K., Tetz V., Vecherkovskaya M. et al., 2023. Seed dressing with M451 promotes seedling growth in wheat and reduces root phytopathogenic fungi without affecting endophytes. Front. Plant Sci. 14, 1176553. https://doi.org/10.3389/fpls.2023.1176553

Khan S., Zahoor M., Khan R.S. et al., 2023. The impact of silver nanoparticles on the growth of plants: the agriculture applications. Heliyon 9, e16928. https://doi.org/10.1016/ j.heliyon.2023.e16928

Kim M.J., Manohar M., Dejonghe W. et al., 2025. Comparative efficacies of calcium hypochlorite and peroxyacetic acid treatments in inactivating *Salmonella enterica* on alfalfa seeds and sprouts. Appl. Food Res. 5, 100774. https://doi.org/10.1016/j.afres.2025.100774

Kowalska J., Łukaszyk J., 2022. Metody zaprawiania materiału siewnego dozwolone w rolnictwie ekologicznym. Prog. Plant Prot. 62, 100–108. https://doi.org/10.14199/ppp-2022-012

Lee S.H.I., Cappato L.P., Corassin C.H. et al., 2016. Effect of peracetic acid on biofilms formed by *Staphylococcus aureus* and *Listeria monocytogenes* isolated from dairy plants. J. Dairy Sci. 99, 2384-2390. http://dx.doi.org/10.3168/jds.2015-10007

Madruga F.B., Rossetti C., Saraiva C.R.C. et al., 2023. Seed treatment: importance of products and equipment. Colloq. Agrar. 19, 105–115. https://doi.org/10.5747/ca.2023.v19.h516

Nazarov P.A., Baleev D.N., Ivanova M.I. et al., 2020. Infectious plant diseases: etiology, current status, problems and prospects in plant protection. Acta Naturae 12, 46–59. https://doi.org/10.32607/actanaturae.11026

Rahman Md.S., Chakraborty A., Kibria A. et al., 2023. Effects of silver nanoparticles on seed germination and growth performance of pea (*Pisum sativum*). Plant Nano Biol. 5, 100042. https://doi.org/10.1016/j.plana.2023.100042

Rossini A., Ruggeri R., Rossini F., 2024. Discriminating among alternative dressing solutions for cereal seed treatment: effect on germination and seedling vigor of durum wheat. Int. J. Plant Biol. 15, 230–241. https://doi.org/10.3390/ijpb15020019

Saikumar A., Singh A., Kaur K. et al., 2023. Numerical optimization of hypochlorous acid (HOCl) treatment parameters and its effect on postharvest quality characteristics of tomatoes. J. Agric. Food Res. 14, 100762. https://doi.org/10.1016/j.jafr.2023.100762

Şehirli S., Karabulut O., İlhan K. et al., 2020. Use and efficiency of disinfectants within a hydrocooler system for postharvest disease control in sweet cherry. Int. J. Fruit Sci. 20, S1590–S1606. https://doi.org/10.1080/15538362.2020.1822265

Surovy M.Z., Islam T., von Tiedemann A., 2023. Role of seed infection for the near and far distance dissemination of wheat blast caused by *Magnaporthe oryzae* pathotype *Triticum*. Front. Microbiol. 14, 1040605. https://doi.org/10.3389/fmicb.2023.1040605

Tobiasz-Salach R., Mazurek M., Jacek B., 2023. Physiological, biochemical, and epigenetic reaction of maize (*Zea mays* L.) to cultivation in conditions of varying soil salinity and foliar application of silicon. I*nt. J. Mol. Sci. 24*, 1141. https://doi.org/10.3390/ijms24021141

Vines J.R.L, Jenkins P.D., Foyer C.H. et al., 2003. Physiological effects of peracetic acid on hydroponic tomato plants. Ann. Appl. Biol. 143(2), 153–159. https://doi.org/10.1111/j.1744-7348.2003.tb00281.x

Wilson D.O., 1976. Evaluation of chemical seed coat sterilants. Plant Soil 44, 703–707.

Yang X., Zhang Z., Yuan Y. et al., 2022. Control efficiency of hexaconazole-lentinan against wheat sharp eyespot and wheat crown rot and the associated effects on rhizosphere soil fungal community. Front. Microbiol. 13, 1014969. https://doi.org/10.3389/fmicb.2022.1014969

Yildiz M., Ekiz H., 2014. The effect of sodium hypochlorite solutions on *in vitro* seedling growth and regeneration capacity of sainfoin (*Onobrychis vicifolia* Scop.) hypocotyl explants. Can. J. Plant Sci. 94, 1161–1164. https://doi.org/10.4141/CJPS2013-250

Source of funding: Research received no external funding.

Conflicts of interest: The author declare no conflict of interest.

Received: 25.08.2025
Accepted:19.11.2025
Published: 31.12.2025

AGRONOMY SCIENCE

VOL. LXXX (4) 2025

https://doi.org/10.24326/as.2025.5631

[1] Department of Food Production and Safety, State Academy of Applied Sciences in Krosno, Rynek 1, 38-400 Krosno, Poland
[2] Department of Plant Production Technology and Commodities Science, University of Life Science, Akademicka 15, 20-950 Lublin, Poland
[3] Potato Agronomy Department, IHAR – PIB Branch in Jadwisin, Szaniawskiego 15, 05-140 Serock, Poland
[4] Research Centre for Cultivar Testing, Słupia Wielka 34, 63-022 Słupia Wielka, Poland
*e-mail: barbara.marczak@pans.krosno.pl

BARBARA KROCHMAL-MARCZAK[1*] https://orcid.org/0000-0001-8619-3031
ELŻBIETA PISULEWSKA[1] https://orcid.org/0000-0001-7830-0116
BARBARA SAWICKA[2] https://orcid.org/0000-0002-8183-7624
PIOTR BARBAŚ[3] https://orcid.org/0000-0001-7830-0116
PIOTR PSZCZÓŁKOWSKI[4] https://orcid.org/0000-0002-5907-1984

The temperature influence on the energy and germination capacity of seeds and the effect of the substrate on the yield *the withania somnifera* in the conditions of south-eastern Poland

Wpływ temperatury na energię i zdolność kiełkowania nasion oraz wpływ podłoża na plonowanie *Withania somnifera* w warunkach Polski południowo-wschodniej

Abstract: The aim of this study was to determine the effect of air temperature on the energy and germination capacity of *W. somnifera* seeds and to assess the effect of different substrates on the yield of the aboveground and root parts. An additional aim of the study was to develop agrotechnical recommendations for pioneering cultivation of this species in the temperate climate of south-eastern Poland. Germination energy and capacity were evaluated at 10°C, 20°C, and 30°C. Additionally, the impact of three substrate types – soil (A), a 50 : 50 mixture of soil and compost (B), and pure compost (C) – on the yield of shoots and roots was assessed over the years 2021–2023. The results indicate that the germination energy and capacity of *W. somnifera* seeds were highly dependent on air temperature. The highest germination energy was observed at 30°C in all study years, with an average value of 93.56%,

Citation: Krochmal-Marczak B., Pisulewska E., Sawicka B., Barbaś P., Pszczółkowski P., 2025. The temperature influence on the energy and germination capacity of seeds and the effect of the substrate on the yield *the withania somnifera* in the conditions of south-eastern Poland. Agron. Sci. 80(4), 69–87. https://doi.org/10.24326/as.2025.5631

while the lowest was recorded at 10°C (average: 0.44%). Germination capacity was also highest at 30°C, reaching an average of 95.45%, indicating that this temperature is optimal for maximizing both germination energy and capacity. Substrate type had a significant effect on the yield of both aboveground and root parts. The highest yield of aboveground biomass was obtained on pure compost (C), while the lowest was recorded on the soil-compost mixture (B). Over the three years, substrate C consistently provided the highest root yields, averaging 3.5 t ha^{-1}, followed by substrate B (3.2 t ha^{-1}) and substrate A (3.1 t ha^{-1}). This study demonstrates that *W. somnifera* has high adaptive potential for cultivation in Poland; however, it requires high air temperature during seed germination and appropriate substrate selection. These results allow for the development of agronomic recommendations for the cultivation of *W. somnifera* in south-eastern Poland.

Keywords: *Withania somnifera* L., seeds, temperature, germination capacity, germination energy, herb yield, root yield

INTRODUCTION

The genus *Withania* includes 23 species, two of which – *Withania somnifera* (ashwagandha) and *W. coagulans* (ashutoshbooti) – occur in India. Their dried roots are widely used in traditional medicine, particularly in Ayurveda [Połumackanycz et al. 2020]. *Withania somnifera*, also known as Indian ginseng, belongs to the nightshade family (Solanaceae) and is a xerophytic plant that naturally occurs in dry, hot regions of the Middle East and North Africa [Khabiya et al. 2024]. It is primarily cultivated in subtropical and tropical zones, including India, Africa, and Australia [Obidowska and Sadowska 2004]. In India, ashwagandha is extensively grown as a medicinal plant, particularly in the northwestern region of Madhya Pradesh, on more than 5,000 ha of land. Other major producing states include Rajasthan, Gujarat, Uttar Pradesh, Punjab, Haryana, Andhra Pradesh, and Maharashtra, with a total cultivation area of approximately 10,768 ha [Khabiya et al. 2024]. In Ayurvedic medicine, ashwagandha is used as an adaptogen to help the body cope with stress, and it also exhibits anti-inflammatory, neuroprotective, and antioxidant properties [Afewerki et al. 2021, Mikulska et al. 2023, Mondal and Paul 2023, Dipankar et al. 2025]. The roots are the most valuable plant part [Chauhan et al. 2022], but a bioactive compound in the leaves, withaferin A, has demonstrated anti-cancer potential, increasing the plant's significance in pharmaceuticals. In India, ashwagandha is often cultivated on marginal soils by small-scale farmers in states such as Madhya Pradesh, Andhra Pradesh, Rajasthan, and Karnataka. Its popularity is due to ease of cultivation, high market value of roots, and additional income from leaves and seeds [Mondal and Paul 2023]. The root is the main pharmaceutical raw material used in Ayurvedic and Unani medicine to treat rheumatic diseases, lung infections, stomach ailments, and skin conditions, and it is valued for its anti-inflammatory and aphrodisiac properties [Połumackanycz et al. 2020]. In recent years, interest has grown in cultivating *W. somnifera* in temperate climates, including Poland, due to increasing demand for natural herbal raw materials [Pisulewska et al. 2025]. However, cultivation under these conditions presents several challenges, such as a shorter growing season, lower temperatures, and reduced sunlight. The minimum germination temperature for this species is 18–20°C, while the maximum is 30–32°C; temperatures outside this range may slow germination or inhibit growth [Singh et al. 2015]. In Poland, *W. somnifera* is cultivated as an annual plant, and cultivation success depends on substrate

choice, germination conditions, and agronomic practices. Low seed germination capacity in temperate climates is a major limitation [Kaur et al. 2018], which makes achieving high germination energy and capacity crucial to justify seed costs and ensure profitable yields [Kumar et al. 2016]. The aim of this study was to determine the effect of air temperature on the energy and germination capacity of *W. somnifera* seeds and to assess the effect of different substrates on the yield of the aboveground and root parts. An additional aim of the study was to develop agrotechnical recommendations for pioneering cultivation of this species in the temperate climate of south-eastern Poland.

Alternative hypotheses:

H_1: There is a statistically significant effect of different temperature levels on the germination capacity of *W. somnifera* seeds.

H_2: There is a statistically significant effect of different substrate types on the yield of *W. somnifera*.

Null hypotheses:

H_{01}: There is no statistically significant effect of temperature on the germination capacity of *W. somnifera* seeds.

H_{02}: There is no statistically significant effect of substrate type on the yield of *W. somnifera*.

MATERIALS AND METHODS

The field experiment was conducted over three growing seasons (2021–2023) in the field experiment was conducted over three growing seasons (2021–2023) at the Experimental Field of the State Higher Vocational School in Krosno (49°41'N, 21°47'E) under the climatic conditions of south-eastern Poland. The study was arranged in a randomized block design with three replications. To evaluate the effect of substrate on plant growth and yield, three experimental variants were applied: A (control), consisting of garden soil (S); B, a 50 : 50 mixture of garden soil and compost (S + C); and C, pure compost (C). The clean compost was purchased from Krosno Municipal Holding. Each experimental plot had an area of 13.5 m^2 (9 × 1.5 m).

Seedling preparation and production

The seeds were purchased from a certified seed retailer. Class A seeds were soaked in distilled water for 24 h prior to sowing. They were then sown into multi-cell trays filled with a 50 : 50 mixture of soil and compost, with the top layer covered with perlite to maintain optimal moisture. After reaching the BBCH 19 (Biologische Bundesanstalt, Bundessortenamt und Chemische Industrie) growth stage (approximately 7 cm in height), the seedlings were transplanted into P9 pots containing the same substrate. The plants were subsequently transplanted to the field at the BBCH 29 stage (about 5 weeks after sowing), maintaining a spacing of 30 × 25 cm. Due to the lack of registered plant protection products for *W. somnifera* in Poland, crop maintenance was limited to manual weeding. Harvesting was carried out in two stages: the above ground parts were collected at the beginning of flowering (BBCH 61), while the roots were dug up at the end of October (BBCH 95). The seedling production process and subsequent stages of cultivation are illustrated in figure 1.

Fig. 1. Steps of growing *Withania somnifera* L**.** A – seeds, B – seedling, C – seedling planted in a plantation, D – flowering, E – tsarina plantation, F – fruit formation, G – above-ground part (stem, leaves, fruits) and underground part (root), H – harvesting of roots

Laboratory analysis and soil studies

Between 2021 and 2023, seed germination tests were conducted at the Microbiology Laboratory of the State Academy of Applied Sciences in Krosno. The seeds were disinfected by soaking them for 24 h in 40% ethanol, followed by 8 h in 3% perchloric acid. The prepared seeds were then placed on sterile filter paper in Petri dishes (150 × 25 mm) (100 seeds per dish, in three replicates). Germination was monitored in a Fito 300 incubator (Biogenet, Poland) at a constant relative humidity of 95%, under temperatures of 10°C, 20°C, and 30°C, with a photoperiod of 16 h light/8 h dark. Germinated seeds were counted every 48 h, and germination capacity and germination energy were determined according to ISTA guidelines [ISTA 2004]. Before the start of each growing season (2021–2023), representative soil samples were collected from the topsoil layer (0–30 cm) of each plot in accordance with the Polish Standard [PN-R-04031:1997] and analyzed at the accredited Regional Chemical-Agricultural Station in Rzeszów. Key chemical parameters were assessed, including pH (in 1 M KCl), organic matter content (Tiurin method) [Myślińska 2010], as well as macroelements (P, K, Mg) [Handzel et al. 2017] and microelements (Cu, Mn, Zn, Fe) [Ostrowska et al. 1991].

Physicochemical properties of soil

Table 1 presents the physicochemical properties of three different types of soil substrates analyzed during the years 2021–2023. These substrates include: A) (Z) – soil serving as the control object, B) (Z + K) – a mixture of soil and compost in a 50 : 50 ratio, and C) (K) – pure compost.

Table 1. Chemical composition and soil reaction (2021–2023): macro- and micro-nutrients, humus, calcium carbonate

Micronutrients (mg kg^{-1})				pH (KCl)	Humus (g kg)	CaCO3 (g kg^{-1})	Macronutrients (mg·kg^{-1})			Substrates
Fe	Zn	Mn	Cu				Mg	K_2O	P_2O_5	
1585	14.6	173.9	5.7	5.69	26.8	0.2	241	310	196	A
1798	15.6	184.1	6.1	6.70	29.2	0.4	198	202	123	B
1887	16.4	186.9	4.7	7.10	29.8	0.6	370	380	240	C

Source: Data prepared based on the results obtained from the District Chemical-Agricultural Station in Rzeszów; substrates: A – soil (Z) as a control object, B – soil + compost (Z + K; 50 : 50), C – compost (K)

The analysis shows that substrate C (compost) had the highest content of macronutrients (P_2O_5, K_2O, Mg) and humus compared to the other substrates, reflecting its greater nutritional potential. Substrate C also exhibited the highest pH value (7.10), indicating a slightly alkaline reaction, in contrast to the slightly acidic reaction of substrates A (pH 5.69) and B (pH 6.70). The highest concentrations of iron (Fe = 1887 mg kg^{-1}), manganese (Mn = 186.9 mg kg^{-1}), and copper (Cu = 16.4 mg kg^{-1}) were also observed in the compost substrate. On the other hand, the control substrate A had the lowest content of these elements. Additionally, substrate A showed the lowest levels of both $CaCO_3$ and humus, making it the least nutrient rich. Substrate B (soil + compost) was intermediate in terms of $CaCO_3$ and humus content, while substrate C (compost) stood out with the highest values, indicating the greatest potential for enriching the soil and improving its physicochemical properties (tab. 1). This suggests that the use of compost (substrate C) can significantly enhance plant growth conditions by enriching the soil with essential nutrients and improving its structure. The weather pattern during the growing season of the ashwagandha was variable, as illustrated in table 2.

According to data from the meteorological station in Dukla, the weather conditions during the vegetation period of ashwagandha in the years 2021–2023 were characterized by considerable variability. Three key parameters were analyzed: precipitation, air temperature, and humidity, expressed by the Hydrothermal Coefficient (HTC).

Precipitation

The total precipitation sum for the April–September period was lower than the long-term average. The driest year was 2021, with mean monthly precipitation of 17.9 mm. Exceptionally low precipitation was recorded in June 2022 (6.5 mm) and in July 2023 (11.7 mm), which could have led to water stress in plants. In contrast, the highest precipitation was observed in May 2022 (61.4 mm) and in June 2023 (52.9 mm).

Table 2. Meteorological conditions during the growing season of ashwagandha 2021–2023, according to the Dukla Meteorological Station

Years	Months						Mean (IV–IX)
	IV	V	VI	VII	VIII	IX	
Rainfalls (mm)							
2021	7.1	16.1	14.0	20.9	31.2	41.5	17.9
2022	23.8	61.4	6.5	16.1	13.0	10.2	24.2
2023	23.3	35.7	52.9	11.7	15.3	22.0	27.8
The average sum of 2021–2023	55.9	95.6	100.9	116.5	30.1	53.1	79.8
Air temperature (°C)							
2021	15.5	18.8	20.9	21.3	21.6	13.0	19.6
2022	10.6	13.7	23.0	20.2	20.6	12.4	17.6
2023	10.0	12.4	17.1	20.4	21.3	15.5	16.2
Long-term average (2004–2023)	9.2	13.6	16.4	19.0	19.4	14.0	15.5
Hydrothermal coefficient (HTC)							
2021	0.5	0.9	0.7	1.0	1.4	3.2	0.9
2022	2.2	4.5	0.3	0.8	0.6	0.8	1.7
2023	2.3	2.9	3.1	0.6	0.7	1.4	1.9

The ranges of this index values were classified as follows: $K \leq 0.4$ – extremely dry month; $0.4 < K \leq 0.7$ – very dry; $0.7 < K \leq 1.0$ – dry; $1.0 < K \leq 1.3$ – quite dry; $1.3 < K \leq 1.6$ – optimal [Cherszkowicz 1971]; $1.6 < K \leq 2.0$ – moderately humid; $2.0 < K \leq 2.5$ – humid; $2.5 < K \leq 3.0$ – very humid; $K > 3.0$ – extremely humid [Skowera and Wojnowski 2003]

Air temperature

The average air temperature in 2021–2023 was higher than the long-term mean (15.5°C), which was favorable for the vegetation of the thermophilic ashwagandha. The warmest period was August 2021 (21.6°C). The lowest average temperature was recorded in April 2023 (10.0°C). Despite the overall warming trend, the cool beginning of the 2023 season may have delayed early plant development.

Air humidity

Humidity was assessed using the Hydrothermal Coefficient (HTC), with values categorized according to the classification of Skowera and Wojkowski [2003]. The analysis revealed considerable variability in humidity conditions across months and years. For instance, May 2022 (HTC = 4.5) was a very humid month, which could have positively influenced plant development, whereas June 2022 (HTC = 0.3) and July 2023 (HTC = 0.6)

were very dry, posing challenges for cultivation. The overall mean HTC values for the respective years indicated a predominance of dry to moderately humid conditions.

Statistical calculations

The experimental data were analyzed using a two-way analysis of variance (ANOVA) with interaction effects to evaluate the influence of experimental factors (substrate type, meteorological conditions) on response variables (germination capacity, yield, biomass parameters) [Sokal and Rohlf 1995, Quinn and Keough 2002]. For post-hoc comparisons between group means (e.g. different substrates or years), Tukey's Honestly Significant Difference (HSD) test was applied [Tukey 1949, Zar 2010]. This conservative multiple comparison procedure maintains the experiment-wise error rate at $\alpha \leq 0.05$. The results were presented using standard ANOVA tables showing F-statistics, degrees of freedom, and significance levels [Press Underwood 1997], as well as boxplots for visualizing comparisons between groups [McGill 1978, Crawley 2013]. All analyses were performed using the R statistical software [Core and Team 2023] with the Agricola [Mendiburu 2021] and ggplot2 [Wickham 2016] packages for statistical computations and data visualization, respectively.

RESULTS

Seed germination capacity and energy

One of the basic yield-forming factors in plant production is seed material, and seed germination energy and germination capacity are the first steps towards successful cultivation of ashwagandha. The results of seed germination are presented in tables 3 and 4.

Table 3. Germination capacity of ashwagandha seeds at different temperatures (%)

Air temperture	Years			Mean
	2021	2022	2023	
10°C	1.3 ±0.0 [c]	1.7 ±0.0 [c]	1.3 ±0.0 [c]	1.6 [c]
20°C	44.7 ±1.0 [b]	44.7 ±1.2 [b]	44.7 ±1.0 [b]	44.6 [b]
30°C	96.0 ±1.1 [a]	95.7 ±2.2 [a]	96.0 ±1.1 [a]	95.5 [a]
LSD $p \leq 0.05$	7.22			2.4
Mean	47.3[a]	47.3 [a]	46.9[a]	47.2
LSD $p \leq 0.05$	ns*			–

Statistically significant differences in means within groups (lines) are marked with letters,
± – standard deviation,
* not significant at $p \leq 0.05$

The germination capacity of ashwagandha significantly varied depending on the air temperature, which means that the temperature significantly affected the results obtained. The highest germination capacity was recorded at 30°C, reaching an average of 95.45%, which indicates that this is the most optimal temperature for germinating ashwagandha seeds. At 20°C, the germination capacity was on average 44.56%, which is significantly

lower than at 30°C, but still significantly higher than at the lowest air temperature. The lowest germination capacity was recorded at 10°C, where the results were almost zero (1.6%). This shows that such a low temperature is not suitable for germinating this plant (tab. 3). Differences between years: the average germination capacity in 2021–2023 was: 47.3% (2021), 47.3% (2022) and 46.9% (2023), respectively. The differences between years were not statistically significant, indicating that the germination capacity of seeds was not dependent on the variability of conditions in individual years in a statistically significant manner (tab. 3). This study highlights the need to ensure appropriate thermal conditions for optimal ashwagandha growth.

No significant differences were observed between years in individual temperatures, emphasizing that temperature is the main factor determining the germination capacity of seeds. Therefore, the obtained results clearly indicate that for ashwagandha, the optimal temperature for seed germination is around 30°C, which is in line with the literature on this plant, which prefers warm, subtropical conditions. A temperature of 20°C, although it allows germination of some seeds, is not high enough to achieve the full germination potential. On the other hand, a temperature of 10°C completely prevents effective seed germination. For commercial cultivation of ashwagandha, it is therefore recommended to use thermal conditions close to 30°C to achieve high germination capacity and ensure the success of the crop. In conclusion, temperature is a key factor influencing the germination capacity of ashwagandha seeds, and the optimal thermal conditions are 30°C. Ashwagandha seed germination varied significantly under different temperature regimes, with the highest values observed at 30°C, indicating optimal conditions for rapid and uniform seedling emergence. Lower temperatures (10°C) resulted in minimum germination energy, highlighting the species' preference for warmer climate during the initial growth phase (tab. 4). The standard deviation for this feature (e.g. 94.7 ±4.1 for a temperature of 30°C) confirmed that the measurements were very precise and repeatable (tab. 4).

Table 4. Germination energy of ashwagandha seeds at different temperatures (%)

Air temperture	Years			Mean
	2021	2022	2023	
10°C	0.3 ±0.0 [c]	0.3 ±0.0 [c]	0.7 ±0.1 [c]	0.4 [c]
20°C	44.7 ±1.2 [b]	45.7 ±1.9 [b]	45.3 ±1.6 [b]	45.2 [b]
30°C	92.7 ±3.1 [a]	94.7 ±4.1 [a]	93.3 ±3.6 [a]	93.6 [a]
LSD $p \leq 0.05$	7.22			2.37
Mean	45.9 [a]	46.9 [a]	46.4 [a]	46.4
LSD $p \leq 0.05$	ns			–

Statistically significant differences in means within groups (lines) are marked with letters, not significant at $p \leq 0.05$

The results of our own research indicate that the germination energy of ashwagandha seeds was significantly dependent on the germination temperature. The highest germination energy was observed at 30°C in all the years of the study, with an average value of 93.6%, which indicates that this temperature provides optimal conditions for seed vigor

and early seedling development. Moderate germination energy was recorded at 20°C (average: 45.2%), while the lowest germination energy was observed at 10°C (average: 0.44%), which highlights the adverse effect of low temperatures on seed metabolic activity and germination potential. LSD analysis confirmed significant differences between temperature treatments, without significant changes between the years of the study.

The interaction between temperature and years indicates that the effect of temperature on germination energy of ashwagandha seeds was stable in the years studied (2021–2023). The results show that temperature was crucial for germination energy, and the highest values were consistently recorded at 30°C regardless of the year, which indicates the repeatability and independence of this result from environmental conditions in individual years (tab. 4).

In contrast, at 20°C, germination energy values were moderate and stable between years, suggesting that this temperature provides acceptable, although suboptimal conditions. On the other hand, at 10°C, the interaction was the least pronounced, as germination energy was very low and similar each year. The lack of significant differences between years (LSD = ns) indicates that germination energy was more influenced by temperature than possible differences resulting from annual conditions.

Yield of the aboveground and underground parts of the Withania somnifera

Soil substrates significantly affected the yield of the aboveground part of the *Withania somnifera*. The highest yield of the tested trait was achieved in the substrate with compost, while the lowest in the substrate made of soil and compost (B). Statistical analysis showed that in the first year of the study, the yield of the aboveground part of *Withania somnifera* significantly depended on the substrate used and was the highest in the treatment with compost. The treatment with compost alone increased the herb yield by 12.4%, compared to the control treatment (A). In the treatment where compost was added to the soil in a 50 : 50 ratio, the value of the tested trait was only higher by approx. 2%, compared to the control treatment (tab. 5). The standard deviation for fresh mass of above ground parts of ashwagandha (e.g. 15.1 ±1.1 for compost substrate) confirmed that the measurements were repeatable (tab. 5).

Table 5. Fresh mass yield of above-ground parts of ashwagandha (t ha^{-1})

Substrates	Years			Mean
	2021	2022	2023	
A	9.7 ±0.9 ^{b}	11.0 ±0.9 ^{ab}	12.1 ±1.0 ^{b}	10.9 ^{c}
B	13.6 ±0.8 ^{a}	12.6 ±1.0 ^{a}	14.4 ±1.2 ^{a}	13.5 ^{b}
C	13.8 ±1.0 ^{a}	14.1 ±1.0 ^{a}	15.1 ±1.1 ^{a}	14.4 ^{a}
LSD $p \leq 0.05$	2.49			2.37
Mean	12.4 ^{b}	12.6 ^{b}	13.9 ^{a}	13.0
LSD $p \leq 0.05$	ns*			–

Statistically significant differences in means within groups (lines) are marked with letters, ± – standard deviation, substrates: A – soil (S) as a control object, B – soil + compost (S + C) (50 : 50), C – compost

Year × substrate interaction is a statistical term used in analysis of variance (ANOVA) that refers to a situation in which the effect of one factor (in this case, year) on the outcome of an experiment depends on the level of a second factor (in this case, substrate). The interaction between substrates and years in relation to the fresh mass of the above-ground parts of ashwagandha indicates a varied response of plants to the type of substrate in individual years (fig. 3). Substrate A (control object): Fresh mass was the lowest in all years, confirming that soil alone (without compost addition) does not provide optimal conditions for maximum yield. However, an increasing trend was observed in subsequent years (from 9.7 t ha^{-1} in 2021 to 12.1 t ha^{-1} in 2023), which may suggest improved environmental conditions or the influence of increasing plant adaptation. Substrate B (soil + compost, 50 : 50): The test results were higher than in the control substrate in each year. The average fresh mass increased from 13.6 t ha^{-1} in 2021 to 14.4 t ha^{-1} in 2023, indicating that compost addition had a positive effect on yield and that the effectiveness of this substrate was stable between years. Substrate C (compost): This all-compost substrate provided the highest fresh mass in each year, with a peak yield of 15.1 t ha^{-1} in 2023. These results suggest that compost as a substrate provided optimal growth conditions, likely due to its high nutrient content and improved physical soil properties (fig. 3).

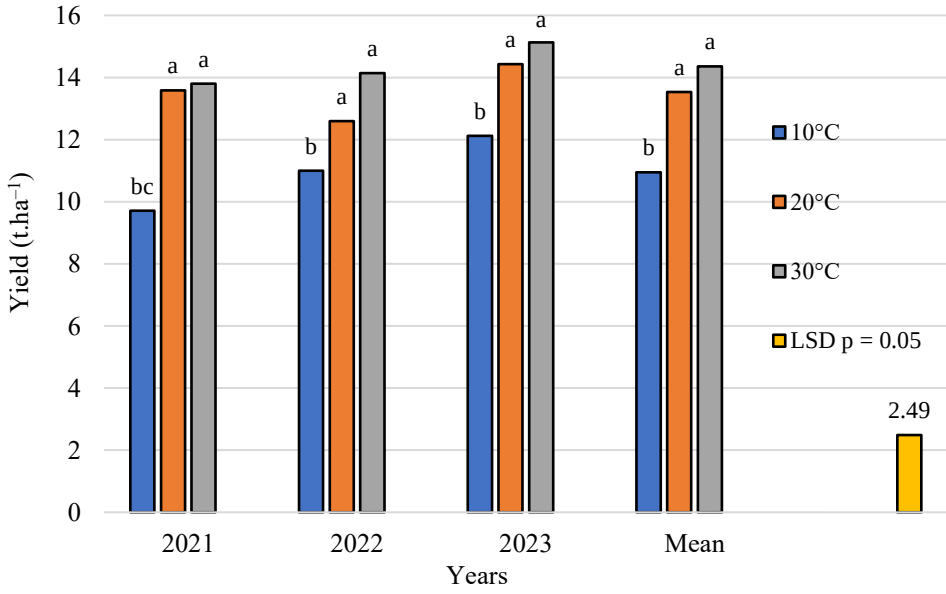

Fig. 3. Interaction of substrates and years of research on the yield of aboveground biomass of ashwagandha

Year and substrate interaction: Although there was an overall improvement in yield between years, regardless of substrate, the difference between substrates was significant. Substrate type had the greatest effect on fresh mass, with years having only a moderate effect (fig. 3). This suggests that the main factor influencing yield is the soil quality, while environmental conditions in individual years played a secondary role.

Table 6 shows the dry matter yield data of the above-ground parts of ashwagandha (t ha^{-1}) over three years (2021–2023) under different substrate conditions (A, B and C). The standard deviation for dry matter of above-ground parts of ashwagandha (e.g. 3.1 ±0.1 to 3.4 ±0.3) for a compost substrate) confirmed that the measurements were repeatable (tab. 6).

Table 6. Yield of dry matter of above-ground parts of ashwagandha (t ha^{-1})

Substrates	Years			Mean
	2021	2022	2023	
A	2.0 ±0.1^{c}	2.0 ±0.2^{b}	2.9 ±0.3^{b}	2.3^{c}
B	2.5 ±0.1^{b}	2.5 ±0.2^{b}	3.1 ±0.2^{a}	2.7^{b}
C	3.1 ±0.1^{a}	3.2 ±0.1^{a}	3.4 ±0.3^{a}	3.3^{a}
LSD $p \leq 0.05$	0.4			2.37
Mean	2.5^{b}	2.6^{b}	3.1^{a}	2.8
LSD $p \leq 0.05$	ns			–

Statistically significant differences in means within groups (lines) are marked with letters, ± – standard deviation, substrates: A – soil (S) as a control object, B – soil + compost (S + C; 50 : 50), C – compost

Effect of substrates: substrate A (as control, soil only): consistently resulted in the lowest dry matter yield in all years, with an average of 2.31 t ha^{-1}. This indicates that soil alone provides limited nutrients and is less effective in supporting optimal plant growth. Substrate B (soil + compost, 50 : 50) showed higher yields, as compared to substrate A, with an average of 2.69 t ha^{-1}. This suggests that the addition of compost increases soil fertility and nutrient availability, promoting better growth. Finally, substrate C (compost only) gave the highest yield in all years, with an average of 3.25 t ha^{-1}. This highlights the higher effectiveness of compost in providing nutrients and creating favorable growth conditions. Year effect: in all substrates, the aboveground dry matter yield increased consistently over the three years, with average values of 2.5 t ha^{-1} (2021), 2.6 t ha^{-1} (2022) and 3.1 t ha^{-1} (2023). This may indicate an improvement in environmental conditions or an increase in the efficiency of experimental management. The LSD values ($p \leq 0.05$) for substrates and years (0.1) indicate that the differences between substrates and between years are statistically significant (tab. 7). This only strengthens the conclusion that both the choice of substrate and the year of cultivation have a significant effect on yield.

Interaction: consistent classification of substrate C > substrate B > substrate A in all years suggests that the effect of substrate type is strong and is not dependent on year-to-year changes. Thus, the obtained results of the study show that compost (substrate C) is the most effective substrate for obtaining high dry matter yields of ashwagandha, followed by soil and compost mixture (substrate B) – tab. 6. Soil alone (substrate A) gives the lowest results. The improvement in yields over the years suggests either better environmental conditions or adaptive management practices during the study period.

Table 7 illustrates the yield of fresh root mass of *V. somnifera* depending on the year and type of substrate. The standard deviation for yield of fresh mass of roots of ashwagandha (e.g. from 3.1 ±0.6 to 4.0 ±0.2) for a compost substrate) confirmed that the measurements were repeatable (tab. 7).

Table 7. Yield of fresh mass of roots of ashwagandha (t ha^{-1})

Substrates	Years			Mean
	2021	2022	2023	
A	3.1 ±0.3 ^{b}	3.1 ±0.4 ^{a}	3.0 ±0.3 ^{a}	3.1 ^{c}
B	3.5 ±0.3 ^{b}	3.1 ±0.2 ^{a}	3.0 ±0.4 ^{a}	3.2 ^{b}
C	4.0 ±0.2 ^{a}	3.5 ±0.2 ^{a}	3.1 ±0.6 ^{a}	3.5 ^{a}
LSD $p \leq 0.05$	0.5			2.37
Mean	3.5 ^{a}	3.2 ^{b}	3.0 ^{c}	3.3
LSD $p \leq 0.05$	ns			–

Statistically significant differences in means within groups (lines) are marked with letters, ± – standard deviation, substrates: A – soil (S) as a control object, B – soil + compost (S+C) (50 : 50), C – compost

The data obtained indicate that the use of compost, either alone (substrate C) or mixed with soil (substrate B), increases the yield of ashwagandha root fresh weight compared to soil alone (substrate A). Over the three years, substrate C consistently produced the highest yield, averaging 3.54 t ha^{-1}, followed by substrate B with 3.19 t ha^{-1} and substrate A with 3.07 t ha^{-1}. The least significant difference (LSD) at $p \leq 0.05$ for the mean values is 0.17, indicating that the differences between substrates C and A, as well as between C and B, are statistically significant, whereas there is no difference between substrates A and B. This suggests that the inclusion of compost in the growing medium can significantly improve the yield of ashwagandha root (tab. 7). These results are consistent with previous studies showing that organic nutrient sources such as compost positively affect the yield and quality of ashwagandha. For example, a field experiment investigating the effect of organic nutrient management on ashwagandha showed increased yield and quality parameters with the use of organic amendments.

Analysis of the interaction between years and substrate types in relation to the yield of fresh root mass of *Withania somnifera* indicates significant differences in performance depending on the substrate used and the year of cultivation. A (control object): Fresh root yields were relatively stable over the years of the study, with a slight decrease from 3.1 t ha^{-1} in 2021 to 3.0 t ha^{-1} in 2023. Substrate B (soil + compost in a ratio of 50 : 50), where a decrease in yields was observed from 3.5 t ha^{-1} in 2021 to 3.0 t ha^{-1} in 2023, which suggests a decreasing efficiency of this substrate in the following years. Substrate C (compost), where the highest yields were obtained in this substrate, from 4.0 t ha^{-1} in 2021, however, a decrease in fresh root yield was observed to 3.1 t ha^{-1} in 2023 (tab. 7).

In 2021 the highest yields were obtained in substrate C (4.00 t ha^{-1}) and the lowest in substrate A (3.1 t ha^{-1}). In 2022, substrate C continued to outperform the others (3.51 t ha^{-1}), while substrate B had a slightly higher yield (3.1 t ha^{-1}) than substrate A (3.1 t ha^{-1}). In 2023, although substrate C maintained the highest yield (3.1 t ha^{-1}), the differences between substrates were smaller and all substrates showed a decreasing trend compared

to previous years. Summary: Substrate C (compost) showed the highest efficiency in increasing ashwagandha root fresh mass yields in all years, but a decreasing trend is noticeable over time. Substrate B (soil + compost) did not bring the expected benefits compared to substrate A (control soil) and even showed a decrease in yields in 2023 (tab. 7). The overall downward trend in yields from 2021 to 2023 suggests the possibility of substrate nutrient depletion or other environmental factors, which require further investigation. Crop rotation, substrate regeneration, or additional fertilization may also be considered to maintain high yields over the longer term (tab. 7). Table 8 illustrates the influence of substrates and years on the yield of dry root mass of *Withania somnifera*.

Table 8. Yield of dry mass of ashwagandha roots (t ha^{-1})

Substrates	Years			Mean
	2021	2022	2023	
A	1.4 ±0.1 ^{b}	1.3 ±0.1 ^{b}	1.2 ±0.1 ^{b}	1.3 ^{c}
B	1.5 ±0.1 ^{a}	1.4 ±0.1 ^{a}	1.3 ±0.2 ^{a}	1.4 ^{b}
C	1.8 ±0.3 ^{a}	1.5 ±0.2 ^{a}	1.4 ±0.1 ^{a}	1.6 ^{a}
LSD $p \leq 0.05$	0.2			0.1
Mean	1.6 ^{a}	1.4 ^{b}	1.3 ^{c}	1.4
LSD $p \leq 0.05$	0.1			–

Statistically significant differences in means within groups (lines) are marked with letters, ± – standard deviation, substrates: A – soil (S) as a control object; B – soil + compost (S+C) (50 : 50); C – compost

Table 8 data shows that substrate composition significantly affects the root dry matter yield of ashwagandha. Over the three-year period (2021–2023), substrate C (compost) consistently produced the highest mean root dry matter yield of 1.55 t ha^{-1}, followed by substrate B (soil + compost) with 1.4 t ha^{-1} and substrate A (soil) with 1.3 t ha^{-1}. The least significant difference at $p \leq 0.05$ was 0.1, suggesting that the differences between these means are statistically significant. This trend was consistent across all three years of the study, with substrate C significantly outperforming the others, indicating that the use of compost as a substrate increases the root dry matter yield of ashwagandha. The interaction between years and substrates shows that although there are some differences in yields between years, the superiority of the C substrate remains consistent, highlighting the beneficial effect of compost on root biomass production (tab. 8). The standard deviation for yield of dry mass of ashwagandha roots (e.g. from 1.4 ±0.1 to 1.8 ±0.3) for a compost substrate and for an object B soil + compost (S + C, 50 : 50; e.g. from 1.31 ±0.2 to 1.5 ±0.1) confirmed that the measurements were repeatable (tab. 8).

These results are consistent with previous studies indicating that organic nutrient sources such as compost positively affect the yield and quality of ashwagandha. A field experiment evaluating the effect of organic nutrient management on ashwagandha showed increased yield values with the use of organic amendments. In conclusion, the incorporation of compost into the growing medium can significantly increase the root dry matter yield of ashwagandha, offering a viable strategy for improving crop productivity in sustainable agricultural practices.

DISCUSSION

Our research provides a comprehensive assessment of the factors influencing the cultivation of *Withania somnifera* in a temperate climate, with particular emphasis on the conditions prevailing in south-eastern Poland. The results obtained from both field and laboratory experiments are consistent and confirm that both biotic factors (soil quality) and abiotic factors (temperature) play a key role in determining the success of cultivation.

Energy and germination of seeds

Germination capacity and germination energy are critical determinants of early plant development and play a decisive role in crop productivity [Kucera et al. 2005, Nonaka et al. 2010, Faligowska and Szukała 2012, Faligowska et al. 2018, Genze et al. 2020, Mohamed et al. 2021]. These parameters directly influence seedling uniformity, vigor, and the ability to adapt to field conditions. As reported by Mohamed et al. [2021] and Rymuza and Radka [2021], seeds exhibiting high germination energy produce robust and uniform seedlings, which is essential for successful crop establishment and subsequent yield potential. Therefore, optimizing germination conditions is a fundamental aspect of agronomic management.

Our results indicate that a temperature of 30°C is optimal for both germination capacity and germination energy of *W. somnifera* seeds, yielding the highest recorded values of 95.45% and 93.56%, respectively (tab. 3 and 4). These findings are consistent with existing literature, which classifies *W. somnifera* as a thermophilic species that thrives in the warmer conditions characteristic of subtropical climates. Maintaining optimal temperature during germination is therefore essential to ensure uniform seedling emergence and vigorous early growth.

The germination process involves a series of complex physiological and biochemical changes, beginning with water uptake, which activates hydrolytic enzymes responsible for mobilizing stored nutrient reserves, and culminating in the emergence of the embryonic radicle, indicating the breaking of the seed coat [Kambizi et al. 2006, Faligowska and Szukała 2012, Faligowska et al. 2018, Mohamed et al. 2021, Rymuza and Radka 2021, Khaim et al. 2022, Kumar et al. 2022, Sharma et al. 2023]. Enzymes such as α-amylase and proteases are particularly critical, facilitating the conversion of starches and proteins into soluble forms that fuel embryonic growth [Xia et al. 2024]. Suboptimal temperatures can suppress enzymatic activity, leading to delayed or incomplete germination. Our observations indicate that temperatures below 20°C markedly reduce germination rates, while exposure to 10°C nearly inhibits germination entirely.

Conversely, high temperatures (~30°C) likely stimulate the synthesis of heat shock proteins (HSPs), which protect cellular structures and enzymes from thermal stress, thereby enhancing germination efficiency and producing uniform seedlings [Faligowska and Szukała 2012, Porter et al. 2016, Faligowska et al. 2018]. Unlike the findings of Kumar et al. [2016], who observed high germination under fluctuating temperatures (15/35°C), our study focused on constant temperature conditions, providing a clearer understanding of the thermal optimum for *W. somnifera*. These results complement existing literature, confirming that stable high temperatures are critical for successful germination of this species.

For cultivation in temperate climates, where early spring temperatures are often suboptimal, producing seedlings under controlled conditions, such as polytunnels or greenhouses maintained at approximately 30°C, is essential to ensure uniform emergence and robust early growth. Seedling vigor at this stage is particularly important, as it affects the plant's capacity to compete for resources and withstand environmental stresses in the field.

Future research should explore thermo-priming techniques, which involve preliminary thermal conditioning of seeds to enhance seedling tolerance to low temperatures, potentially extending the cultivation range of *W. somnifera* [Lim et al. 2015]. Additionally, the identification and selection of genotypes with superior adaptability to variable climatic conditions represent a promising strategy for improving crop resilience and ensuring sustainable production under changing environmental conditions [Singh et al. 2024].

The effect of substrate and environmental conditions on yield

Our research demonstrates that substrate type is the primary factor influencing the yield of both above-ground and root parts of *W. somnifera*. The highest fresh (14.36 t ha^{-1}) and dry matter (3.25 t ha^{-1}) yields from above-ground parts were obtained on substrate C (pure compost), which can be directly attributed to its high fertility [Patel and Rank 2022]. Physicochemical analysis (tab. 1) confirmed that substrate C had the highest concentrations of essential macronutrients (P_2O_5, K_2O, Mg) and micronutrients (Zn, Fe, Mn), along with a neutral pH of 7.10. These characteristics are known to favor optimal nutrient uptake and plant development. This finding aligns with previous studies highlighting the critical role of soil pH and nutrient availability in determining *W. somnifera* growth and productivity [Helfenstein et al. 2016, Neina 2019, Xia et al. 2024].

Soil pH plays a crucial role in controlling nutrient bioavailability [Lim et al. 2015], particularly for phosphorus and zinc, which are essential for enzymatic activity, energy transfer, and overall metabolic processes in plants. Acidic conditions, such as those observed in the control substrate (A) with a pH of 5.69, limit nutrient availability and consequently reduce both vegetative growth and yield [Singh et al. 2024]. Over the period 2021–2023, an increase in yield was observed on all substrates, likely reflecting a combination of improved meteorological conditions and progressive plant adaptation to the local environment, underscoring the interactive effects of edaphic and climatic factors on crop performance.

The highest fresh (3.54 t ha^{-1}) and dry root mass (1.55 t ha^{-1}) were also recorded on substrate C, confirming the exceptional nutrient-retention and fertility properties of high-quality compost [Patel and Rank 2022]. These results are consistent with numerous studies demonstrating that organic nutrient sources, such as compost and manure, significantly enhance both biomass accumulation and secondary metabolite content in *W. somnifera* [Patel and Rank 2022, Singh et al. 2024]. The availability of organic matter not only provides essential nutrients but also improves soil structure, water-holding capacity, and microbial activity, all of which contribute to improved root development and plant vigor.

Interestingly, while above-ground yields generally increased, root yields exhibited a downward trend across all substrates over the years 2021–2023. This observation cannot be fully explained by meteorological conditions alone, which were relatively favorable, particularly in 2023. Potential factors contributing to the decline in root biomass include:

Nutrient depletion: despite the initially high fertility of the substrates, continuous cultivation without adequate substrate regeneration may have gradually reduced nutrient availability, particularly in the root zone.

Lack of crop rotation: Monoculture practices can lead to the accumulation of soil-borne pathogens, negatively impacting root development and overall plant health [Noworolnik 2015, Helfenstein et al. 2016, Porter et al. 2016, Neina 2019, Xia et al. 2024].

These findings emphasize that even the most fertile organic substrates require a comprehensive, long-term management strategy. Substrate regeneration, rotational practices, and supplementary fertilization are necessary to maintain soil fertility and sustain high yields over multiple growing seasons. This highlights an important practical consideration often overlooked in single-season studies, underlining the need for long-term experiments to fully understand substrate effects on crop productivity.

Furthermore, these results have implications for optimizing cultivation protocols for *W. somnifera*, especially in regions with marginal soils or limited access to high-quality compost. Integrating organic amendments with targeted nutrient management and adaptive agronomic practices can enhance both above-ground biomass and root yield, contributing to sustainable production systems and maximizing the medicinal potential of this species.

CONCLUSIONS

The results of the study confirmed hypothesis H_1, indicating that temperature had a statistically significant effect on the germination capacity of *W. somnifera* seeds. The null hypothesis H_{01} was therefore rejected. Similarly, the obtained results confirmed hypothesis H_2, showing that different substrate types had a significant effect on the yield of *W. somnifera*. Consequently, the null hypothesis H_{02} was also rejected.

The study clearly demonstrated that both germination temperature and substrate type play a crucial role in the successful cultivation of *Withania somnifera* L. The optimal germination temperature was found to be 30°C, at which the highest germination capacity and energy (over 90%) were recorded, confirming the plant's strong preference for warm, subtropical conditions. Lower temperatures, especially 10°C, almost completely inhibited effective germination, ruling out the possibility of cultivation in cooler climates without temperature control.

The composition of the substrate was equally important – the highest yields of both aerial parts and roots were obtained on a substrate consisting exclusively of compost (substrate C), indicating the high fertilization value of organic matter and its positive effect on the physical and chemical properties of the soil. Although a slight decrease in yields was observed in the third year of the study, the results confirmed that compost significantly improves both the quality and quantity of ashwagandha production.

In the context of sustainable agriculture and the growing demand for medicinal plant raw materials, it is recommended to implement practices such as substrate rotation, regeneration, and further optimization of organic fertilization. Future efforts should focus on maintaining high productivity while ensuring the quality of raw materials and the long-term sustainability of cultivation.

REFERENCES

Afewerki H.K., Ayodeji A.E., Tiamiyu B.B. et al., 2021. Critical review of *Withania somnifera* (L.) Donal: ethnobotany, pharmacological efficacy, and commercialization significance in Africa. Bull. Natl. Res. Cent. 45(1), 176. https://doi.org/10.1186/s42269-021-00635-6

Chauhan S., Madiya T., Jain D. et al., 2022. Early selective strategies for higher-yielding bio-economic Indian ginseng based on genotypic study through metabolic and molecular markers. Saudi J. Biol. Sci. 29(4), 3051–3061. https://doi.org/10.1016/j.sjbs.2022.01.030

Cherszkowicz E., 1971. Hydrothermischer coefficient (HTK) VI, VII, VIII Karte Agraklimatische Ressourcen des Territoriums der sozialistischen Länder Europas. Sofia, 123.

Core R., Team R.A., 2023. Language and environment for statistical computing.

Crawley M.J., 2013. The R book. John Wiley & Sons Ltd., Chichester.

Dipankar S.P., Dani M.M., Anirudhan R. et al., 2025. Pharmacological Insights into ashwagandha (*Withania somnifera*). A Review of its immunomodulatory and neuroprotective properties. Cureus 17(8), e89856. https://doi.org/10.7759/cureus.89856

Faligowska A., Panasiewicz K., Szymańska G. et al., 2018. Wpływ sposobu i gęstości siewu na produktywność i jakość nasion łubinu białego. Część II. Wartość siewna i wigor nasion. Fragm. Agron. 35(3), 47–54 [in Polish].

Faligowska A., Szukała J., 2012. Influence of sprinkling irrigation and soil tillage systems on vigor and sowing value of yellow lupine seeds. Sci. Natur. Technol. 6(2), #26.

Genze N., Bharti R., Grieb M. et al., 2020. Accurate machine learning-based germination detection, prediction and quality assessment of three grain crops. Plant Methods 16(1), 157. https://doi.org/10.1186/s13007-020-00699-x

Handzel A., Krawczyk J.B., Latawiec A.E. et al., 2017. Determination of element contents and physicochemical properties of selected soils. Infrastructure Ecol. Rur. Areas 1(2), 419–432.

Helfenstein J., Müller I., Grater R. et al., 2016. Organic wheat farming improves grain zinc concentration. PLoS ONE 11(8), e0160729. https://doi.org/10.1371/journal.pone.0160729

ISTA – International Seed Testing Association, 2004. Seed Sci. Technol. 21, Supplement.

Kambizi L., Adebol P.O., Afolayan A.J., 2006. Effects of temperature, prechilling and light on seed germination of *Withania somnifera*; a high-value medicinal plant. S. Afr. J. Bot. 72(1), 11–14.

Kaur A., Pratap B.S., Pati K. et al., 2018. Organic cultivation of Ashwagandha with improved biomass and high content of active withanolides: use of vermicompost. PLoS ONE 13(4), e0194314. https://doi.org/10.1371/journal.pone.0194314

Khabiya R., Choudhary G.P., Jnanesha A.C. et al., 2024. An insight into the potential varieties of Ashwagandha (Indian ginseng) for better therapeutic efficacy. Ecol. Frontiers. 44(3), 444–450.

Kucera B., Cohn M.A., Leubner-Metzger G., 2005. Plant hormone interactions during seed dormancy release and germination. Seed Sci. Res. 15(4), 281–307. https://doi.org/10.1079/SSR2005218

Kumar B., Yadav R., Singh S. et al., 2016. Seed germination behavior of *Withania* spp. under different temperature regimes. J. Crop Improv. 30(3), 287–292. https://doi.org/10.1080/15427528.2016.1151849

Kumar S., Verma S.K., Yadav A. et al., 2022. Tillage-based crop establishment methods and zinc application enhance productivity, grain quality, profitability and energetics of direct-seeded rice in potentially zinc-deficient soil in the subtropical conditions of India. Commun. Soil Sci. Plan. 53(9), 1085–1099. https://doi.org/10.1080/00103624.2022.2043340

Lim S.L., Yeong W.T., Lim P. et al., 2015. The use of vermicompost in organic farming: overview, effects on soil and economics. J. Sci. Food Agric. 95(6), 1143–1156. https://doi.org/10.1002/jsfa.6849

McGill R., 1978. American Statistician 32, 12–16.

Mendiburu F., 2021. Agricola: Statistical Procedures for Agricultural Research. R package.

Mikulska P., Malinowska M., Ignacyk M. et al., 2023. Ashwagandha (*Withania somnifera*) –current research on the health-promoting activities. A narrative review. Pharma 15(4), 1057. https://doi.org/10.3390/pharmaceutics15041057

Mohamed S.O., Kandiel M.A., Abo Zaid O.A.R. et al., 2021. Biochemical effect of *Nigella sativa* seeds on fatty acids, lipid profile, and antioxidants of laying hens. J. World Poult. Res. 11(3), 338–343. https://dx.doi.org/10.36380/jwpr.2021.40

Mondal K., Paul A., 2023. Challenges and opportunities in the cultivation of Ashwagandha (*Withania somnifera* Donal). Agric. Food 5(5), 424–426.

Myślińska E., 2010. Laboratoryjne badania gruntów i gleb. Wanito UW, Warszawa [in Polish].

Neina D., 2019. The role of soil pH in plant nutrition and soil remediation. Appl. Environ. Soil Sci., 1–9. https://doi.org/10.1155/2019/5794869

Nonaka H., Bassel G.W., Bewley J.D., 2010. Germination – still a mystery. Plant Sci. 179(6), 574–581. https://doi.org/10.1016/j.plantsci.2010.02.010

Noworolnik K., 2015. Warunki glebowe a plonowanie zbóż i ich współdziałania z czynnikami agrotechnicznymi. Stud. Rap. IUNG-PIB 44(18), 119–133 [in Polish].

Obidoska G., Sadowska A., 2004. Próby uprawy polowej *Withania somnifera* (L.) Dun. oraz ocena plonu i wartości surowca krajowego. Biul. Inst. Hod. Akl. Rośl. 233, 173–180 [in Polish].

Ostrowska A., Gawliński S., Szczesiakowa Z., 1991. Metody analizy i oceny właściwości gleb i roślin. Inst. Ochr. Roślin. 310 [in Polish].

Patel R.J., Rank H.D., 2022. Water use efficiency of wheat under different irrigation regimes using high discharge drip irrigation system. Agric. Eng. Today. 44(2), 19–31. https://doi.org/10.52151/aet2020442.1518

Pisulewska E., Krochmal-Marczak B., Jędrzejewska P. et al., 2025. Yield and antioxidant properties of herb and root of ashwagandha (*Withania somnifera* L.) grown with permaculture under subcarpathian conditions. Herbalism 1(11), 7–21. https://doi.org/10.12775/HERB.2025.001

PN-R-04031:1997. Analiza chemiczno-rolnicza gleby. Pobieranie próbek. Polski Komitet Normalizacyjny, Warszawa [in Polish].

Połumackanycz M., Forencewicz A., Wesołowski M., 2020. Viapiana A. Ashwagandha (*Withania somnifera* L.) the plant with proven health-promoting properties. Farm. Pol. 76(8), 442–447.

Porter H., Fiorani F., Pieruschka R. et al., 2016. Pampered inside, pestered outside? Differences and similarities between plants growing in controlled conditions and in the field. New Phytol. 212(4), 838–855. https://doi.org/10.1111/nph.14243

Press Underwood A.J., 1997. Experiments in ecology: their logical design and interpretation using analysis of variance. Cambridge Univ. Press, Cambridge, 504.

Quinn G.P., Keough M.J., 2002. Experimental design and data analysis. Cambridge Univ. Press.

Rymuza K., Radka E., 2021. Assessment of the germination capacity of soybeans depending on the pH of the substrate. Prog. Plant Prot. 61, 201–206. https://doi.org/10.14199/ppp-2021-022

Sharma H., Kumari A., Raigar O.P. et al., 2023. Strategies for improving tolerance to the combined effect of drought and salinity stress in crops. In: A. Kumar, P. Dhansu, A. Mann (eds), Salinity and drought tolerance in plants. Springer Nature, 137–172. https://doi.org/10.1007/978-981-99-4669-3_8

Singh M., Bhutani S., Dinkar N. et al., 2024. Assessment of pharmacological activities of specialized metabolites of *Withania somnifera* (L.). S. Afr. J. Bot. 166, 259–271. https://doi.org/10.1016/j.sajb.2024.01.039

Singh P., Guler R., Singh V. et al., 2015. Biotechnological interventions in *Withania somnifera* (L.) Donal. Biotechnol. Genet. Eng. Rev. (1–2), 1–20. https://doi.org/10.1080/02648725.2015.1020467

Skowera B., Wojnowski J., 2003. Changes of hydrothermal conditions in Poland in the period 1931–1990. Studia Geogr. 23, 250–261.

Sokal R.R., Rohlf F.J., 1995. Biometry: the principles and practice of statistics in biological research, 3rd ed. W.H. Freeman and Co., New York.

Tukey J.W., 1949. Comparing individual means in the analysis of variance. Biometrics 5, 99–114. https://doi.org/10.2307/3001913

Wickham H., 2016. ggplot2: elegant graphics for data analysis. Springer. J. Statist. Software, 260. http://www.springer.com/gp/book/9783319242750

Xia Y., Feng J., Zhang H. et al., 2024. Effects of soil pH on the growth, soil nutrient composition, and rhizosphere microbiome of *Ageratina adenophora*. Peer J. 16(12), e17231. https://doi.org/10.7717/peerj.17231

Zar J.H., 2010. Biostatistical analysis, 5th ed. Pearson.

Source of funding: This research received no external funding.

Received: 19.10.2025
Accepted: 26.11..2025
Published: 31.12.2025

AGRONOMY SCIENCE

VOL. LXXX (4) 2025

https://doi.org/10.24326/as.2025.5577

[1] Institute of Horticulture Production, University of Life Science, Głęboka 28, 20-612 Lublin, Poland
[2] Plant Nutrition R & D Department, Centre Mondial de l'Innovation of Roullier Group, 35400 Saint Malo, France
[3] Department of Applied Mathematics and Computer Sciences, University of Life Science, Głęboka 28, 20-612 Lublin, Poland
* e-mail: kamila.klimek@up.lublin.pl

MAGDALENA KAPŁAN[1] https://orcid.org/0000-0002-3833-9275
SYLVAIN PLUCHON[2]
KAMILA KLIMEK[3]* https://orcid.org/0000-0001-6638-894X

Assessment of the impact of growth biostimulants on the effects of stimulating branching in maiden apple tree

Ocena wpływu biostymulatorów wzrostu na efekty stymulacji rozgałęzienia u okulantów jabłoni

Abstract. Modern methods of cultivating trees in a nursery plants require nursery stock of very good quality, free from viruses, with an extensive root system, strong growth and, most importantly, with the correct structure of the tree crown, i.e. the number of lateral shoots. High-quality planting material, properly branched, determines the productive efficiency of the trees in a nursery in subsequent years of cultivation and its profitability. The research was conducted in 2017–2019 at a private nursery farm near Lublin. The purpose of the research was to analyze the effect of mixtures of biostimulants with growth regulators of natural origin on the effectiveness of chemical treatment to stimulate the emergence of lateral shoots in apple trees of the Gloster. The study showed that the height of maiden apple trees of the Gloster. significantly depended on the concentration of growth regulators. The best results were achieved using a mixture of AGRIMIX PRO (35 ml) and Maxifruit, producing trees 6% taller than the control. The number of side shoots, the average length of one shoot and the sum of the lengths of side shoots significantly depended on the number of growth regulator applications. Double application of AGRIMIX PRO resulted in an increase in the number of side shoots by 37.5% compared to single application, while in the case of a mixture of growth regulators with a biostimulant this effect was less pronounced and amounted to 17.0%.The biostimulation treatment with Maxifruit does not guarantee improved tree growth and quality, but its use in combination with the growth regulator AGRIMIX PRO improves the effectiveness of treatments that stimulate apple branching.

Keywords: biostimulants for growth, branching stimulation, nursery, apple tree

Citation: Kapłan M., Pluchon S., Klimek K., 2025. Assessment of the impact of growth biostimulants on the effects of stimulating branching in maiden apple tree Agron. Sci. 80(4), 89–101. https://doi.org/10.24326/as.2025.5577

INTRODUCTION

The efficiency and profitability of a nursery farm depends on the quality of the plants produced there. On the other hand, the use of high-quality nursery stock in horticultural cultivation determines the productive efficiency of the trees in subsequent years of cultivation [Gudarowska 2002, Rejman et al. 2002, Basak 2009, Czynczyk 2012, Kumawat et al. 2023, 2025], and thus its profitability [Skrzyński and Poniedziałek 2000, Bielicki and Pąśko 2013, Kapłan et al. 2017].

Modern methods of cultivating trees in a nursery plants require planting material of very good quality, free of viruses, with an extensive root system [Zhalnerchyk et al. 2015], with strong growth and the right structure of the tree crown, i.e. the number of lateral shoots [Skrzyński and Poniedziałek 2000, Bielicki and Pąśko 2013, Kapłan et al. 2017]. Producing plants with such characteristics is a complex process, often taking several years, e.g., trees on a 3-year cycle (the so-called knip-boom) or on a 2-year cycle [Gudarowska 2002, Basak 2009, Czynczyk 2012].

The quality of the nursery stock produced is influenced by a number of factors, starting with the growth strength of the rootstock used [Gudarowska 2002, Kviklys 2004, 2006, Kapłan and Baryła 2006, Nečas et al. 2018, 2020], the predisposition of the cultivar to form lateral shoots [Kapłan and Baryła 2006] and ending with external factors, i.e. the type and effectiveness of treatments to stimulate branching, soil and climatic conditions related to the location of the nursery and weather conditions during the initiation and growth of lateralshoots [Gudarowska and Szewczuk 2002, Jacyna 2002, Matysiak and Adamczewski 2009, Kapłan et al. 2017, Laňar et al. 2020].

Many popular apple tree cultivars at the nursery stage have a problem with the formation of a crown consisting of 5–8 lateral shoots. The reason for this is the apical dominance of the main shoot. In an attempt to prevent this phenomenon, nurserymen use mechanical treatments to stimulate branching of young trees, such as pinching the apical shoot, twisting the apex of growth by 180°, removing lateral shoots from the lower parts of the tree and rootstock [Rejman et al. 2002, Kapłan 2016] and chemical treatments [Kopytowski and Markuszewski 2009, Elfving 2010, Dorić et al. 2015, Lordan et al. 2017, Nečas et al. 2018].

Horticultural production is constantly looking for innovative solutions that have a beneficial effect on plant productivity, and the introduced EU restrictions require them to be environmentally friendly at the same time [Pacholczak et al. 2012, Kozak et al. 2016, Buraczyk et al. 2020, Laňar et al. 2020]. Therefore, in nursery cultivation one can notice an increase in interest in biopreparations, which can be such a group combining both features, i.e. stimulate the growth and development of plants (e.g. growth of the root system and aboveground parts), and, in addition, contain substances that have little impact on the environment [Hetman and Adamiak 2003, Kapłan et al. 2021]. Biostimulants meet these challenges.

According to the EU definition for Member States, a plant biostimulant means a material containing substance(s) or microorganisms, intended for application to the plant, seed or root zone to stimulate natural processes that increase nutrient use efficiency, abiotic stress tolerance and/or yield quality, the effect of which does not depend on nutrient content [Traon et al. 2014]. These are natural or synthetic compounds, which include free amino acids, humic substances, extracts from marine algae, the polysaccharide chitosan,

equivalents of natural phytohormones, phosphites, effective microorganisms and vitamins [Gawrońska and Przybysz 2011]. Biostimulants are safe and all-purpose preparations that support various physiological processes of plants and positively affect their overall condition, and the demonstration of their positive effect on plants depends largely on the preparation used and the plant species [Matyjaszczyk 2015].

The aim of the study was to analyze the influence of mixtures of growth biostimulants: AGRIMIX PRO and Maxifruit SL on the effectiveness of chemical growth stimulation on the growth and quality of maiden apple trees of the Gloster, budded on the M9 rootstock in the Lublin region in eastern Poland.

MATERIAL AND METHODS

Description of the experimental design

The study was conducted in 2017–2019 years at a private nursery farm located in the Lublin district, 5 km from Lublin (GPS: 51.285260, 22.616847). The experimental material was an apple Gloster budded on M.9 RN 29 rootstocks. The experiment evaluated the growth and quality of apple cv. apple trees after the application of treatments to stimulate branching. The experiment was set up in a randomized block design and included 11 combinations in 5 repetitions (one repetition was a plot with 10 plants). In each of the tested combinations, 50 plants were observed and measured.

The following combinations were used in the experiment:

Control – trees not sprayed, not treated to stimulate branching,
2. AGRIMIX PRO 25 ml per 1 liter of water – 1 application,
3. AGRIMIX PRO 35 ml per 1 liter of water – 1 application,
4. AGRIMIX PRO 25 ml + Maxifruit SL 0.2% per 1 liter of water – 1 application,
5. AGRIMIX PRO 35 ml + Maxifruit SL 0.2% per 1 liter of water – 1 application,
6. AGRIMIX PRO 25 ml per 1 liter of water – 2 applications,
7. AGRIMIX PRO 35 ml per 1 liter of water – 2 applications,
8. AGRIMIX PRO 25 ml + Maxifruit SL 0.2% per 1 liter of water – 2 applications,
9. AGRIMIX PRO 35 ml + Maxifruit SL 0.2% per 1 liter of water – 2 applications,
10. Maxifruit SL 0.2% per 1 liter of water – 1 application,
11. Maxifruit SL 0.2% per 1 liter of water – 2 applications.

Principles and application methods of growth regulators and biostimulation

Each year, the experiment was established in June, when the maiden apple trees reached a height of approximately 75 cm. The six youngest, well-developed lateral buds and leaves just below the cone were sprayed with a water solution. Applications were performed once or twice during the growing season – the first application after the maiden apple trees reached an average height of approximately 75 cm, while the second application, in the case of the double-application combination, was performed 10 days after the first spray. Chemical treatments for branching stimulation consisted of application in the form of an aqueous solution of AGRIMIX PRO (manufacturer Agrimix s.r.l.) at a dose of 25 and 35 ml per liter of water. AGRIMIX PRO [GA_{4+7} gibberellins – 19.1 g/l (1.8%) and

6-benzyladenine – 19.1 g/l (1.8%)] is the Italian equivalent of the Promalin 3.6 SL formulation. Depending on the combination, the AGRIMIX PRO preparation was applied as a single-component solution or a mixture, i.e. the growth biostimulant Maxifruit (manufacturer Timac Agro) was added to the prepared solution. Maxifruit (NMX® Complex, N 3%, P 7%, K 7%, Mn 0.05%, Zn 0.1%), contains extracts from plants living in extreme conditions (marine, desert and tropical), phytohormone precursors and transmitters for their expression and nutrients that support the action of substances that stimulate the production of natural phytohormones in the plant. The adjuvant Superam 10 AL was added to the prepared solution each time. During the experiment, regular protection against diseases, pests and weeds was carried out, and all treatments were carried out in accordance with the current nursery stock protection program. Adjuvant was used only in combinations where growth regulators were used.

Measurements and observations

In autumn, after October 10 and the end of apple tree growth, the height, number of side shoots and length of all lateral shoots were measured. The height of the trees from the ground to the apical bud of the main shoot was measured with a scaler with an accuracy of 1.0 cm. On each maiden apple trees, lateral shoots were counted and their length was measured. Based on the measurements, the following were calculated: the sum of the length of the lateral shoots and the average length of the lateral shoot.

Statistical analysis

The results obtained in the experiment were statistically analyzed using the one-way analysis of variance method. Additionally, the results were presented graphically using a dendrogram. Correlations between parameters determining the growth and quality of maiden apple trees and weather conditions were estimated by calculating Pearson correlation coefficients. Inference was based on significance $p < 0.05$. All statistical analyses were performed in SAS Enterprise Guide 5.1 software.

RESULTS

The average air temperature for the 2017–2019 growing season was higher than the multi-year average (in 2017 by 1.5°C, while in 2018 and 2019 by 2.5°C). The above dependence were also observed in the individual months of the growing season. The warmest month in all the analyzed years was August, while the coolest month was April (tab. 1).

Table 1 shows the total precipitation for the 2017–2019 period, which varied significantly by growing season. In the first year it was 292.00 mm higher than the multi-year average, in 2018 it was 61.00 mm, while in 2019 it was equal to the multi-year average. The highest precipitation was recorded in 2017 in June (282.00 mm), 2018 in July (124.00 mm), and in 2019 in August (102.00 mm).

Table 1. Average monthly air temperatures and total precipitation according to the Agrometeorological Station in Lublin during the months of April to October in 2017–2019

Air temperature (°C)								
Year	IV	V	VI	VII	VIII	IX	X	average
2017	8.0	14.1	19.6	18.9	20.2	13.5	8.5	14.7
2018	7.5	16.7	18.8	20.6	20.8	15.5	10.0	15.7
2019	9.5	13.4	21.5	19.4	20.3	14.5	11.0	15.7
Multi-year average	7.4	13.0	16.3	18.0	17.2	12.6	7.6	13.2
Total precipitation (mm)								
Year	IV	V	VI	VII	VIII	IX	X	sum
2017	55.0	29.1	282.0	107.9	48.0	80.0	90.0	692.0
2018	40.0	56.0	65.0	124.0	72.0	68.0	36.0	461.0
2019	49.0	93.0	37.0	38.0	102.0	52.0	29.0	400.0
Multi-year average	39.0	60.7	65.9	82.0	70.7	53.7	40.1	400.0

The height of maiden apple trees ranged from 153.92 to 166.07 cm (tab. 2). It was shown that the trait under study was significantly influenced by branching and biostimulation treatments. In the case of maiden apple trees treated with growth regulators, no significant effect of the number of applications on the studied trait was shown. A significant effect of the number of treatments was shown only in the case of biostimulant application. It was found that significantly the highest maiden apple trees were after the application of Maxifruit, while significantly the lowest were after AGRAMIX PRO. Within the maiden apple trees treated with growth regulators, a significantly favorable effect of biostimulation on the final height of the studied apple trees was shown (tab. 2).

The number of lateral shoots of maiden apple trees of the Gloster ranged from 0.84 to 4.36 units (tab. 2). A significant effect of branching and biostimulation treatments and the number of applications on the studied trait was shown. In the case of maiden apple trees treated with branching, it was found that two applications of growth regulators significantly increased the number of shoots compared to a single application. In maiden apple trees treated with a biostimulant preparation, the relationships were significantly opposite. A significantly beneficial effect of growth regulators on the studied trait was demonstrated. The trees in the above-mentioned combinations formed significantly more lateral shoots than the control and biostimulation-treated trees. Within the combinations where AGRAMIX PRO was applied, it was shown that the addition of the biostimulant to the solution significantly positively increased its effect. The maiden apple trees treated with the biostimulant preparation formed significantly fewer lateral shoots than the control (tab. 2).

Analyzing the average length of one shoot showed that this trait depended significantly on the number of applications and branching and biostimulation treatments (tab. 2). Regardless of the combination, trees treated twice with growth regulators and biostimulant had significantly longer shoots than those treated once. AGRIMIX PRO had a significantly beneficial effect on lateral shoot length compared to trees treated with biostimulants and controls. Within the combinations where chemical branching treatment with AGRAMIX PRO was applied, a significantly unfavorable effect of biostimulation on the tested parameter was shown. Control trees formed significantly shorter shoots than after application of Maxifruit (tab. 2).

Table 2. Influence of the number of applications on the growth and quality of maiden apple trees Gloster

Parameter	Number of applications	Control	Maxifruit	AGRIMIX PRO	AGRIMIX PRO + Maxifruit	p-value
Height of maiden apple trees in autumn (cm)	1	156.36 ±14.22 ^{Ac}	165.18 ±15.02 ^{Ba}	153.92 ±14.00 ^{Ad}	161.12 ±14.65 ^{Ab}	0.0001
	2		166.07 ±15.10 ^{Aa}	156.00 ±14.18 ^{Ac}	162.66 ±14.79 ^{Ab}	0.0001
	p-value	0.9874	0.0001	0.1045	0.6252	–
Number of lateral shoots (pcs)	1	1.28 ±0.12 ^{Ac}	1.04 ±0.09 ^{Ad}	2.88 ±0.26 ^{Bb}	3.72 ±0.34 ^{Ba}	0.0001
	2		0.84 ±0.08 ^{Bd}	3.96 ±0.36 ^{Ab}	4.36 ±0.40 ^{Aa}	0.0001
	p-value	0.9621	0.0001	0.0001	0.0027	–
Average length of one shoot (cm)	1	2.56 ±0.23 ^{Ad}	15.62 ±1.42 ^{Bc}	25.10 ±2.28 ^{Ba}	22.07 ±2.01^{Bb}	0.0001
	2		17.24 ±1.57 ^{Ac}	28.49 ±2.59 ^{Aa}	27.24 ±2.48 ^{Ab}	0.0001
	p-value	0.9854	0.0001	0.0473	0.0001	–
Total length of lateral shoots (cm)	1	3.28 ±0.30 ^{Ad}	16.24 ±1.48 ^{Ac}	72.62 ±6.60 ^{Bb}	82.30 ±7.48 ^{Ba}	0.0001
	2		14.48 ±1.32 ^{Bc}	112.28 ±10.21 ^{Ab}	118.50 ±10.77 ^{Aa}	0.0001
	p-value	0.9631	0.0001	0.0001	0.0001	–

Different letters A, B, C in the same column and a, b, c in the same line indicate statistically significant differences ($p < 0.05$)

The sum of lateral shoot lengths ranged from 3.28 to 118.50 cm and significantly depended on the number of applications and branching and biostimulation treatments (tab. 2). Trees treated twice with AGRAMIX PRO were characterized by a significantly higher sum of lateral shoot lengths than after a single application. The opposite relationship was found for trees treated with Maxifruit. Trees treated with branching had a significantly higher sum of lateral shoots than the others. Within the maiden apple trees treated with growth regulators, it was found that the addition of the biostimulant treatment significantly positively affected the level of the evaluated parameter. Maxifruit-treated maiden apple trees had significantly higher sum of lateral shoot lengths than controls (tab. 2).

Table 3 shows the effect of the concentration of growth regulators in the form of the AGRAMIX PRO preparation and a mixture of AGRAMIX PRO and Maxifruit preparations on the height and quality parameters of maiden apple trees of the 'Gloster', regardless of the examined year and the number of applications. The height of apple tree maiden in autumn in combinations with AGRAMIX PRO preparations treated with a lower concentration, i.e. 25 ml, was significantly lower than the others. In the case of a mixture of AGRAMIX PRO and Maxifruit preparations, it was shown that the maiden apple trees treated with a higher concentration of growth regulators, i.e. 35 ml, were significantly the highest. Analyzing the structure of the crown, which consists of such parameters as the number and average length of lateral shoots and the sum of the length of syleptic shoots, showed an unambiguous significantly beneficial effect of growth regulators. There was no significant effect of the dose of AGRAMIX PRO preparation on the evaluated quality parameters of apple trees, this tendency persisted in the case of the combination with AGRAMIX PRO preparation and the mixture of AGRAMIX PRO and Maxifruit preparations (tab. 3).

Table 3. Effect of the concentration of AGRIMIX PRO preparation on the growth and quality of maiden apple trees of the Gloster

Preparation	Dose	Height of maiden apple trees (cm)	Number of lateral shoots (pcs)	Average length of one shoot (cm)	Total length of lateral shoots (cm)
AGRIMIX PRO	control	156.36 ±14.22 ^{A}	1.28 ±0.12 ^{B}	2.56 ±0.23 ^{B}	3.28 ±0.30 ^{B}
	25 ml	153.74 ±2.65 ^{B}	3.60 ±0.61 ^{A}	26.49 ±0.72 ^{A}	94.98 ±13.65 ^{A}
	35 ml	156.18 ± 0.37 ^{A}	3.24 ±0.57 ^{A}	27.11 ±4.43 ^{A}	89.92 ±29.80 ^{A}
	p-value	0.0173	0.0001	0.0001	0.0001
AGRIMIX PRO + Maxifruit	control	156.36 ±14.22 ^{B}	1.28 ±0.12 ^{B}	2.56 ±0.23 ^{B}	3.28 ±0.30 ^{B}
	25 ml	158.16 ±4.21 ^{B}	3.84 ±0.53 ^{A}	24.71 ±3.49 ^{A}	96.16 ±26.12 ^{A}
	35 ml	165.62 ±2.52 ^{A}	4.24 ±0.18 ^{A}	24.61 ±2.17 ^{A}	104.64 ±13.54 ^{A}
	p-value	0.0001	0.0001	0.0001	0.0001

* Different letters A, B, C in the same column and a, b, c in the same line indicate statistically significant differences ($p < 0.05$)

Table 4 shows the impact of biostimulation in the form of Maxifruit on the effectiveness of AGRIMIX PRO regardless of the number of applications and year of study. In the case of a lower dose of AGRIMIX PRO, no significant effect of biostimulation on the growth and quality of apple tree maiden was shown. A similar tendency occurred in the

combination where a higher dose of AGRIMIX PRO was applied, when the average length of one shoot and the sum of the length of lateral shoots were evaluated. A significantly beneficial effect of the higher dose of AGRIMIX PRO + Maxifruit was found for the height of maiden apple trees in autumn and the number of lateral shoots (tab. 4).

Table 4. Effect of biostimulation on the effectiveness of growth regulators regardless of the number of applications and year of study

Dose	Preparation	Height of maiden apple trees (cm)	Number of lateral shoots (pcs)	Average length of one shoot (cm)	Total length of lateral shoots (cm)
25 ml	AGRIMIX PRO	153.74 ±2.65 A	3.60 ±0.61 A	26.49 ±0.72 A	94.98 ±13.65 A
	AGRIMIX PRO + Maxifruit	158.16 ±4.21 A	3.84 ±0.53 A	24.71 ±3.49 A	96.16 ±26.12 A
	p-value	0.0545	0.4835	0.2509	0.9238
35 ml	AGRIMIX PRO	156.18 ±0.37 B	3.24 ±0.57 B	27.11 ±4.43 A	89.92 ±29.80 A
	AGRIMIX PRO + Maxifruit	165.62 ±2.52 A	4.24 ±0.18 A	24.61 ±2.17 A	104.64 ±13.54 A
	p-value	0.0001	0.0021	0.2431	0.2964

* Different letters A, B, C in the same column and a, b, c in the same line indicate statistically significant differences ($p < 0.05$)

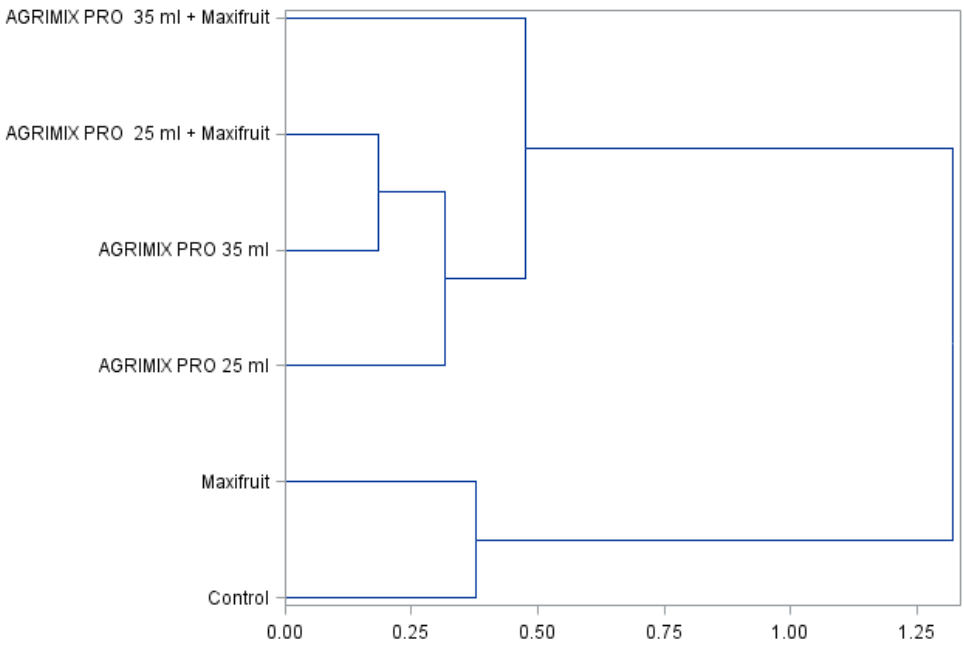

Fig. 1. Cluster analysis of parameters determining the branching quality of maiden apple trees of the Gloster

Figure 1 shows a cluster analysis of the crown structure of the Gloster of apple trees regardless of the year of study and number of applications. The dendogram below shows two distinct clusters. The first cluster refers to combinations in which growth regulators and mixtures of growth regulators and biostimulation were applied. Within the large cluster, we can distinguish a subgroup that includes combinations showing very high similarity, i.e. AGROMIX PRO 25 ml + Maxifruit and AGROMIX PRO 35 ml. The next similarity was observed with AGRO-MIX PRO 25 ml and AGROMIX PRO 35 ml + Maxifruit. Controla and the Maxifruit combination formed a separate cluster.

It was observed that the number and total length of lateral shoots correlated with average air temperature, while the height of maiden apple trees and average length of one shoot did not show this relationship. The analyzed traits showed no correlation with the sum of precipitation and the year of the study (tab. 5).

Table 5. Correlation of growth and quality of maiden apple trees with weather conditions during the plant growth period (April–October) and the year of study

Specification	Average air temperature (°C)	Rainfall totals (mm)	Year of study
Height of maiden apple trees in autumn (cm)	–0.1248	–0.3551	–0.2987
Number of lateral shoots (pcs)	0.5189*	0.1157	0.2684
Average length of one shoot (cm)	0.3703	0.1381	0.3111
Total length of lateral shoots (cm)	0.4875*	0.1447	0.2631

DISCUSSION

Biostimulants contain biologically active substances that positively affect plant growth and development. They improve the tolerance of plants to unfavorable environmental conditions, and some can affect the development of the root system [Hetman i Adamiak 2002, Jankowski and Dubis 2008, Kapłan et al. 2021, Kapłan et al. 2023]. Extracts from marine algae are used in horticultural practice as agents that increase the size and quality of crops [Matysiak and Adamczewski 2009, Pacholczak et al. 2012]. In the work of Klimek et al. [2018] demonstrated the is-total effect of a growth regulator and its dosage as well as biostimulation on the height of Szampion Reno maiden apple trees. These studies demonstrated that the use of AGRIMIX PRO at the highest dose, 35 ml, resulted in a significant reduction in the height of the trees under evaluation. This could be attributed to the extensive branching of the plants and their well-developed side shoots. Biostimulant applications in the form of Asahi SL in the study by Klimek et al. [2018] had a significantly beneficial effect on the evaluated parameter, which was also confirmed in the present study. Kaplan and Baryła [2006] showed no significant effect of the preparation dose on the height of the maiden apple trees of two-year-old apple trees. The growth of maiden apple trees was significantly independent of average air temperature and precipitation sum, these relationships did not confirm the previous results of Klimek et al. 2018 and Kaplan and Baryła [2006]. Gąstoł et al. [1999, 2012] using preparations based on bezyladein (BA) and gibberellins (GA_3 and GA_{4+7}) showed no significant effect on the height of maiden apple trees of Boskoop and Mutsu cultivars. In a study by Hetman and

Adamiak [2003], the application of Asahi SL in the form of plant sprays produced beneficial effects in the cultivation of multiflora rose rootstock. The application of Asahi SL concentrations from 0.1% to 0.6% had a stymulative effect on the diameter and length of the root neck, as well as the weight of the aboveground part and the root system. The result was a good quality of multifloral rose rootstocks, which grew to periculations already in the first half of August despite the not favorable weather conditions immediately after the establishment of the experiment. Similar observations were demonstrated in a newly established apple orchard, where the application of biostimulants had a beneficial effect on the growth and development of apple trees of the Gala Must cultivar [Kapłan et al. 2021]. This study demonstrated that the number of lateral shoots is influenced by the dose and number of AGRIMIX PRO applications and the biostimulation treatment. Maiden apple trees treated with growth regulators and biostimulation produced significantly more lateral shoots than control trees. These relationships have been confirmed in numerous papers [Gąstoł et al. 1999, Klimek et al. 2018, Kapłan 2006]. An inconclusive effect on the degree of branching of two-year-old apple trees was shown by Kaplan and Baryła [2006]. In the above study, more lateral shoots were obtained in combinations treated with growth regulators than in the control, but the effect was not always significant. The number of lateral shoots was observed to significantly increase after the application of the Maxifruit biostimulant. This phenomenon likely stems from the fact that the effectiveness of exogenous growth regulators depends on numerous environmental factors, and the use of the biostimulant supported and enhanced the branching effect. Hetman and Adamiak [2003], evaluating the effect of Asahi SL on the quality of large-flowered roses, showed that the least effective effect of the biostimulant was observed at the number of first-order shoots compared to plants growing in control plots. The average length per shoot depended significantly on the number of applications and branching and biostimulation treatments. Klimek et al. [2018] showed that the maiden apple trees of the cultivar Szampion Reno treated with the lowest dose of AGRIMIX PRO produced istotally longer shoots than after application at a dose of 35 ml and in the control trial. The aforementioned study showed a significantly beneficial effect of the Asahi SL preparation on the studied parameter. The sum of lateral shoot lengths significantly depended on the number of applications and branching and biostimulation treatments.

Klimek et al. [2018] showed that maiden apple trees treated with growth regulators formed a higher sum of all shoot lengths compared to the control. They found that as the concentration of AGRIMIX PRO increased, the sum of syleptic shoot lengths increased significantly.Similar results were obtained by Gąstoł et al. [1999]. In the study of Poniedziałek and Porębski [1992], a significant effect on the sum of lateral shoot lengths was exerted by spraying with a mixture of BA + GA_3 (Arbolin 036 SL), while the preparation Paturyl 100 SL (BA) had only a slight effect on increasing the sum of increments, since the resulting shoots are too short. In an earlier study by these authors Poniedzialek and Porębski [1992], the formulations Promalin 3.6 SL and Arbolin 036 SL affected the average sum of shoot length, but no significant differences were found between the formulations used.

CONCLUSIONS

1. The height of maiden apple trees of the Gloster significantly depended on the concentration of applied growth regulators. Trees treated with a higher concentration (35 ml) were significantly higher than those treated with a lower dose (25 ml). A significantly beneficial effect of the Maxifruit biostimulator on the height of the examined maiden apple trees was demonstrated with the use of a higher dose of AGRIMIX PRO.

2. The number of side shoots, average length of a single shoot, and the sum of side shoot lengths were significantly dependent on the number of growth regulator applications. A double application of AGRIMIX PRO had a beneficial effect on crown structure parameters of maiden trees of the Gloster cultivar compared to a single application.

3. The crown structure of maiden apple trees of the Gloster cultivar, determined by the number and length of lateral shoots and their sum, is significantly correlated with the average air temperature during the growing season, which indicates a significant influence of thermal conditions on the effectiveness of tree branching and should be taken into account when planning treatments stimulating the development of trees in the nursery.

4. Using the Maxifruit biostimulator alone does not significantly improve the growth or quality of young apple trees of the Gloster. However, its use in combination with growth regulators such as AGRIMIX PRO significantly increases the number of lateral shoots, promotes branching development, and improves crown structure parameters, indicating the significant value of this combination in nursery practice.

REFERENCES

Basak A., 2009. Regulatory wzrostu w matecznikach, szkółkach i młodych sadach. Plantpress Warszawa.

Bielicki P., Pąśko M., 2013. Effect of the rootstocks on the quality of apricot maiden trees produced in the organic nursery. J. Res. Appl. Agric. Eng. 58(3).

Buraczyk W., Żybura H., Ostaszewska E. et al., 2020. Zastosowanie biostymulatorów w hodowli i ochronie sadzonek dębu szypułkowego (*Quercus robur* L.) w gruntowej szkółce leśnej. Sylwan 164(4), 292−299.

Czynczyk A., 2012. Szkółkarstwo sadownicze. Powszechne Wydawnictwo Rolnicze i Leśne, Warszawa.

Dorić, M., Keserović, Z., Magazin, N., Milić, B., 2015. The effects of BA and BA + GA4 + 7 on the main shoot growth dynamics and the feather formation in two-year-old 'knip-boom' apple trees. In: Proceedings of 50th Croatian & 10th International Symposium on Agriculture. Opatija, Croatia, 16–20 February 2015, University of Zagreb, 555–559.

Elfving D.C., 2010. Plant bioregulators in the deciduous fruit tree nursery. Acta Hortic. 884, 159–166. https://doi.org/10.17660/ActaHortic.2010.884.18.

Gawrońska H., Przybysz A., 2011. Biostymulatory: mechanizmy zastosowania i przykłady zastosowań. Materiały konferencyjne TSW. Warszawa, 5−6 stycznia 2011 r.,7−13.

Gąstoł M., Poniedziałek W., Banach P., 1999. Wpływ preparatu Arbolin 36SL na rozgałęzianie sięokulantów jabłoni. Zesz. Nauk. AR Krak. 351, 81–85.

Gudarowska E., 2002. Wpływ wysokości przycięcia jednorocznych okulantów pięciu odmian jabłoni na wysokość otrzymanych drzewek dwuletnich. Zesz. Nauk. ISiK 10, 75–82

Gudarowska E., Szewczuk A., 2002. Wpływ czynników agrotechnicznych i bioregulatorów na stopień rozgałęziania jednorocznych i dwuletnich drzewek jabłoni odmian ‘Gala’ i ‘Alwa’ na podkładce M.26. Zesz. Nauk. ISiK 10, 29–37.

Hetman J., Adamiak J., 2002. Wpływ Asahi SL na jakość podkładki róży wielkokwiatowej (*Rosa multiflora* THUNB.). Zesz. Probl. Post. Nauk Rol. 491, 61–67.

Jacyna T., 2002. Factors influencing lateral-branch formation in woody plants. Acta Agrobaot., 55(2), 5–25.

Jankowski K., Dubis B., 2008. Biostimulators in plant field production. Mat. Conf. Biostimulators in Modern Plant Breeding. Plant Press, Warsaw, 24–25.

Kapłan M., Baryła P., 2006. The effect of growth regulators on the quality of two- year-old apple trees of ‘Sampion’ and ‘Jonica’ cultivars. Acta Sci. Pol. Hortorum Cultus, 5(1), 79–89.

Kapłan M., 2012. Mechaniczne metody stymulacji rozgałęzienia drzew. Szkółkarstwo 3, 67–70.

Kapłan M., Jurkowski G., Krawiec M. et al., 2017. Wpływ zabiegów stymulujących rozgałęzianie na jakość okulantów jabłoni. Ann. Hortic. 27(3), 5–20.

Kapłan M., Lenart A., Klimek K. et al., 2021. Assessment of the possibilities of using cross-linked polyacrylamide (agro hydrogel) and preparations with biostimulation in building the quality potential of newly planted apple trees. Agron.-Basel 11(1), 125. https://doi.org/10.3390/agronomy11010125

Kapłan M., Klimek K., Buczyński K. et al., 2023. Evaluation of the effect of biostimulation on the yielding of Golden Delicious apple trees. Appl. Sci.-Basel 13(16), 9389. https://doi.org/10.3390/app13169389

Klimek K., Kapłan M., Najda A., 2018. Effect of growth regulators on quality of apple tree maidens. Acta Agrophys. 25, 3.

Kopytowski J., Markuszewski B., 2009. Wpływ Arbolinu 036 SL i uszczykiwania liści szczytowych na rozgałęzianie się drzewek jabłoni w szkółce. Zesz. Probl. Postępów Nauk Roln. 539(1), 333–339.

Kozak M., Wondołowska-Grabowska A., Serafin-Andrzejewska M. et al., 2016. Biostymulatory – wczoraj, dziś i jutro. In: D. Łuczyńska D. (ed.), Rolnictwo XXI wieku – problemy i wyzwania. Idea Knowledge Future, Wrocław, 114−122.

Kumawat K.L., Raja W.H., Chand L. et al., 2023. Influence of plant growth regulators on growth and formation of sylleptic shoots in one-year-old apple cv. ‘Gala Mast’. J. Env. Biol. 44, 122–133.

Kumawat K.L., Raja W.H., Mir J.I. et al., 2025. Effect of genotype and leader type on benzyladenine induced sylleptic branching in apple nursery trees. Hort. Sci. (Prague) 52, 33–41.

Kviklys, D., 2004. Apple rootstock effect on the quality of planting material. Acta Hortic. 658, 641–645. https://doi.org/10.17660/ActaHortic.2004.658.97

Kviklys, D., 2006. Induction of feathering of apple planting material. Agronomijas Vestis 9, 58–63.

Laňar L., Měszáros M., Kyselová K. et al., 2020. Branching of nursery apples and plums using various branching inducing methods. J. Central Eur. Agric. 21(1), 113–123. https://doi.org/10.5513/JCEA01/21.1.2459

Lordan J., Robinson T.L., Sazo M.M. et al., 2017. Use of plant growth regulators for feathering and flower suppression of apple nursery trees. HortScience 52(8), 1080–1091. https://doi.org/10.21273/HORTSCI11918-17

Matyjaszczyk E., 2015. Wprowadzanie biostymulatorów do obrotu handlowego w Polsce. Sytuacja bieżąca i uwarunkowania prawne. Przem. Chem. 94(10), 1841–1844.

Matysiak K., Adamczewski K., 2009. Regulatory wzrostu i rozwoju roślin – kierunki badań w Polsce i na świecie. Prog. Plant Prot. 49(4), 1810–1816.

Nečas T., Wolf J., Kiss T. et al., 2018. Use of different plant growth regulators for control of shoot branching in apple and pear trees. Acta Hortic. 1206, 225–232. https://doi.org/10.17660/ActaHortic.2018.1206.31

Nečas T., Wolf J., Kiss T. et al., 2020. Improving the quality of nursery apple and pear trees with the use of different plant growth regulators. Eur. J. Hortic. Sci. 85, 430–438.

Pacholczak A., Szydło W., Jacygrad E. et al., 2012. Effect of auxins and the biostimulator algaminoplant on rhizogenesis in stem cuttings of two dogwood cultivars (*Cornus alba* 'AUREA' AND 'ELEGANTISSIMA'), Acta Sci. Pol. Hort. Cult. 11(2), 93–103.

Poniedziałek W., Porębski S., 1992. Wpływ regulatorów wzrostu i uszczykiwania wierzchołków na tworzenie się bocznych pędów u okulantów jabłoni odmiany 'Melrose'. Zesz. Nauk. AR Krak. 267, 21–33.

Rejman A., Ścibisz K., Czarnecki B., 2002. Szkółkarstwo roślin sadowniczych. Państwowe Wydawnictwo Rolnicze i Leśne, Warszawa.

Skrzyński J., Poniedziałek W., 2000. Wzrost i plonowanie odmiany 'Jonagold' na kilku podkładkach wegetatywnych. Zesz. Nauk. Inst. Sadow. Kwiac. Skiern. 8, 53–58.

Traon D., Amat L., Zotz F., du Jardin P., 2014. A legal framework for plant biostimulants and agronomic fertilizer additives in the EU. Report for the European Comission Enterprise & Industry Directorate – General, Arcadia International.

Zhalnerchyk P., Przybyła A., Jaumień F., 2015. Influence of chemicals of arbolin group on branching of maiden trees of three apple cultivars. J. Hortic. Res. 23(2), 95–104. https://doi.org/10.2478/johr-2015-0019

Source of funding: This work received no external funding.

Received: 30.07.2025
Accepted: 11.12.2025
Published: 31.12.2025

AGRONOMY SCIENCE
VOL. LXXX (4) 2025

Lista recenzentów
List of reviewers

dr hab. Jakub Bekier (Uniwersytet Przyrodniczy we Wrocławiu, Polska)

dr hab. inż. Jan Buczek (Uniwersytet Rzeszowski, Polska)

assoc. prof dr Civan Çelik (Isparta University of Applied Sciences, Türkiye)

dr Mykhaylo Chernetskyy (Uniwersytet Marii Curie-Skłodowskiej w Lublinie, Polska)

dr hab. Eugenia Czernyszewicz, prof. UPL (Uniwersytet Przyrodniczy w Lublinie, Polska)

dr Francesca Degola (University of Parma, Italy)

dr hab. Renata Dobosz (Instytut Ochrony Roślin – Państwowy Instytut Badawczy w Poznaniu, Polska)

prof. dr hab. Teresa Doroszewska (Instytut Uprawy Nawożenia i Gleboznawstwa – Państwowy Instytut Badawczy w Puławach, Polska)

dr Adam Gawryluk (Uniwersytet Przyrodniczy w Lublinie, Polska)

dr hab. Dariusz Gozdowski, prof. SGGW (Szkoła Główna Gospodarstwa Wiejskiego w Warszawie, Polska)

dr Grzegorz Gryń (Instytut Hodowli i Aklimatyzacji Roślin – Państwowy Instytut Badawczy w Bydgoszczy, Polska)

dr inż. Joanna Horoszkiewicz-Janka (Instytut Ochrony Roślin – Państwowy Instytut Badawczy w Poznaniu, Polska)

dr hab. Agata Jabłońska-Trypuć, prof. PB (Politechnika Białostocka, Polska)

dr hab. inż. Magdalena Jakubowska (Instytut Ochrony Roślin – Państwowy Instytut Badawczy w Poznaniu, Polska)

dr hab. inż. Wacław Jarecki, prof. UR (Uniwersytet Rzeszowski, Polska)

dr ing. Jiří Kadlec (Mendel University in Brno, Czech Republic)

dr hab. inż. Paweł Kiełbasa, prof. URK (Uniwersytet Rolniczy im. Hugona Kołłątaja w Krakowie, Polska)

prof. dr hab. inż. Anna Kocira (Państwowa Akademia Nauk Stosowanych w Chełmie, Polska)

prof. dr hab. Jolanta Kowalska (Instytut Ochrony Roślin – Państwowy Instytut Badawczy w Poznaniu, Polska)

dr inż. Aneta Kramek (Uniwersytet Przyrodniczy w Lublinie, Polska)

dr hab. inż. Barbara Lilianna Krochmal-Marczak, prof. PANS (Państwowa Akademia Nauk Stosowanych w Krośnie, Polska)

prof. dr hab. Cezary Kwiatkowski (Uniwersytet Przyrodniczy w Lublinie, Polska)

prof. dr hab. Anetta Kuczyńska (Instytut Genetyki Roślin Polskiej Akademii Nauk, Polska)

dr hab. inż. Krystyna Kurowska, prof. UWM (Uniwersytet Warmińsko-Mazurski w Olsztynie, Polska)

dr hab. Marek Liszewski, prof. UPW (Uniwersytet Przyrodniczy we Wrocławiu, Polska)

dr hab. Joanna Majkowska-Gadomska, prof. UWM (Uniwersytet Warmińsko-Mazurski w Olsztynie, Polska)

dr hab. Janetta Niemann, prof. UPP (Uniwersytet Przyrodniczy w Poznaniu, Polska)

dr hab. Anna Nowak, prof. UPL (Uniwersytet Przyrodniczy w Lublinie, Polska)

prof. dr hab. Elżbieta Patkowska (Uniwersytet Przyrodniczy w Lublinie, Polska)

dr hab. inż. Joanna Puła, prof. URK (Uniwersytet Rolniczy im. Hugona Kołłątaja w Krakowie, Polska)

dr Michał Pylak (Instytut Agrofizyki im. Bohdana Dobrzańskiego PAN, Polska)

dr Monika Rewers (Politechnika Bydgoska, Polska)

prof. dr hab. Barbara Sawicka (Uniwersytet Przyrodniczy w Lublinie, Polska)

assoc. prof. dr. Emre Sevindik (Adnan Menderes University, Türkiye)

assoc. prof. dr Miroslav Šlosár (Slovak University of Agriculture in Nitra, Slovakia)

dr hab. Zbigniew Sobisz, prof. UP, Herbarium (Uniwersytet Pomorski, Polska)

dr hab. Jarosław Stalenga (Instytut Uprawy Nawożenia i Gleboznawstwa – Państwowy Instytut Badawczy w Puławach, Polska)

dr hab. inż. Arkadiusz Stępień, prof. UWM (Uniwersytet Warmińsko-Mazurski w Olsztynie, Polska)

prof. dr hab. Stefan Stojałowski (Zachodniopomorski Uniwersytet Technologiczny, Polska)

prof. dr hab. inż. Ewa Szpunar-Krok (Uniwersytet Rzeszowski, Polska)

dr hab. inż. Elżbieta J. Szymańska, prof. SGGW (Szkoła Główna Gospodarstwa Wiejskiego, Polska)

dr hab. Sławomir Świerczyński (Uniwersytet Przyrodniczy w Poznaniu, Polska)

prof. dr hab. Mirosław Tyrka (Politechnika Rzeszowska, Polska)

dr Sylwester Wereski (Uniwersytet Marii Curie-Skłodowskiej w Lublinie, Polska)

dr Yared Seifu Woldeyohannis (Dire Dawa University, Ethiopia)

dr hab. Elżbieta Wołejko, prof. PB (Politechnika Białostocka, Polska)

dr hab. Elżbieta Wójcik-Gront, prof. SGGW (Szkoła Główna Gospodarstwa Wiejskiego w Warszawie, Polska)

dr inż. Urszula Wydro (Politechnika Białostocka, Polska)

dr Maria Zuba-Ciszewska (Katolicki Uniwersytet Lubelski Jana Pawła II, Polska)